INFORMATION TO USERS

This manuscript has been reproduced from the microfilm master. UMI films the text directly from the original or copy submitted. Thus, some thesis and dissertation copies are in typewriter face, while others may be from any type of computer printer.

The quality of this reproduction is dependent upon the quality of the copy submitted. Broken or indistinct print, colored or poor quality illustrations and photographs, print bleedthrough, substandard margins, and improper alignment can adversely affect reproduction.

In the unlikely event that the author did not send UMI a complete manuscript and there are missing pages, these will be noted. Also, if unauthorized copyright material had to be removed, a note will indicate the deletion.

Oversize materials (e.g., maps, drawings, charts) are reproduced by sectioning the original, beginning at the upper left-hand corner and continuing from left to right in equal sections with small overlaps.

Photographs included in the original manuscript have been reproduced xerographically in this copy. Higher quality 6" x 9" black and white photographic prints are available for any photographs or illustrations appearing in this copy for an additional charge. Contact UMI directly to order.

ProQuest Information and Learning
300 North Zeeb Road, Ann Arbor, MI 48106-1346 USA
800-521-0600

Université d'Ottawa · University of Ottawa

The Role of Liquid Mixing in Evaporation of Complex Multi-Component Mixtures: Modelling using Continuous Thermodynamics

Zainab Abdel-Qader

The thesis is submitted to

The School of Graduate Studies and Research in partial fulfillment of the

requirements for the degree of

Master of Applied Science

in the

Department of Chemical Engineering

University of Ottawa

September 2000

ACKNOWLEDGMENTS

I would like to dedicate this work to my mother for all that she has done for me. I would like also to express gratitude and special thanks to Prof. W. Hallett for giving me the chance to make this study, for all his help, support, guidance, patient and for all the time he gave me. Special thanks to my husband for all his patience through the last two years and for my family because they have always encouraged me to go on. Finally, many thanks to all my friends for their help.

ABSTRACT

"Continuous thermodynamics" is a technique for modelling mixtures with large numbers of components which uses a probability density function rather than discrete components to represent the mixture composition. It has proved to be a practical and useful technique for modelling mixtures with dozens or even hundreds of components. An unresolved issue in the use of these models so far has been the role of mixing in the liquid phase, all the previous work having assumed a well-mixed droplet. With two- or three-component mixtures it is known that there are significant differences between the two extremes of well-mixed and diffusion limited droplets, the latter referring to mixing which occurs by molecular diffusion only.

This paper presents a numerical solution for diffusion within a droplet of multi-component mixture modelled using continuous thermodynamics. Transport equations for the mean and variance of the fuel composition distribution function in the droplet are derived. The molecular diffusivity of the liquid mixture is calculated using a continuous thermodynamics extension of the well-known Wilke-Chang diffusivity correlation. The effects of enhanced mixing caused by internal circulation are modelled by increasing the effective diffusivity of the liquid. Vapour and liquid phase solutions are coupled at the liquid surface by matching the fluxes of the distribution moments. The results are compared to other models, including a continuous mixture version of the quasi-steady liquid phase model of Law and Law (1981). Conclusions for practical spray modelling are drawn.

SOMMAIRE

La "thermodynamique continue" est une technique pour décrire les mélanges avec un grand nombre de composantes. Elle représente le mélange avec une fonction de probabilité au lieu de donner les composantes individuelles. Elle est une technique pratique pour représenter des mélanges avec des douzaines ou des centaines de composantes. Dans cette thèse, la thermodynamique continue est utilisée pour calculer la vaporisation d'une goutte de mélange qui rassemble un carburant commercial liquide. La thèse s'occupe particulièrement de la question des processus du mélange dans la phase liquide. Tous les écrits sur cet thème ont assumé une goutte bien mélangé, mais pour des mélanges de deux ou de trois composantes, il est bien reconnu que les processus de mélange peuvent être significatifs.

Cette thèse présente une solution numérique pour la diffusion dans une goutte de mélange avec plusieurs composantes en utilisant la thermodynamique continue. Des équations de transport pour le moyen et l'écart-type de la fonction de probabilité qui décrit la composition du carburant sont dérivées pour la phase liquide. La diffusivité moléculaire du mélange est calculée par une formulation continue de la correlation Wilke-Chang. Les effets du mélange par l'écoulement du liquide dans la goutte sont simulés par une diffusivité augmentée. Les solutions pour la phase liquide et la phase vapeur sont reliées par des relations de flux à la surface. Les résultats sont comparés avec d'autres modèles, y inclus le modèle quasi-stationnaire de Law et Law. Des conclusions pour la modélisation pratique des aérosols de carburants en sont tirées.

NOMENCLATURE

A	droplet surface area (m^2)
c	vapour molar density ($kmol/m^3$)
c_L	liquid molar density ($kmol/m^3$)
$\overline{c}_L$	Average over the droplet of the liquid molar density ($kmol/m^3$)
$\overline{C}_P$	mixture specific heat (kJ/kmol.K)
D_{im}	effective diffusivity of component i in the vapour mixture (m^2/s)
D_{lim}	effective diffusivity of component i in the liquid mixture (m^2/s)
$\overline{D}, \widetilde{D}, \hat{D}$	average diffusivities weighted with respect to the mol fraction, the mean of the distribution and the variance of the vapour distribution (m^2/s)
$\overline{D}_L, \widetilde{D}_L, \hat{D}_L$	average diffusivites weighted with respect to the mol fraction, the mean of the distribution and the variance of the liquid distribution (m^2/s)
f(I)	vapour phase probability density function
$f_L(I)$	liquid phase probability density function
$f_N(I)$	vapour flux probability density function
G_{ij}	binary interaction parameter
h_{fg}	enthalpy of vaporization, (J/kmol)
I	distribution parameter (= species molecular mass)

J_i^*	molar flux (kmol/m^2.s)
M	molecular mass (kg/kmol)
N	molar flux from the droplet (kmol/m^2.s)
n_i	number of moles of species i (kmol)
P	total pressure (kPa)
P_v	vapour pressure (kPa)
P_{ATM}	atmospheric pressure (kPa)
q	heat flux to the droplet surface by conduction (J/m^2.s)
r	radial position (m)
R	droplet radius (m)
$\dot{R}$	droplet surface rate of recession (m/s)
S_{fg}	entropy of vaporization (kJ/kmol.K)
t	time (sec)
T	temperature (K)
T_B	boiling temperature (K)
V	droplet volume (m^3)
v^*	vapour molar average velocity (m/s)
v_L^*	liquid molar average velocity (m/s)
w	vapour velocity relative to ξ coordinate
w_L	liquid velocity relative to ξ coordinate
x	liquid mole fraction (kmol/kmol)

$\bar{x}$	liquid mean mole fraction (kmol/kmol)
y	vapour mole fraction (kmol/kmol)

Greek Letters

$\alpha, \beta, \alpha_L, \beta_L$	parameters of the gamma distribution of the vapour and liquid phase respectively
γ	origin of the distribution
Γ	gamma function
$\theta, \theta_L, \theta_N$	mean molecular mass of the vapour, liquid and vapour flux distribution respectively (kg/kmol)
$\bar{\theta}_L$	average over the droplet of the liquid distribution mean, (kg/kmol)
σ^2, σ^2_L	variance of the vapour and liquid distributions respectively
ψ, ψ_L, ψ_N	second moment about the origin of the vapour, liquid and vapour flux distribution respectively
$\bar{\Psi}_L$	average over the droplet of the liquid distribution second moment (kg/kmol)
σ	Stefan-Boltzmann constant.
α_R	absorptivity of the droplet
η	viscosity (cp)
ϕ	association factor
χ	mixing factor, multiplying the liquid diffusivity

λ	thermal conductivity (W/m.K)
$\xi = r/R$	dimensionless radial coordinate
ρ_L	mass density of the liquid (kg/m^3)
Δ	difference

Subscripts:

A, F	refers to air and fuel respectively
E, W	eastern and western grid point respectively
i	chemical species
L	liquid
m	mixture
N	number of grid points in the vapour phase
NN	number of grid points in the liquid phase
P	grid point
R	at the droplet surface
T_{cr}	critical temperature, (K)
∞	ambient condition
$_o$	initial conditions

Superscripts

^{o}	previous time step

TABLE OF CONTENTS

LIST OF FIGURES

CHAPTER 1: INTRODUCTION

1.1 Continuous Thermodynamics:

Liquid petroleum has played and still plays a very important role from the beginning of the 20th century as one of the main power sources in the world. Petroleum fuel mixtures are generally composed of hundreds of components of different types of hydrocarbons with a boiling point range from 65°C up to 500°C. These mixtures can vary in properties and specifications depending on the contribution of each compound, where a range of different molecular weights, volatilities, carbon numbers and boiling points can be present. These variations in properties will make it very complex to perform a discrete treatment of each component in a mixture simulation. Even if computers are used to simulate mixture behavior in terms of discrete components, one is limited to a fairly small number of components because of limitations on storage memory and computational time.

Different techniques were therefore invented to deal with such mixtures, such as the pseudo-component technique, the continuous thermodynamics technique and the semi-continuous mixtures technique.

The pseudo-component technique is based on lumping individual components of similar properties together in groups. Each group is represented as one component ("pseudo-

component"). Although this is convenient for some mixture calculations and can yield satisfactory results, it is considered somewhat arbitrary and depends greatly on proper selection of the pseudo-components.

The continuous thermodynamics technique was a revolution in simulation work for complex mixtures. The principle of continuous thermodynamics is the description of the fuel mixture by a continuous probability density function instead of by discrete components. The probability density function can be any function that is able to describe the fuel mixture over the desired domain. Its independent variable is some appropriate characterizing quantity such as boiling point or molecular weight. The three parameter gamma function has been the most common choice in previous work and will be used in this research to describe the fuel mixture in both vapour and liquid phases with the molecular weight as the characterizing variable. The continuous thermodynamics technique can save significantly in computational complexity over existing pseudo-component calculation methods, and can be a more accurate representation of the mixture if a large number of components are present.

The semi-continuous technique is based on describing a few of the components as identifiable discrete components while a continuous probability density function describes all other components. The reason for doing this can be the existence of compounds such as fuel additives, which can not be described by the continuous function. This technique can be valid if the number of discrete components is low, but for large number of discrete components, the same computational problems of pseudo-components will be faced.

To describe mixtures with different groups of compounds - for example, fuels with paraffin, naphthene and aromatic fractions - a multi-distribution continuous thermodynamic technique should be used. This technique is based on describing the fuel mixture with two or more distribution functions: each distribution will fit a certain combination of components that have closely related properties or structures.

1.2 Droplet Evaporation:

Liquid fuels are usually fired in the form of sprays. The fuel is atomized into fine droplets in order to enlarge the surface area and as a result get faster evaporation and combustion. The fuel droplets subsequently vaporize as they are dispersed in the combustor. Many studies in the field of droplet combustion and/or ignition were performed for various types of engines which indicate that the resulting combustion and/or ignition characteristics depend significantly on the vaporization process of the fuel droplet.

The droplet evaporation process was the concern of many researchers due to its importance in combustion in engines and in other similar fields. Accurate models of single droplet evaporation are essential to calculations of spray evaporation and combustion.

Fuel droplet evaporation as a basic idea is simple and it can be summarized by a combination of heat and mass transfer inward and outward the droplet. The main physical features of these processes are shown in Figure1.

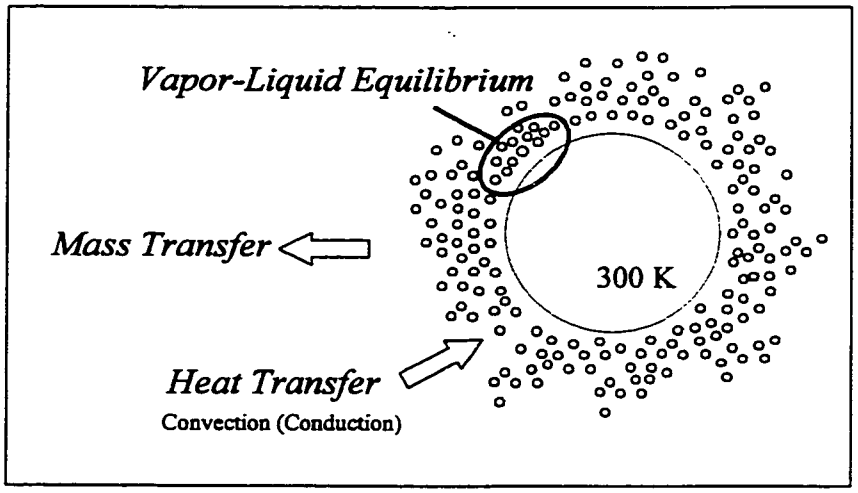

Figure 1.1: Mass and heat transfer processes through droplet evaporation.

A heat flux from the surrounding atmosphere is transferred inward to the fuel droplet by conduction due to the temperature difference between the surrounding atmosphere and the liquid droplet. A part of this heat will be used to heat the fuel droplet up to a temperature approaching its proper boiling point, while the other part of the heat will be used for evaporation of the liquid into vapour. The concentration of the fuel vapour will be maximum at the droplet surface and will decrease towards the surroundings of the fuel droplet. A concentration gradient will thus occur outwards, causing a fuel mass flux away from the droplet (See Figure 2). At the droplet surface an equilibrium will be established between the vapour and liquid phases. This equilibrium can be described by a vapour pressure relation, such as Raoult's law and the Clausius-Clapeyron equation. Through the evaporation process, a change in droplet size will take place.

For a droplet of a mixture of several components, the vapour phase composition and

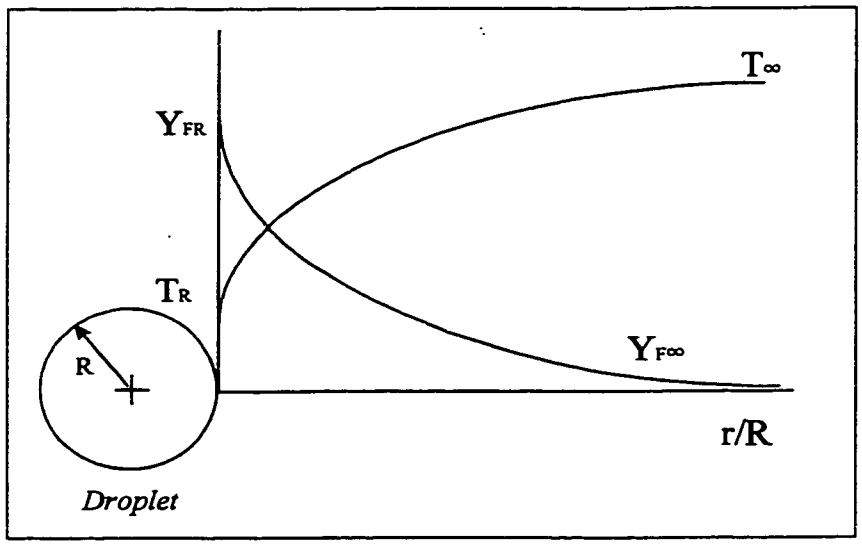

Figure 1.2: Vapour mole fraction and temperature profiles in gas phase through droplet evaporation.

evaporation rate depend on the liquid composition at the surface, which in turn is controlled by mixing within the droplet. The effect of mixing in the liquid-phase of the fuel droplet will be the interest of this research which will simulate different models of internal mixing by using an effective liquid-phase diffusivity. The state of mixing inside the liquid droplet can be described by two main limiting models:

- The well-mixed model: This model assumes complete mixing inside the liquid droplet, which will be enough to cause the temperature and composition inside the liquid droplet to be uniform.
- The diffusion limited model: This model assumes no motion inside the liquid droplet, so that the transport within the droplet occurs by molecular diffusion alone.

Some work has been done on the effect of liquid phase processes on the evaporation process, although many researchers assume a uniform temperature and composition of the liquid phase. Most work on mixture droplets has examined two-component mixtures, but

continuous thermodynamics techniques are now being applied to droplets to allow mixtures more typical of commercial fuels to be modelled. This was first done by Tamim and Hallett (1995), whose model is being extended in this thesis to include the variation of liquid phase composition in space as well as in time.

1.3 Objectives

Multi-component droplet evaporation has been the subject of various theoretical, numerical and experimental investigations due to its importance for the efficient utilization of fuel sprays. Liquid-phase internal mixing is an important factor which affects the evaporation and combustion behaviour of multi-component single droplets. Previous work which applied continuous thermodynamics to droplets used the well-mixed model for describing the liquid-phase internal mixing. Work on the effects of mass diffusion in the liquid-phase has so far been restricted to two-component droplet evaporation.

The main object of this work is therefore to study the effect of liquid-phase internal mixing on the evaporation process of a multi-component droplet using a continuous thermodynamics model for the mixture. Different liquid-phase internal circulation models will be compared with each other and with the quasi-steady model for a multi-component single droplet derived by Hallett (2000).

1.4 Outline of Thesis

To achieve the above, continuous thermodynamics principles will be applied to the liquid-phase transport equations. The liquid-phase internal circulation will be modelled using an effective liquid diffusivity as first suggested by Talley and Yao (1986).

Tamim and Hallett (1995) applied the assumption of the well-mixed liquid droplet which implies uniform liquid phase temperature and composition all over the droplet lifetime. They only included in their model the variation of vapour phase mole fraction in space and time. The numerical model developed is an extension of the multi-component single droplet evaporation model derived by Tamim and Hallett (1995). The following are the main modifications required to model the liquid-phase internal mixing:

- A gamma distribution will be used to describe the liquid-phase mole fraction.
- Liquid-phase transport equations will be derived in continuous form.
- Finite volume techniques will be used to solve the continuous liquid-phase transport relations.
- Correlation equations to describe the liquid-phase transport properties in terms of the distribution characterizing variable will be developed.
- Flux relations at the droplet surface will be derived to include the role of the liquid-phase composition.
- Variable liquid-phase transport properties will be developed.

A further extension to earlier continuous thermodynamics models will also be presented. Commercial fuel mixtures can be composed of different groups of components, each group containing a large number of components. Each group can be a different hydrocarbon family

(e.g. n-paraffins, aromatics, etc.). Dealing with this type of commercial fuel can be facilitated by using a multi-distribution technique in which a separate distribution will be used for each group in the fuel.

The next chapter will present a detailed literature survey done on droplet evaporation fundamentals, multi-component droplet evaporation and fundamentals of the continuous thermodynamics technique. A mathematical model development of multi-component droplet evaporation using the diffusion-limited model to describe liquid mixing in the droplet based on principles of continuous thermodynamics will be presented in Chapter 3. The numerical methods chosen to solve the problem are presented in Chapter 4. Results and discussion follows in Chapter 5. Chapter 6 will describe the modelling of multi-component droplet evaporation using multiple distributions followed by results and discussion. General conclusions and recommendations for further work will be presented in Chapter 7.

CHAPTER 2: LITERATURE SURVEY

2.1 Introduction

The current development in the field of diesel engines highlights the importance of liquid fuel droplet evaporation and combustion. The evaporation of fuel droplets is of considerable importance because it is the first step of combustion. Liquid-phase internal circulation plays an important role in droplet evaporation. This chapter will review previous studies performed in the fields of droplet evaporation, multi-component droplet evaporation (including internal mixing) and continuous thermodynamics.

2.2 Droplet Evaporation

The theory of fuel droplet vaporization has been intensively developed during the past several decades. The classical droplet vaporization model explained in many text books (e.g. Hallett (1997), Spalding (1979) and Kanury (1975)) deals with an isolated pure component single droplet suddenly exposed to a hot environment at low pressure. Since the droplet temperature is lower than the surrounding atmosphere temperature a net driving force due to temperature difference will transfer heat into the droplet, which will be used to supply energy for vaporization as well as for heating the liquid. In the early part of the droplet life time, most of the energy will go into heating the droplet until it reaches a steady-state

temperature, at which time all the energy supplied will be used for liquid vaporization. As the droplet heats up, the vapour concentration will start to build up at the liquid-vapour interface where equilibrium between the liquid and vapour exists; this will be a function of interface temperature and the total atmospheric pressure. The vapour will start to diffuse into the surrounding air, resulting a net mass flux outward from the droplet. Air does not dissolve in the droplet except at high pressures. At low pressures, near atmospheric pressure as in this research, air absorption by the liquid can be neglected.

The classical theory of droplet vaporization is based on the following main assumptions:

- Spherical symmetry: Real droplets are nearly symmetrical, but the field of vapour concentration and temperature around them becomes distorted by natural and forced convection, which are ignored in the theory.
- Constant gas phase transport properties.
- Constant pressure.
- No chemical reaction.
- Liquid-phase temperature and concentration uniform throughout the droplet but time varying.
- Quasi-steady vapour-phase. It is assumed that at any instant in time the fields of temperature and concentration of the vapour-phase are in a quasi-steady state, so that the transient terms ($\partial/\partial t$) can be dropped from the governing equations. As the droplet temperature and radius change during the evaporation process, the vapour field is assumed to adjust to a new steady-state almost instantaneously. This

assumption is based on the fact that vapour density is much less than liquid density and the vapour velocity is much higher than the droplet surface regression rate.

These assumptions lead to a simple solution for evaporation rate and heat transfer, such that the model becomes a steady, one dimensional flow governed by ordinary differential equations. The quasi-steady vapour-phase assumption has been used widely for spray combustion modelling as in Sirignano and Law (1978) and Abramzon and Sirignano (1989).

For a pure fuel with a constant liquid temperature, the theory shows that the square of the droplet diameter varies linearly with time (Wood, Wise and Inami, 1960), the so-called d^2-law.

Temperature gradients in the liquid-phase tend to be reduced by internal circulation within the droplet. El-Wakil and co-workers (1956) performed experiments on single component droplets which showed that enough internal circulation exists even in a stationary droplet to cause mixing of the fluid.

Sirignano and Law (1978) studied the effect of non-uniform liquid-phase temperatures on a single component fuel droplet by considering that internal motion does not exist and diffusion is the only heat transport mechanism. They compared this case with that of a uniform liquid-phase temperature (complete mixing model) and they concluded that the droplet size variations and consequently the droplet vaporization time can be predicted with

good accuracy regardless of the model of internal heat transfer.

For more detailed models, in which some or all of the assumptions of the quasi-steady theory are related, numerical solutions are required (for example, the transient behaviour in the vapour phase was studied for single component droplets by Faeth and Olson (1968) and Bergeron and Hallett (1989a)). Faeth and Olson (1968) also examined the role of variable and constant property assumptions. A comparison of predicted temperature profiles for two different vapour concentrations at the droplet surface shows that the constant property assumption can produce a very large error in predicted temperatures, and based on that they used variable properties throughout their work. A detailed numerical solution was used by Hubbard et al. (1975) to study the effect of vapour phase property variations; they concluded that if the gas phase transport properties were assumed to be constant, they should be evaluated at a properly defined reference temperature and vapour molar fraction.

2.3 Multi-Component Droplets

Commercial fuels are multi-component mixtures of many different hydrocarbons that have a boiling point range of about 65°C - 500°C. Also, other alternative fuels can be a mixture of alcohol and hydrocarbons, coal/oil or water/oil. Previous experimental and theoretical results all indicate that the evaporation and combustion characteristics of multi-component droplets may differ both quantitatively and qualitatively from those of single component droplets (Law, Prakash and Sirignano, 1976). Modelling of multi-component droplet

evaporation has two complexities absent in similar analysis for the single component droplet:

- The phase change process at the multi-component fuel surface, and the transport of the fuel-vapour mixture in the vapour-phase need to be properly described.
- The evaporation process is inherently time-varying due to continuous change in the composition and temperature of the droplet as vaporization proceeds; hence, an understanding of the heat and mass transport processes within the droplet is required (Law, 1976).

Several studies of two-component droplet evaporation, combustion and/or ignition were based on the quasi-steady vapour phase assumption as in the classical droplet evaporation theory for simplifying the droplet model. Examples of studies based on this assumption are Wood, Wise and Inami (1960), Faeth (1970), Law (1976), Law, Prakash and Sirignano (1976), Law and Law (1981), Tong and Sirignano (1984), Talley and Yao (1984), Shaw and Williams (1990) and Kneer et al. (1993a & b).

Introducing transient effects in the vapour-phase of multi-component droplet evaporation improves the accuracy of multi-component droplet evaporation models. Transient effects in the vapour-phase were investigated in different studies performed by Newbold and Amundson (1973), Law (1976), Aggarwal (1987), Bergeron and Hallett (1989b), Hallett and Ricard (1992) and Mawid and Aggarwal (1991).

The assumption of constant vapour-phase transport properties was applied also for two-component droplets as well as for single component droplets. Faeth (1970) and Law and Law (1981) used constant vapour-phase transport properties calculated at reference temperature and concentration values. Aggarwal (1987), Kneer et al. (1993a & b) used variable vapour-phase transport properties through their models. They found a remarkable deviation when they compared results from constant property calculations with those employing variable properties. These deviations depends on the selection of the reference values for the constant properties.

Most of the previous work was done or applied for two-component fuel droplets with two exceptions. Newbold and Amundson (1973) developed a quasi-steady model with a well-mixed droplet to solve the vaporization problem for a three-component mixture. Hallett and Ricard (1992) applied a well-mixed model to ignition of a seven-component fuel droplet.

The major factors that should be considered when trying to understand multi-component fuel droplet behaviour are:

- The relative concentrations and volatilities of the liquid components.
- The miscibility of the liquid constituents, which controls the phase change characteristics.
- The intensity of liquid mixing and motion, which controls the rate at which the components are exposed to the surface of the droplet (Law, 1982).

Based on the fact that the liquid fuel can only vaporize once it is exposed to the surface, this makes the intensity of the mixing and internal motion in the liquid phase of the multi-component droplet an important subject. Two different limiting cases for the transport of the heat and mass within the liquid phase can be identified:

- Well-Mixed Model.
- Diffusion-Limited Model.

2.3.1 Well-Mixed Model:

This model is relevant for low viscosity mixtures where the internal circulation is fast enough that the droplet temperature and composition are maintained nearly spatially uniform, yet still temporally varying. The vaporization of the droplet is controlled by the relative volatilities of the components: the more volatile components are continuously brought to the surface where they are preferentially vaporized, so that the droplet becomes gradually more concentrated in the less volatile components. This makes the vaporization process equivalent to a batch distillation. The liquid motion can be caused either by the buoyant motion of air and vapour around the droplet or as a result of the droplet velocity acquired at injection (Sirignano and Law, 1978, Law, Prakash and Sirignano, 1976, Law, 1976 and Law, 1982).

Many studies have been performed on multi-component droplet evaporation using the assumption of a well-mixed liquid. El-Wakil et al. (1956) had proved experimentally the existence of internal circulation within a binary droplet. Wood, Wise and Inami (1960) assumed the existence of uniform composition within the liquid at every instant. They found

that the composition of the liquid-phase was changing in a manner which can be described as a batch distillation. Law (1976) applied the assumption of uniform temperature and composition within the droplet to his own theoretical model. Sample solutions indicated that the components vaporize approximately sequentially in the order of their relative volatilities, and that the vaporization rate is insensitive to the mixture composition during combustion as well as during evaporation in a hot environment. The liquid temperature rises steadily as distillation proceeds. Law, Prakash and Sirignano (1976) assumed a uniform temperature within the droplet. They found that the intensity of internal circulation increases as liquid viscosity is reduced. Hallett and Ricard (1992) and Tamim and Hallett (1995) also assumed a well-mixed model to describe liquid-phase internal mixing in their studies.

2.3.2 Diffusion-Limited Model:

This model is relevant to a very viscous fluid mixture in which internal motion does not exist, such that transport within the droplet occurs by molecular diffusion alone. The liquid-phase mass diffusion is extremely slow compared with droplet surface regression rates. The concentration changes very steeply in a thin surface layer, while the interior core of the droplet remains at the initial composition until approached by the receding surface. Because of this, the relative volatility of the components has less effect on the vaporization. Also, the liquid phase temperature and composition are not uniform (Sirignano and Law, 1976, Law, 1976, Law, Prakash and Sirignano, 1976, Landis and Mills, 1974, Law, 1982, Tamim and Hallett, 1995 and Hallett, 2000).

Several studies have used the diffusion-limited model to describe liquid-phase internal mixing for multi-component droplets. Landis and Mills (1974) studied the effect of liquid-phase mass diffusional resistance on the evaporation of a two-component droplet. Their results showed that the internal concentrations approach an almost constant profile shortly after an initial transient period and this behaviour persists until the droplet has almost completely disappeared. It was therefore concluded that liquid-phase mass diffusion is extremely slow and controls the surface composition.

Tong and Sirignano (1984) examined the transient diffusional model for liquid internal mixing for vaporization of a two-component droplet in a hot convective environment. From their results, they recommended the transient diffusion model in the liquid-phase for the stagnant situation where there is no relative gas motion.

Mawid and Aggarwal (1991), Kneer et al. (1993a & b) and Shaw and Williams (1990) studied liquid-phase mass fraction profiles through the evaporation process of a binary fuel droplet. Shaw and Williams (1990) assumed a uniform temperature inside the liquid-phase and a transient diffusional liquid-phase concentration. They showed that at the surface of the droplet a boundary layer arises in which the mass fraction of the low volatility component increases with time.

Sirignano and Law (1978) and Aggarwal (1987) studied both limiting cases of internal mixing in binary droplet: the well-mixed model and the diffusion-limited model. They noticed considerable differences between results when using the diffusion-limited model and the well-mixed model.

Law and Law (1981) applied the diffusion-limited model for modelling mixing in the liquid

phase and they concluded that the extremely slow rate of liquid-phase mass diffusion causes the droplet concentration distribution to attain an almost constant state during much of the droplet life time. Hence, they argue that the quasi-steady assumption can be applied to the liquid-phase in order to simplify the multi-component droplet evaporation modelling. The vapour phase mass and thermal diffusivities, which are of the order of 10^{-1} cm^2/sec, are much higher than the liquid phase thermal and mass diffusivities, which are of the order of 10^{-3} to 10^{-5} cm^2/sec. This permitted the derivation of an analytical solution for the liquid phase.

On the other hand, Wang, Liu and Law (1984) and Law (1986) applied the diffusion-limited model of the liquid phase internal mixing for binary droplets and came to the conclusion that the importance of the diffusion-limited model to describe the liquid-phase internal mixing increases for immiscible fuel mixtures and is of moderate importance for miscible fuel mixtures. The vaporization mechanism of a miscible fuel mixture is intermediate between those of the well-mixed model and the diffusion-limited model. Law (1986) emphasized that the importance of the diffusion-limited model to describe liquid phase internal mixing is further increased with increasing volatility differentials between mixture constituent.

2.3.3 Droplet with Internal Circulation:

Mixing in most real droplets occurs by molecular diffusion and internal circulation. Talley and Yao (1984) studied both mixing models, the well-mixed model and the diffusion-limited model. They noticed that the liquid phase heat and mass transfer with internal circulation is intermediate between these limiting cases. Talley and Yao (1986) have suggested a simple

model to describe mixing in a real droplet with internal circulation which uses an enhanced liquid diffusion in the radial direction, represented by multiplying the molecular diffusivity D_L by a factor χ. Law, Prakash and Sirignano (1976), Sirignano and Law (1978), Abramzon and Sirignano (1989), Haywood, Nafziger and Renksizbulut (1989) and Shaw and Williams (1990) calculated the flow field of the internal motion in a liquid droplet generated by an external gas stream flow by assuming that the viscous effects in both the gas and liquid phases are confined to thin boundary layers across the interface. They found out that a reduction in liquid and vapour density and viscosity ratios produces a significant change in the interfacial velocity profile: the liquid phase becomes more fluid, hence resulting in a higher interfacial velocity and much thinner liquid boundary layer and consequently a reduction in the evaporation rate.

2.4 Continuous Thermodynamics

Many of the fluid mixtures in nature and in the chemical industry are composed of large numbers of components. Examples of such complex mixtures are higher petroleum fractions, coal-derived liquids, polydisperse polymers, and mixtures of fatty acids or esters in vegetable oils. These mixtures can be part of any chemical or industrial process. Engineering calculations of systems involving these mixtures will depend upon determining the concentration or mole fraction of each component. Since the mixtures consist of a large number of components this means that a solution of hundreds of material balances would have to be performed, which leads to a very complicated solution. In the past the "pseudo-

components method" was used for such mixtures, and it was based on representing each group of components of similar properties by one "pseudo-component". Hence, instead of dealing with hundreds of components, the number of components can be reduced significantly.

The pseudo-component method is convenient, but its main disadvantage is that the selection of pseudo-components is arbitrary and the results are sensitive to the selection. An alternative approach is to describe the fluid mixture by a continuous distribution function instead of discrete components. This frame work is called "Continuous Thermodynamics", which is shorter but equivalent to the more descriptive term "Thermodynamics of Continuous Mixtures". This concept was introduced more than sixty years ago. Katz and Brown (1933) presented a method for calculating the vapour pressure of petroleum fractions, in which the complex mixture composition was expressed in terms of true boiling point obtained from an efficient distillation column. They assumed that the properties of the mixture vary continuously throughout the range of composition, so that properties of a fraction at any point on the true boiling point curve were given by those of corresponding pure hydrocarbon. This is considered to be the first paper on Continuous Thermodynamics.

The main principle of "Continuous Thermodynamics" is to describe the fluid mixture with a continuous distribution function f(I), where I is the characterizing variable for the mixture, which can be any convenient physical property, such as molecular weight, carbon number, boiling point temperature, or others. Therefore, only the distribution parameters (i.e., mean, variance) are required for characterization of a multi-component fluid mixture.

Advances in Continuous Thermodynamics were discussed through the literature in three

areas:

- Characterization and presentation of composition in a many-component mixture;
- Development and application of molecular thermodynamic models for continuous mixtures; and,
- Implementation of efficient numerical techniques for solving material-balance and phase-equilibrium equations.

Earlier works established the basic principles of continuous thermodynamics by converting thermodynamic relations into continuous distribution function form (Kehlen and Rätzsch, 1980, Gualtieri, Kincaid and Marrison, 1982 and Briano and Glandt, 1983). Continuous Thermodynamics was shown to be computationally simpler yet more accurate than the traditional Pseudo-component method (Cotterman and Prausnitz, 1985, Willman and Teja, 1986 and Peng, Wu and Batycky, 1987).

The principles of Continuous Thermodynamics have been applied in many fields:

- Phase-equilibria calculations using an equation of state for petroleum mixtures (Gualtieri, Kincaid and Marrison, 1982, Briano and Glandt, 1983, Peng, Wu and Batycky, 1987, and Angelos and Ewing, 1988).
- Flash calculations for petroleum mixtures (Cotterman and Prausnitz, 1985 & 1990, Kehlen and Rätzsch, 1983, and Rätzsch, Kehlen and Schumann, 1988).
- Simulation of gas-condensate systems (Du and Mansoori, 1986)
- Application to multi-stage absorption and distillation (Chou and Prausnitz, 1986, and Kehlen and Rätzsch, 1987).
- Dew point calculations for natural gas mixtures (Cotterman, Bender and Prausnitz,

1985, and Willman and Teja, 1986, 1987).

- Solvent loss in a high pressure absorber to recover intermediate hydrocarbons from natural gas (Cotterman, Bender and Prausnitz, 1985).
- Liquid-Liquid phase equilibria for polymer fractions (Cotterman, Bender and Prausnitz, 1985).

Solving problems using the continuous thermodynamics technique requires special attention to the following:

- Selection of a proper and representative distribution function;
- Selection of the proper characterizing variable;
- Selection of the proper phase-equilibrium relation, if necessary.

To describe the composition of the continuous mixture, a suitable function f(I) must be selected to represent the distribution of concentration over I. If f gives the distribution of the number of moles, f is a molar probability density function; for a weight distribution, f is a mass probability density function. The choice of f is determined primarily by its ability to represent reality to a sufficient degree of approximation. However, another consideration in the choice of f is mathematical convenience: some functions are more suitable than others for solving certain mathematical equations (Cotterman, Bender and Prausnitz, 1985). Different distribution functions were used throughout the literature. The Gaussian distribution function was used by Kehlen and Rätzsch (1980, 1983, 1985, 1988, 1989). Others such as Cotterman and Prausnitz (1985), Chou and Prausnitz (1986), Peng, Wu and Batycky (1987), Willman and Teja (1987), Behrens and Sandler (1988), Tamim and Hallett

(1995), Lippert and Reitz (1997) , Hallett (1998) and Hallett (2000) used the gamma distribution function. Willman and Teja (1986) have used a log-normal distribution function, while Peng, Wu and Batycky (1987) used a beta distribution density function.

The choice of the characterizing variable of the distribution function is as important as the selection of the distribution function. The characterizing variable can be any convenient physical or chemical property. Different characterizing variables were used such as:

- Component molecular weight (Cotterman and Prausnitz, 1985, Du and Mansoori, 1986, Peng, Wu and Batycky, 1987, Tamim and Hallett, 1995, Lippert and Reitz, 1997, Hallett, 1998 and Hallett, 2000).
- Component carbon number (Behrens and Sandler, 1988, Willman and Teja, 1987 and Browarzik, Kowalewski and Kehlen, 1998).
- Component boiling point temperature (Kehlen and Rätzsch, 1984).
- Willman and Teja (1986) used a two-variable distribution, with boiling point temperature and specific gravity as characterizing variables.

Vapour-liquid equilibrium for mixtures was one of the most important applications of continuous thermodynamics. Different approaches were discussed in the literature to describe the phase equilibrium relation. Kehlen and Rätzsch (1980, 1983, 1985, 1988, 1989) used the assumption of ideal solution behaviour in all the systems they studied, applying Raoult's law to describe vapour-liquid equilibrium for the mixture, and using the Clausius-Clapeyron equation and Trouton's rule to express the component vapour pressures in terms of the

distribution variable. This gives simple relationships between the distribution parameters in the vapour and liquid phases. Cotterman and Prausnitz (1985) also used Raoult's law and the Clausius-Clapeyron equation.

Several authors have used an equation of state to describe vapour-liquid equilibrium for continuous mixtures. Different equations of state used were:

- Van der Waals equation of state (Gualtieri, Kincaid and Marrison, 1982)
- Soave-Redlich-Kwong equation of state (Chou and Prausnitz, 1986, Browarzik, Kowalewski and Kehlen, 1998, Cotterman, Bender and Prausnitz, 1985, Cotterman and Prausnitz, 1985).
- Peng-Robinson equation of state (Du and Mansoori, 1986, Peng, Wu and Batycky, 1987, Behrens and Sandler, 1988, Angelos and Ewing, 1988).
- Patel-Teja equation of state (Willman and Teja, 1986)
- Virial equation of state (Willman and Teja, 1987)

Most of the applications of continuous thermodynamics so far have been directed to fields in which the transport processes (diffusion and convection) are not important. However, continuous thermodynamics has great potential for modelling the transport processes of complex fluid mixtures in the combustion field, particularly in the evaporation of multi-component fuel droplets. Tamim and Hallett (1995) first developed a model for evaporation of a multi-component fuel droplet using the continuous thermodynamics technique. Lippert and Reitz (1997) applied this model to a complete model for the evaporation of a fuel spray in a Diesel engine cylinder. Hallett (1998) modelled the ignition of multi-component single

droplet exposed to hot environment at atmospheric pressure using continuous thermodynamics technique. Also, Hallett (2000) derived a simplified version of the Tamim and Hallett (1995) model for quasi-steady multi-component droplet evaporation using continuous thermodynamics. These efforts have provided the first realistic models of commercial liquid fuels in combustion.

2.5 Conclusions

The main conclusions that can be drawn from reviewing the literature survey are:

- The continuous thermodynamics technique has proved to be a successful and computationally efficient technique to deal with fuel mixtures with a large number of components.
- The assumption of uniform temperature inside the liquid droplet is reasonable.
- Liquid phase internal mixing plays an important role in multi-component droplet evaporation.
- The effect of liquid-phase internal circulation was studied only for two-component droplets, while there was no study to deal with this matter for multi-component droplets.
- A simplified model derived by Law and Law (1981) uses the quasi-steady model for both vapour and liquid phases, leading to an analytical solution. This can facilitate the work and be used instead of our model if it proves to be correct.

- The use of variable transport properties in vapour and liquid phases can improve the accuracy of the results significantly.

The main goal of this study is to model the liquid-phase with the diffusion-limited model using the continuous thermodynamics technique. The classical relations describing the liquid-phase will be converted into the continuous form in terms of the distribution variable. All liquid-phase relations will be solved with the vapour-phase relations in order to find a complete solution that considers transient effects in both the vapour and liquid phase.

CHAPTER 3: MATHEMATICAL MODEL

3.1 Introduction

The purpose of this model is to study the effect of liquid-phase internal mixing on the evaporation process of a multi-component droplet suddenly exposed to a hot environment, using the continuous thermodynamics technique to model the mixture.

Previous work done by Tamim and Hallett (1995) developed a model for multi-component droplet evaporation using continuous thermodynamics. They assumed a well-mixed liquid-phase; hence, the concentration of the liquid-phase was uniform but time varying. Our model will test the validity of this assumption: it will study the diffusion effect of the liquid phase by using an effective diffusivity expression; hence, the liquid-phase concentration will vary in space as well as in time. In this chapter, the following sections will be a detailed description of the present model which includes the liquid-phase main transport relations, a brief review of vapour-phase relations derived by Tamim and Hallett (1995), the flux relations at the droplet surface, the liquid phase energy balance, the distribution function used in this model, vapour-liquid equilibrium relations, a derivation of the liquid phase transport properties, balances on liquid phase distribution parameters, and finally a brief description of the alternative quasi-steady model.

To simplify the model, the following main assumptions were made:

- The droplet temperature is uniform in space but may vary in time.

- No chemical reaction is included in the model (pure evaporation).
- Spherical symmetry of the droplet and surroundings is assumed, so that only radial transport is possible.

These assumptions are standard common assumptions in most modelling work of droplet evaporation.

3.2 Liquid-Phase Transport Relations

As discussed in chapter 2, liquid phase mixing can be described by two limiting models, the diffusion-limited model, or the well-mixed model. Real droplets generally have some degree of internal circulation, and fall part way between these two extremes in their behaviour. Liquid phase mixing has been studied for two-component droplets, and it has been found that the degree of liquid phase mixing has little effect on evaporation if the mixture has two components with closely spaced boiling points, which makes the assumption of a well-mixed model valid in this case. A significant effect of liquid phase mixing can be noticed, on the other hand, for two components with very different boiling points, and as a result the diffusion effects become important (Randolph, Makino and Law, 1986). For droplets with widely differing boiling points, "micro-explosion" can occur, in which bubbles of the most volatile component expand and burst in the droplet. Tamim and Hallett (1995) developed a model for multi-component droplet evaporation using the assumption of a well-mixed liquid phase. The present model will be based on the Tamim and Hallett (1995) model except that the liquid phase will not be well-mixed, and diffusion in the liquid will be included. This will

be achieved by the derivation of the following equations:

- Liquid phase continuity and diffusion equations.
- Flux relations at the droplet surface including the effect of the liquid phase composition.
- Vapour-liquid equilibrium relations at the droplet surface.
- Liquid-phase transport properties.

All these equations will be developed in continuous thermodynamics form.

Real droplet behaviour is something in between these two limiting models. Talley and Yao (1986) developed a more accurate model which included liquid phase internal motion based on a recirculating vortex flow, and compared it to a model with radial diffusion alone. They found that mixing in a real liquid droplet can be approximated as equivalent to enhanced diffusion in the radial direction, represented by multiplying the molecular diffusivity D_L by a factor χ. Changing the mixing factor value from one to a very large number will allow different liquid motion models to be run: ($\chi = 1$) gives the diffusion-limited model, (χ = large) approximates a well-mixed model and moderate values (i.e. $\chi = 10$) approximate real droplet behaviour with some internal flow.

3.2.1 Liquid phase Basic Equations

The physical transport equations governing the present problem are those of diffusion and continuity for the liquid phase of the droplet. These are written here in vector form for generality.

Continuity equation

The continuity equation describes the liquid flow velocity field and is formulated as follows for the mixture:

$$\frac{\partial c_L}{\partial t} + \nabla \cdot c_L v_L^* = 0 \qquad (3.2\text{-}1)$$

where c_L is the liquid molar density (kmol/m^3) and v_L^* is the liquid molar average velocity (m/s). Although no bulk fluid motion was assumed, v_L^* can still be non-zero as a result of changes in c_L. It is assumed that there is no reaction, otherwise the right hand side would be non-zero. Molar densities and mole fractions are used throughout instead of mass units to avoid the need to convert from mass to mole fraction and back again when dealing with phase equilibrium at the droplet surface.

Diffusion equation

The diffusion equation describes the concentration of species i of liquid fuel as a function of position and time and is formulated as follows for a single discrete component i

$$\frac{\partial (c_L x_i)}{\partial t} + \nabla \cdot \left(c_L v_L^* x_i \right) = \nabla \cdot \left(c_L \chi D_{Lim} \nabla x_i \right) \qquad (3.2\text{-}2)$$

where c_L is the liquid molar density (kmol/m^3), x_i is the mole fraction of i in the liquid phase, χ is the mixing factor (following Talley and Yao, 1986) and D_{Lim} is the molecular diffusivity of component i in the liquid mixture (m^2/s). Since in a complex mixture the concentration

of any individual fuel component will be small because of the large number of components, it has been assumed that multi-component diffusion can be approximated by Fick's law.

Energy Equation

The liquid droplet temperature was assumed uniform in space and only changes with time as per the value of the temperature at the droplet surface. This means that the temperature gradients inside the droplet are zero. This assumption was based on experiments of El-Wakil and co-workers (1956) which showed that the temperature gradients in the liquid droplet tend to be reduced by internal circulation of the fluid. Also, assuming uniform temperature in the liquid phase will isolate the dependence of the evaporation rate on changes in the droplet composition from those on the transient heating or cooling processes, which will help to focus only on the mass diffusion effects in the liquid phase.

3.2.2 Species Transport Equations in Continuous Form

The main task in developing a continuous thermodynamics model of this process is to convert the equations in the previous section to continuous thermodynamics form. Two continuous thermodynamics equations equivalent to the system equations given in section (3.2.1) were developed based on the following:

First, a distribution function has to be chosen with a suitable characterizing variable. Then, the governing equations are written and derived in terms of this distribution. For the liquid phase, a single variable distribution function $f_L(I)$ was chosen to represent the molar concentration of species of a continuous mixture. The mole fraction of a species i is then

given by

$$x_i = x_F f_L(I)_i \Delta I_i \tag{3.2-3}$$

where ΔI_i is the interval in I centred about the value of I corresponding to species i and x_F is the overall concentration of fuel in the liquid. The distribution variable I can be any variable of concern; for this research, I was selected to be the molecular weight. The distribution has the property that

$$\int_0^\infty f_L(I)dI = 1 \tag{3.2-4}$$

The distribution is characterized by its mean θ_L and second central moment ψ_L defined as

$$\theta_L = \int_0^\infty f_L(I) I dI \tag{3.2-5}$$

$$\Psi_L = \int_0^\infty f_L(I) I^2 dI = \theta_L^2 + \sigma_L^2 \tag{3.2-6}$$

where σ_L^2 is the variance of the liquid distribution function. A transport equation can also be derived for σ_L^2 instead of ψ by using $(I-\theta_L)^2$ as a weighting function rather than I^2, but since θ_L itself varies in space and time, the resulting equations would be much more complex than those for ψ_L, because the variation of θ_L would have to be accounted for when integrating.

The liquid fuel in droplet is present with overall mol fraction x_F (F= "fuel"), the remainder being air (A) so that

$$x_A = 1 - x_F \tag{3.2-7}$$

At high pressure some air can be dissolved in the liquid phase, but at low and moderate pressure, the amount of air dissolved in the liquid phase can be ignored to simplify the numerical solution. So, the total molar concentration of the liquid fuel can be considered to be equal to one.

$$x_F = 1, \qquad x_A = 0 \tag{3.2-8}$$

Although $x_F = 1$ for all calculations in this work, the equations are derived for $x_F \leq 1$ for generality. Diffusion in the mixture is described by deriving transport equations for the distribution function. Substituting the component mol fraction x_i above in eq.(3.2-2) gives

$$\frac{\partial}{\partial t}\left(c_L x_F f_L(I)_i \Delta I_i\right) + \nabla \cdot \left(c_L v_L^* x_F f_L(I)_i \Delta I_i\right) =$$

$$\nabla \cdot \left(c_L \chi D_{Lm}(I) \nabla \left(x_F f_L(I)_i \Delta I_i\right)\right) \tag{3.2-9}$$

Note that the diffusivity has now become $D_{Lm}(I)$, and that it has been allowed to vary, reflecting the fact that species diffusivity depends on molecular mass and other properties. Allowing the interval ΔI_i to become infinitesimally small, and integrating over I from 0 to ∞ yields:

- First term of the left hand side of equation (3.2-9):

$$\int_0^\infty \frac{\partial}{\partial t}\left(c_L x_F f_L(I)dI\right) = \frac{\partial}{\partial t}\left(c_L x_F\right) \tag{3.2-10}$$

- Second term of the left hand side of equation (3.2-9):

$$\int_0^\infty \nabla.\left(r^2 c_L v_L^* x_F f_L(I)dI\right) = \nabla.\left(r^2 c_L v_L^* x_F\right) \tag{3.2-11}$$

- Right hand side term of equation (3.2-9):

$$\int_0^\infty \nabla.\left[r^2 c_L \chi D_{Lm}(I)\nabla\left(x_F f_L(I)dI\right)\right] = \nabla.\left[x_F \nabla\left(c_L \chi \overline{D}_L\right) + \left(c_L \chi \overline{D}_L \nabla x_F\right)\right.$$

$$\left. - x_F \int_0^\infty f_L(I)\frac{\partial}{\partial r}\left(c_L \chi D_{Lm}(I)\right)dI\right] \tag{3.2-12}$$

where an average liquid diffusivity $\overline{D}_L$ is defined by

$$\overline{D}_L = \int_0^\infty D_{Lm}(I) f_L(I).dI \tag{3.2-13}$$

The transport equation, in continuous form, for the vaporizing substance as a whole is then given as:

$$\frac{\partial}{\partial t}\left(c_L x_F\right)+\nabla\cdot\left(c_L v_L^{*} x_F\right)=\nabla\cdot\left[c_L\chi\overline{D}_L\nabla x_F+x_F\nabla\left(c_L\chi\overline{D}_L\right)\right.$$

$$\left.-x_F\int_0^{\infty}f_L(I)\nabla\left(c_L D_{Lm}(I)\right)dI\right] \qquad (3.2\text{-}14)$$

and $D_{Lm}(I)$ is the component diffusivity as a function of I. Weighting equation (3.2-9) by I before integrating in the same way equation (3.2-14) was derived yields a transport equation for the mean θ_L of the distribution (i.e., the mean molecular weight of the liquid fuel):

$$\frac{\partial}{\partial t}\left(c_L x_F\theta_L\right)+\nabla\cdot\left(c_L v_L^{*} x_F\theta_L\right)=\nabla\cdot\left\{c_L\chi\widetilde{D}_L\nabla\left(x_F\theta_L\right)+x_F\theta_L\nabla\left(c_L\chi\widetilde{D}_L\right)\right.$$

$$\left.-x_F\int_0^{\infty}f_L(I)I\nabla\left(c_L D_{Lm}(I)dI\right)\right\} \qquad (3.2\text{-}15)$$

where a second average liquid diffusivity must be defined as

$$\widetilde{D}_L\theta_L=\int_0^{\infty}I.D_{Lm}(I)f_L(I).dI \qquad (3.2\text{-}16)$$

and θ_L is the liquid distribution mean. Finally, weighting equation (3.2-9) by I^2 and integrating in the same manner as previously results in

$$\frac{\partial}{\partial t}\left(c_L x_F \Psi_L\right) + \nabla \cdot \left(c_L \vec{v}_L x_F \Psi_L\right) = \nabla \cdot \left\{c_L \chi \hat{D}_L \nabla\left(x_F \Psi_L\right) + x_F \Psi_L \nabla\left(c_L \chi \hat{D}_L\right)\right.$$

$$\left. - x_F \int_0^\infty f_L(I) I^2 \nabla\left(c_L D_{Lm}(I) dI\right)\right\} \qquad (3.2\text{-}17)$$

where yet another average liquid diffusivity must be defined as

$$\hat{D}_L \Psi_L = \int_0^\infty I^2 . D_{Lm}(I) f_L(I) . dI \qquad (3.2\text{-}18)$$

and ψ_L is the second moment about the origin of the liquid distribution.

Equations (3.2-14), (3.2-15) and (3.2-17) describe the variation of liquid phase composition in space and time by means of the "fuel" mole fraction x_F and the distribution parameters θ_L and ψ_L (or σ_L^2). They are general and allow for transport property variation in space and time.

Boundary Conditions for the Liquid Phase Droplet Problem:

At the droplet surface, the values of x_F, θ_L and ψ_L are considered known; they will be calculated later from liquid-vapour phase equilibrium and flux relations. At the droplet centre (r = 0), symmetry dictates that gradients in the fuel properties are zero, resulting in the following boundary conditions:

- at the droplet surface (r = R): $x_F = x_{FR}$; $\theta_L = \theta_{LR}$; $\psi_L = \psi_{LR}$

(Values of x_{FR}, θ_{LR}, ψ_{LR} will be found later by flux matching at the surface - see section 3.4)

- at the droplet centre (r = 0): $$\frac{\partial x_F}{\partial r} = \frac{\partial (x_F \theta_L)}{\partial r} = \frac{\partial (x_F \Psi_L)}{\partial r} = 0$$

and the initial conditions are:

- at (t = 0): $x_F = x_{Fo}$; $\theta_L = \theta_{Lo}$; $\psi_L = \psi_{Lo}$ for all r values

Simplification of the Transport Equations

To simplify the transport equations in the liquid phase, it can be noted that in each of equation (3.2-14), (3.2-15) and (3.2-17) the last two terms are identical or nearly identical in finite difference approximation, and hence together make very little contribution to the equations. This is shown in detail in Appendix A for the last two terms of equation (3.2-14), and the same simplification procedure applies for equations (3.2-15) and (3.2-17). This reduces the equations to

$$\frac{\partial}{\partial t}(c_L x_F) + \nabla \cdot (c_L v_L^* x_F) = \nabla \cdot (c_L \overline{D}_L \nabla x_F) \qquad (3.2\text{-}19)$$

$$\frac{\partial}{\partial t}(c_L x_F \theta_L) + \nabla \cdot (c_L v_L^* x_F \theta_L) = \nabla \cdot (c_L \chi \tilde{D}_L \nabla (x_F \theta_L)) \qquad (3.2\text{-}20)$$

$$\frac{\partial}{\partial t}(c_L x_F \Psi_L) + \nabla \cdot (c_L v_L^* x_F \Psi_L) = \nabla \cdot (c_L \chi \hat{D}_L \nabla (x_F \Psi_L)) \qquad (3.2\text{-}21)$$

These are the equations to be solved here.

3.3 Brief Review of Vapour phase Transport Relations

For generality, the transport equations were developed in vector form. The basic physical transport equations necessary for solving the droplet vaporization problem in the vapour phase are those of diffusion, continuity and energy. These equations were derived by Tamim and Hallett (1995) with the same procedure that has been used for the derivation of the liquid phase transport equations explained in section 3.2, and are given here for convenience. The vapour phase distribution function is f(I); it has a mean θ, a second moment ψ, and an overall fuel mol fraction y_F.

Continuity equation

The continuity equation describes the vapour flow velocity field and is formulated as follows for the mixture:

$$\frac{\partial c}{\partial t} + \nabla \cdot c\mathbf{v}^* = 0 \tag{3.3-1}$$

Diffusion equation

$$\frac{\partial}{\partial t}\left(cy_F\right) + \nabla \cdot \left(c\mathbf{v}^* y_F\right) = \nabla \cdot \left(c\overline{D}\nabla y_F\right) \tag{3.3-2}$$

The first and second moment transport equations of the vapour distribution are

$$\frac{\partial}{\partial t}\left(cy_F\theta\right) + \nabla \cdot \left(c\mathbf{v}^* y_F\theta\right) = \nabla \cdot \left(c\tilde{D}\nabla\left(y_F\theta\right)\right) \tag{3.3-3}$$

$$\frac{\partial}{\partial t}\left(cy_F\Psi\right)+\nabla\cdot\left(cv^{*}y_F\Psi\right)=\nabla\cdot\left(c\hat{D}\nabla\left(y_F\Psi\right)\right) \qquad (3.3\text{-}4)$$

Energy equation

$$\overline{C_P}\frac{\partial(cT)}{\partial t}+\overline{C_P}\nabla\cdot\left(cv^{*}T\right)=\nabla\cdot\lambda\nabla T+\left[\left(a_C-C_{PA}\right)c\overline{D}\nabla y_F+b_C\theta c\widetilde{D}\nabla y_F\right]\cdot\nabla T \qquad (3.3\text{-}5)$$

where a_C, b_C are constants in a fuel species specific heat equation of the form:

$$C_P=a_C+b_CI \qquad (3.3\text{-}6)$$

For any clarifications or details, please refer to Tamim and Hallett (1995).

3.4 Flux Relations at the Droplet Surface

Liquid and vapour phases are coupled by molar and heat fluxes at the liquid surface. The variation in droplet temperature and composition as the droplet heats and vaporizes have a great effect on the molar and heat fluxes in the vapour phase and hence on the droplet lifetime. The assumption of the diffusion-limited model for the liquid phase means that the composition of the liquid phase changes in time and space. A mole balance on the droplet gives the total molar flux N from the droplet surface as

$$N = -\frac{1}{A}\frac{d(\bar{c}_L V)}{dt} \tag{3.4-1}$$

where A and V are the droplet surface area and volume respectively and $\bar{c}_L$ is the mean molar density of the whole droplet. Equation (3.4-1) can be solved for the rate of recession of the surface to yield

$$\frac{dR}{dt} = -\frac{1}{\bar{c}_L}\left[\frac{R}{3}\frac{d\bar{c}_L}{dt} + N\right] \tag{3.4-2}$$

N is obtained from matching component fluxes at the surface for both vapour and liquid phase. For a single discrete component i, the molar flux at the surface can be described for the liquid phase by the sum of convection and diffusion to the surface as

$$N_i = Nx_{iR} - c_L D_{Lim}\left.\frac{\partial x_i}{\partial r}\right|_R \tag{3.4-3}$$

The same flux at the surface can be described for the vapour phase as

$$N_i = Ny_{iR} - cD_{im}\left.\frac{\partial y_i}{\partial r}\right|_R \tag{3.4-4}$$

Equating equations (3.4-3) and (3.4-4) gives

$$N\left(x_i - y_i\right)_R = c_L D_{Lim}\left.\frac{\partial x_i}{\partial r}\right|_R - cD_{im}\left.\frac{\partial y_i}{\partial r}\right|_R \tag{3.4-5}$$

Introducing the distribution functions into equation (3.4-5) and integrating gives an equation for the total flux N:

$$N\left(x_{FR} - y_{FR}\right) = c_L\overline{D}_L\left.\frac{\partial x_F}{\partial r}\right|_R - c\overline{D}\left.\frac{\partial y_F}{\partial r}\right|_R + x_F\frac{\partial}{\partial r}\left(c_L\overline{D}_L\right) - y_F\frac{\partial}{\partial r}\left(c\overline{D}\right)$$

$$+\left[y_F\int_0^\infty f(I)\frac{\partial\left(cD(I)\right)}{\partial r}dI\right]_R - \left[x_F\int_0^\infty f_L(I)\frac{\partial\left(c_L D_L(I)\right)}{\partial r}dI\right]_R \tag{3.4-6}$$

The last four terms of equations (3.4-6), like the analogous terms in (3.2-14), can shown to be equal in finite difference form and can be neglected. As a further simplification $x_{FR} = 1.0$ will be substituted into these equations:

$$N\left(1 - y_{FR}\right) = -c\overline{D}\left.\frac{\partial y_F}{\partial r}\right|_R \tag{3.4-7}$$

Weighting equation (3.4-5) by I and I^2 respectively, integrating and simplifying in the same way yields equations for the liquid phase distribution parameters:

$$N\theta_{LR} - c_L \tilde{D}_L \frac{\partial \theta_L}{\partial r}\bigg|_R = N y_{FR} \theta_R - c\tilde{D} \frac{\partial (y_F \theta)}{\partial r}\bigg|_R \tag{3.4-8}$$

$$N\Psi_{LR} - c_L \hat{D}_L \frac{\partial \Psi_L}{\partial r}\bigg|_R = N y_{FR} \Psi_R - c\hat{D} \frac{\partial (y_F \Psi)}{\partial r}\bigg|_R \tag{3.4-9}$$

These equations, together with vapour-liquid equilibrium, tie together the solutions for the liquid and vapour phase. The liquid density is calculated from the liquid mass density ρ_L

$$c_L = \rho_L / \theta_L \tag{3.4-10}$$

As the mass densities of members of homologous groups of hydrocarbons show little variation within the group, ρ_L was assumed constant.

3.5 Distribution Function

The distribution function can be any function which is able to describe the fluid mixture over the desired domain. Different distribution functions were used in the literature, such as the gamma distribution, Gaussian distribution and beta distribution. The gamma distribution function was the most popular distribution especially for petroleum fractions, for which it was found to best describe the composition of the mixtures considered (Cotterman et al., 1985, and Willman and Teja, 1987). Tamim and Hallett (1995) used the gamma distribution function to describe both the vapour and liquid phases. Based on that, the gamma distribution function was selected to describe both the vapour and the liquid phases since the two phases are in equilibrium (Cotterman and Prausnitz, 1985). The gamma distribution describing the liquid phase is

$$f_L(I) = \frac{(I-\gamma)^{\alpha_L - 1}}{\beta_L{}^{\alpha_L}\Gamma(\alpha_L)} \exp\left[-\left(\frac{I-\gamma}{\beta_L}\right)\right] \qquad (3.5\text{-}1)$$

where α_L and β_L are the distribution parameters in the liquid phase, $I = \gamma$ is the origin, and $\Gamma(\alpha_L)$ is the gamma function. The mean and the variance are

$$\theta_L = \alpha_L \beta_L + \gamma \qquad (3.5\text{-}2)$$

$$\sigma_L^2 = \alpha_L \beta_L^2 \qquad (3.5\text{-}3)$$

For the vapour phase, the gamma distribution function was also used, but with different values of parameters. The origin γ is assumed to be the same in both phases, reflecting the idea that the lowest molecular mass component will be present in both phases.

3.6 Vapour Liquid Equilibrium

Vapour-liquid equilibrium calculations for continuous mixtures were discussed in most of the literature in terms of Gibbs free energy, fugacity, activity coefficient, chemical potential, etc. Some of the literature used an equation of state to describe the vapour-liquid equilibrium in continuous mixtures, in particular the Soave-Redlich-Kwong equation (Chou and Prausnitz, 1986). Others assumed ideal behaviour of the mixture and applied Raoult's law and the Clausius-Clapeyron equation to find the vapour pressure with good results (Rätzsch, Kehlen et al., 1980, 1983, 1985, 1988 and 1989, and Cotterman and Prausnitz, 1985). Raoult's law and the Clausius-Clapeyron equation were used by Tamim and Hallett (1995) and will be also chosen to be used in this work to describe the vapour-liquid equilibrium at the surface. It is a reasonable approximation for a mixture of hydrocarbons at low pressure (Reid et al., 1986). For a continuous mixture, the final expression of the total vapour phase mole fraction at the droplet surface using Raoult's law is

$$y_{FR} = x_{FR} \int_0^\infty f_L(I) \frac{P_v(I)}{P} dI \qquad (3.6\text{-}1)$$

while integration with I and $(I-\theta)^2$ respectively as weighting functions gives the vapour phase mean and variance:

$$y_{FR}\theta_R = x_{FR} \int_0^\infty f_L(I) I \frac{P_v(I)}{P} dI \qquad (3.6\text{-}2)$$

$$y_{FR}\sigma_R^2 = x_{FR}\int_0^{\infty} f_L(I)\left(I-\theta_L\right)^2 \frac{P_v(I)}{P}dI \qquad (3.6\text{-}3)$$

The component vapour pressure is given by the Clausius-Clapeyron equation:

$$P_v(I) = P_{ATM}\exp\left[\frac{S_{fg}}{R}\left(1-\frac{T_B(I)}{T}\right)\right] \qquad (3.6\text{-}4)$$

For more details, please refer to Tamim and Hallett (1995).

This treatment of vapour-liquid equilibrium equation assumes that:

- the droplet evaporation time is much larger than the molecular relaxation time;
- component vapour pressure is not affected by surface tension (valid for d > ≈1 μm).

3.7 Transport Properties

An important part of this work is to develop transport properties in continuous form for use in the governing equations. Previous work (Bergeron and Hallett, 1989a & b, Ruszalo and Hallett, 1991 and Tamim and Hallett, 1995) assumed that the transport properties of the vapour phase are uniform in space but vary only with time, except for the vapour density. The model of Tamim was later revised by Hallett (1998) to allow all transport properties in the vapour phase to vary in space as well as time. This work will allow the liquid phase transport properties as well as the vapour phase transport properties to vary in space as well as in time.

3.7.1 Liquid Diffusivity

As mentioned previously, the component diffusivities required for these calculations are those of the components in the mixture, and because of the low concentration of each component, it has been assumed that Fick's law holds for each species. The liquid phase diffusivity coefficient is calculated using the Wilke-Chang correlation (Reid et al., 1986, page 618). For a single discrete component i

$$D_{Lim} = 7.4 * 10^{-12} \frac{(\phi M)^{1/2} T}{\eta_m V_i^{0.6}} \qquad (3.7\text{-}1)$$

where the D_{Lim} is in (m^2/sec), M is the molecular weight of the mixture excluding component

i, T is the temperature, η_m is the mixture viscosity in cP, V_i is the pure component molar volume, and ϕ is the association factor for the solvent. For hydrocarbons and other non-polar molecules, $\phi = 1$ (Reid et al., 1986, page 618). For a large number of components, then, ϕM becomes the mixture mean molecular weight.

$$\phi M = \sum_{j=1}^{N} x_j M_j = \theta_L \tag{3.7-2}$$

The molar volume of component i (V_i) at normal boiling point is

$$V_i = \frac{1}{c_{Li}} = \frac{M_i}{\rho_L} = \frac{I}{\rho_L} \tag{3.7-3}$$

where c_{Li} is the component molar density, M_i is the component molecular weight, ρ_L is the liquid mass density which is assumed to be constant, and I is the distribution variable. Substituting equations (3.7-2) and (3.7-3) into equation (3.7-1) yields:

$$D_L(I) = 7.4 * 10^{-12} \frac{\theta_L^{1/2} T \rho_L^{0.6}}{\eta_m I^{0.6}} \tag{3.7-4}$$

This expression assumes that there are no concentration gradients in the solvent (i.e. species i is the only one diffusing). This is untrue in this work because there exist other components than i, but no other methods are available which are simple enough to use for the calculations which follow. To find an expression for $\overline{D}$, equation (3.7-4) will be substituted into equation

(3.2-13). Defining

$$\Xi = 7.4 * 10^{-12} \frac{\theta_L^{1/2} T \rho_L^{0.6}}{\eta_m} \tag{3.7-6}$$

and substituting the gamma distribution (equation (3.5-1)) yields:

$$\overline{D}_L = \frac{\Xi}{\Gamma(\alpha_L)} \int_0^{\infty} \frac{t^{\alpha_L - 1}}{(\beta_L t + \gamma)^{0.6}} \exp(-t) dt \tag{3.7-7}$$

where

$$t = \frac{I - \gamma}{\beta_L} \tag{3.7-8}$$

and thus this integral can be solved by numerical integration. If $\gamma = 0$, equation (3.7-7) can be integrated directly to give

$$\overline{D}_L = \frac{\Xi \Gamma(\alpha_L - 0.6)}{\Gamma(\alpha_L) \beta_L^{0.6}} \tag{3.7-9}$$

The same procedure is performed for $\widetilde{D}_L$ *and* $\hat{D}_L$ to get the following expressions for $\gamma \neq 0$, where again the integration must be performed numerically:

$$\theta_L \tilde{D}_L = \frac{\Xi}{\Gamma(\alpha_L)} \int_0^\infty t^{\alpha_L - 1} (\beta_L t + \gamma)^{0.4} \exp(-t) dt \tag{3.7-10}$$

$$\Psi_L \hat{D}_L = \frac{\Xi}{\Gamma(\alpha_L)} \int_0^\infty t^{\alpha_L - 1} (\beta_L t + \gamma)^{1.4} \exp(-t) dt \tag{3.7-11}$$

These equations can be further simplified for $\gamma = 0$ as follows

$$\theta_L \tilde{D}_L = \frac{\Xi \Gamma(\alpha_L + 0.4) \beta_L^{0.4}}{\Gamma(\alpha_L)} \tag{3.7-12}$$

$$\Psi_L \hat{D}_L = \frac{\Xi \Gamma(\alpha_L + 1.4) \beta_L^{1.4}}{\Gamma(\alpha_L)} \tag{3.7-13}$$

The gamma function $\Gamma(\alpha_L)$ can be calculated using an asymptotic formula given by Abramovitz and Stegun (1970)

$$\ln \Gamma(\alpha_L) \approx \left(\alpha_L - \frac{1}{2}\right) \ln(\alpha_L) - \alpha_L + \frac{1}{2} \ln(2\pi)$$

$$+ \frac{1}{12\alpha_L} - \frac{1}{360\alpha_L^3} + \frac{1}{1260\alpha_L^5} - \frac{1}{1680\alpha_L^7} + \ldots \tag{3.7-14}$$

The values of the three diffusivities $\overline{D}_L$, $\widetilde{D}_L$ *and* $\hat{D}_L$ are very close to each other and they are of the order of 10^{-9} (m^2/sec).

3.7.2 Liquid Mixture Viscosity

The recommended method for finding a liquid mixture viscosity from the viscosity of the components is that of Grunberg and Nissan (Reid et al., 1986, page 474):

$$\ln \eta_m = \sum_{i=1}^{N} x_i \ln \eta_i + \sum^{N} \sum_{i \neq j}^{N} x_i x_j G_{ij} \qquad (3.7\text{-}15)$$

where η_i is the viscosity of component i, N is the total number of components in the mixture and G_{ij} is a binary interaction parameter determined from a group contribution method. The binary interaction parameter term is smaller than the first term of equation (3.7-15) and is small for components of similar molecular weight (Reid et al., 1986, page 475), and in a mixture with many components the individual species mole fractions x_i are small; therefore, the second term can be neglected, and the equation in continuous mixture form for $x_F = 1$ becomes

$$\ln \eta_m = \int_0^{\infty} f_L(I) \ln \eta(I) dI \qquad (3.7\text{-}16)$$

3.7.3 Liquid Component Viscosity

The simplest method to calculate the component viscosity is by using the Orrick and Erbar correlation (Reid et al., 1986, page 456). For a single discrete component i, the liquid viscosity can be estimated as

$$\ln\left(\frac{\eta_i}{\rho_L M_i}\right) = A + \frac{B}{T} \tag{3.7-17}$$

where M_i is the component molecular weight and T is the liquid temperature. A and B for n-paraffins are written using group contributions as

$$A = -(6.95 + 0.21n) \tag{3.7-18}$$

$$B = 275 + 99n \tag{3.7-19}$$

where n is the number of carbon atoms, related to the molecule weight for n-paraffins as

$$M_i = 14n + 2 \tag{3.7-20}$$

Substituting equation (3.7-20) into (3.7-18) and (3.7-19) gives

$$A = a_1 + a_2 I \tag{3.7-21}$$

$$B = b_1 + b_2 I \tag{3.7-22}$$

where $a_1 = -6.92$, $a_2 = -0.015$, $b_1 = 260.9$ and $b_2 = 7.07$

Substituting equations (3.7-21) and (3.7-22) into (3.7-17) yields

$$\ln \eta_i = \ln \rho_L + \ln I + a_1 + \left[a_2 + \frac{b_2}{T} \right] I + \frac{b_1}{T} \tag{3.7-23}$$

To find an expression for liquid mixture viscosity, equation (3.7-23) will be substituted into equation (3.7-16) and integrated over I to yield

$$\ln \eta_m = \ln \rho_L + a_1 + \frac{b_1}{T} + \left(a_2 + \frac{b_2}{T} \right) \theta_L + \int_0^\infty f_L(I) \ln(I) dI \tag{3.7-24}$$

Substituting the gamma distribution gives

$$\ln \eta_m = \ln \rho_L + a_1 + \frac{b_1}{T} + \left(a_2 + \frac{b_2}{T} \right) \theta_L$$

$$+ \frac{1}{\Gamma(\alpha_L)} \int_0^\infty t^{\alpha_L - 1} \exp(-t) \ln(\beta_L t + \gamma) dt \tag{3.7-25}$$

where t has been defined in equation (3.7-8). For $\gamma = 0$, the integral can be integrated to

$$\int_0^\infty f_L(I) \ln(I) dI = \ln(\beta_L) + \Psi(\alpha_L) \tag{3.7-26}$$

where $\Psi(\alpha_L)$ is the digamma function, which can be calculated using an asymptotic formula found in Abramovitz and Stegun (1970)

$$\Psi(\alpha_L) = \ln(\alpha_L) - \frac{1}{2\alpha_L} - \frac{1}{12\alpha_L^2} + \frac{1}{120\alpha_L^4} - \frac{1}{252\alpha_L^6} + \ldots \qquad (3.7\text{-}27)$$

The liquid mixture viscosity for $\gamma = 0$ is therefore

$$\ln \eta_m = \ln \rho_L + a_1 + \frac{b_1}{T} + \left(a_2 + \frac{b_2}{T}\right)\theta_L + \ln(\beta_L) + \Psi(\alpha) \qquad (3.7\text{-}28)$$

For $\gamma \neq 0$, equation (3.7-25) was integrated numerically using the trapezoid rule.

3.7.4 Liquid Heat Capacity

The liquid specific heat was taken from the second order polynomial correlation developed by Tamim and Hallett (1995) for n-paraffins.

3.7.5 Vapour Phase Properties

Expressions for vapour phase properties such as enthalpy of vaporization, heat capacity, thermal conductivity and diffusivity were developed by Tamim and Hallett (1995) and are used in this work to calculate the vapour phase properties.

3.8 Balances on Liquid Phase Distribution Parameters

Balances were performed upon liquid phase distribution parameters θ_L and ψ_L to check if they obey mass balances or not. These were used in checking and debugging the model. Details are explained in Appendix C. The balance is checked by comparing values of $\overline{\theta}_L$ and $\overline{\Psi}_L$ from equation (C-5) and (C-6) with those obtained by integrating equation (C-10) and (C-11) over time. It was found that the previous explained model obeys the mass balances with a maximum error of $\overline{\theta}_L$ balance equal to 0.1913%, for $\overline{\Psi}_L$ balance equal to 0.5017% and for $\overline{\sigma}_L$ balance equal to 4.301E-4%.

3.9 Alternative Quasi-Steady Model

The model developed in the previous sections calculates full transient behaviour in both vapour and liquid phases. The full transient model is complicated and the program used to solve this model is long and requires considerable computer time. Although the addition of the diffusion-limited assumption to the liquid phase means a more accurate solution and a closer approach to real droplet behaviour, it would be desirable to have a faster, but still accurate, solution. If the quasi-steady assumption in the liquid phase is correct and is able to describe multi-component droplet evaporation correctly, this means that it can be used instead of our complicated full transient model.

Some years ago, Law and Law (1981) derived an analytical model for liquid phase diffusion in a multi-component droplet, based on the assumption of a quasi-steady concentration profile in the liquid phase. This solution has recently been extended to a continuous mixture by Hallett (2000), and will here be compared with the results of the full numerical solution outlined previously.

The quasi-steady liquid-phase assumption simply means that at any instant in time the fields of temperature and concentration of the liquid-phase are in a quasi-steady state, so that the transient terms ($\partial/\partial t$) can be dropped from the governing equations. The liquid variables are assumed to adjust to a new steady-state almost instantaneously. The problem with this assumption is the fact that the rate of liquid-phase mass diffusion is extremely slow. Vapour-phase mass and thermal diffusivities are of the order of 10^{-5} m^2/sec, and are much higher than the liquid phase thermal and mass diffusivities, which are of the order of 10^{-7} to 10^{-9} m^2/sec; hence, transients should be much slower in the liquid, and there is some doubt as to whether Law and Law's assumption is valid. It will be tested against the present model.

CHAPTER 4: NUMERICAL SOLUTION

The transport properties of both the liquid and vapour phases were assumed to vary in space as well as in time. The temperature of the liquid phase was assumed to be uniform in space and vary only in time, while the vapour temperature is allowed to vary in time and space. The assumption of spherical symmetry of the droplet makes the problem one dimensional with radius as the only space co-ordinate. The model uses finite volume techniques to solve the governing transport equations in both vapour and liquid phases, as in earlier work performed by Bergeron and Hallett (1989b), Ruszalo and Hallett (1991) and Tamim and Hallett (1995).

4.1 Finite Volume Solution

As in previous work, the governing equations together with the boundary and initial conditions were developed into finite volume form and solved numerically. Before setting up the numerical equations a coordinate transformation is applied. This is needed to keep the first grid point for the vapour phase on the surface of the droplet and also to keep the last grid point for the liquid phase at the droplet surface, otherwise the droplet surface would move with respect to the coordinates as the droplet vaporizes. This is achieved by transforming the coordinates as follows:

$$\xi = \frac{r}{R} \tag{4.1-1}$$

where r represents the radial distance toward or away from droplet surface (depending on which phase need to be described). The rate of droplet recession is defined as

$$\dot{R} = \frac{dR}{dt} \tag{4.1-2}$$

For the Liquid Phase

Although it is assumed that there is no bulk motion in the liquid phase, v_L^* can be non-zero because of changes in c_L; hence we need to define a new velocity

$$w_L^* = v_L^* - \xi \dot{R} \tag{4.1-3}$$

The transformed governing equations relative to the new coordinate system are

Continuity Equations:

$$\xi^2 \frac{dc_L}{dt} + \frac{1}{R}\frac{\partial}{\partial \xi}\left(\xi^2 c_L w_L^*\right) + \frac{\dot{R}}{R} c_L \frac{\partial}{\partial \xi}\left(\xi^3\right) = 0 \tag{4.1-4}$$

Diffusion Equations:

* Equation for x_F (from 3.2-19):

$$\xi^2 \frac{\partial\left(c_L x_F\right)}{\partial t} + \frac{\dot{R}}{R}\left(c_L x_F\right)\frac{\partial \xi^3}{\partial \xi} + \frac{1}{R}\frac{\partial}{\partial \xi}\left(\xi^2 c_L w_L^* x_F\right)$$

$$= \frac{1}{R^2}\frac{\partial}{\partial \xi}\left(c_L \chi \overline{D}_L \xi^2 \frac{\partial x_F}{\partial \xi}\right) \tag{4.1-5}$$

* Equation for ($x_F\theta_L$) (from 3.2-20):

$$\xi^2 \frac{\partial\left(c_L x_F \theta_L\right)}{\partial t} + \frac{\dot{R}}{R}\left(c_L x_F \theta_L\right)\frac{\partial \xi^3}{\partial \xi} + \frac{1}{R}\frac{\partial}{\partial \xi}\left(\xi^2 c_L w_L^*\left(x_F \theta_L\right)\right)$$

$$= \frac{1}{R^2}\frac{\partial}{\partial \xi}\left(c_L \chi \tilde{D}_L \xi^2 \frac{\partial\left(x_F \theta_L\right)}{\partial \xi}\right) \qquad (4.1\text{-}6)$$

* Equation for ($x_F\psi_L$) (from 3.2-21):

$$\xi^2 \frac{\partial\left(c_L x_F \Psi_L\right)}{\partial t} + \frac{\dot{R}}{R}\left(c_L x_F \Psi_L\right)\frac{\partial \xi^3}{\partial \xi} + \frac{1}{R}\frac{\partial}{\partial \xi}\left(\xi^2 c_L w_L^*\left(x_F \Psi_L\right)\right)$$

$$= \frac{1}{R^2}\frac{\partial}{\partial \xi}\left(c_L \chi \hat{D}_L \xi^2 \frac{\partial\left(x_F \Psi_L\right)}{\partial \xi}\right) \qquad (4.1\text{-}7)$$

In the same manner, a coordinate transformation was applied for the vapour phase transport equations, and equivalent relations to (4.1-4) - (4.1-7) were obtained. The new equations derived for both vapour and liquid phase were integrated over a radial control volume using the finite volume technique described by Patankar (1980). The general form of the discretization equation is, for the liquid fuel mole fraction for example:

$$ax_{FP} = bx_{FE} + cx_{FW} + a^{o}x^{o}_{FP} \qquad (4.1\text{-}8)$$

where P denotes the point solved for, E and W are its east and west neighbours respectively (Figure4.1), and the coefficients a, b, c and a^{o} are obtained from the integration of each term over the control volume and over the time interval $t+\Delta t$ (Patankar, 1980, Bergeron and Hallett, 1989b, Ruszalo and Hallett, 1991 and Tamim and Hallett, 1995). Superscript ^{o} (='old') denotes values at the previous time step, and an implicit method used for the time dependence. Details of these equations are in Appendix B. The resulting equations for both phases were solved using a tri-diagonal matrix algorithm.

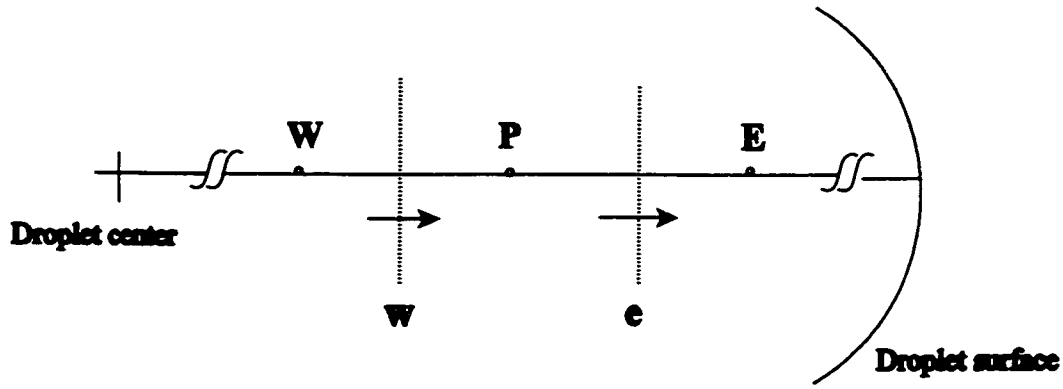

Figure 4.1: Diagram of cell around droplet

4.2 Computational Grid Spacing

Two grids were defined in this work, one inside the droplet for the liquid phase calculations and the other one outside the droplet for the vapour phase calculations. The most important changes take place at the droplet surface where the largest gradients are found in both phases. Based on that, the grid spacing used for both phases gives more points near the droplet surface and fewer points away from the droplet surface; hence the study of the variation very close to the droplet surface can be more precise.

Grid Spacing in the Vapour Phase

A grid similar to that used by Tamim (1996) will be used in this work. The grid spacing in the vapour phase was defined in exponential form as follows

$$\xi(i) = \exp\left[\frac{\ln \xi(N)}{N-1}(i-1)\right] \qquad (4.2\text{-}1)$$

where i is the grid point index and N is the total number of grid points in the vapour phase (outside the droplet Tamim (1996) used a 20 point grid with an outer boundary situated at a distance equal to 500 times the droplet radius.

Grid Spacing in the Liquid Phase

As in the vapour phase solution, a non-uniform grid spacing is desirable. Most of the droplet mass lies near the surface, hence a cubic equation is used for the grid (Ruszalo, 1990) as follows

$$\xi(i) = \left[\frac{(i-1)}{NN-1}\right]^{1/3}, \quad \xi \leq 1 \tag{4.2-2}$$

where i is the grid point index and NN is the total number of grid points inside the droplet (figure 4.2). In this case a 15 point grid was used. The effect of grid spacing on numerical accuracy will be discussed in section 5. The droplet center is at $\xi = 0.0$, while the droplet surface is at $\xi = 1.0$.

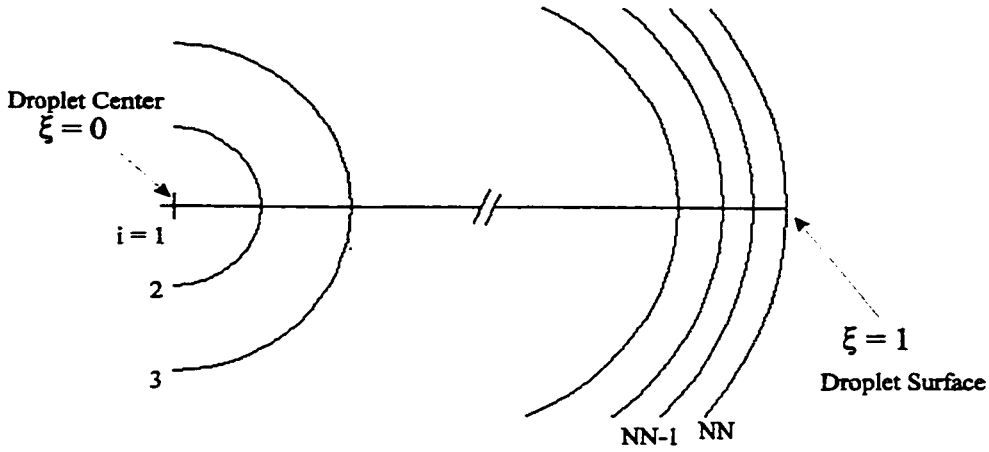

Figure 4.2: Cubic grid spacing in the liquid phase

The first point out from the centre of liquid phase grid is a large way from the center. To give better resolution near the centre, another grid point $\xi_{1.5}$ was added half way between ξ_2 and the centre, such that $\xi_{1.5} = \xi_2 /2$. The points were then renumbered so that $\xi_{1.5}$ becomes ξ_2, ξ_2 becomes ξ_3, etc.

4.3 Program Flow Chart

The equations developed in chapter 3 must be solved by iteration at each time step. Figure 4.3 shows the sequence of calculation used. The structure of the algorithm used in the same as that used by Tamim and Hallett with modifications implemented where required. For trial values of temperature and liquid distribution parameters at the droplet surface, the droplet energy balance, vapour-liquid equilibrium, and the flux relations at the surface are solved , which gives a new surface vapour pressure. The transport and continuity equations for both phases are then solved, which yields new vapour and liquid phase composition distributions. These are checked for convergence.

Vapour-liquid equilibrium and the flux relations at the surface are solved by iteration using a two variable Newton method in a separate subroutine. The objective is to chose values of θ_{LR} and ψ_{LR} that will balance equations (3.4-8 and 3.4-9); hence, objective functions ϕ are defined as

$$\phi_\theta = N\theta_{LR} - c_L \tilde{D}_L \left.\frac{\partial \theta_L}{\partial r}\right|_R - Ny_{FR}\theta_R + c\tilde{D}\left.\frac{\partial \theta}{\partial r}\right|_R \qquad (4.3\text{-}1)$$

with a similar definition for ϕ_ψ. These must be made to equal zero.

An initial guess θ_{LR} , ψ_{LR} gives ϕ_θ, ϕ_ψ. Let the values for the next iteration be ($\theta_{LR} + \Delta\theta_L$, $\psi_{LR} + \Delta\psi_L$), for which the resulting values ϕ'_θ, ϕ'_ψ should be equal to zero. Expanding ϕ_θ, ϕ_ψ in a Taylor series:

$$\phi'_\theta = \phi_\theta + \left(\frac{\partial \phi_\theta}{\partial \theta_L}\right)_\Psi \Delta\theta_L + \left(\frac{\partial \phi_\theta}{\partial \Psi_L}\right)_\theta \Delta\Psi_L \qquad (4.3\text{-}2)$$

Likewise

$$\phi'_\Psi = \phi_\Psi + \left(\frac{\partial \phi_\Psi}{\partial \theta_L}\right)_\Psi \Delta\theta_L + \left(\frac{\partial \phi_\Psi}{\partial \Psi_L}\right)_\theta \Delta\Psi_L \qquad (4.3\text{-}3)$$

Setting $\phi'_\theta, \phi'_\Psi = 0.0$ we get:

$$-\phi_\theta = \left(\frac{\partial \phi_\theta}{\partial \theta_L}\right)_\Psi \Delta\theta_L + \left(\frac{\partial \phi_\theta}{\partial \Psi_L}\right)_\theta \Delta\Psi_L \qquad (4.3\text{-}4)$$

$$-\phi_\Psi = \left(\frac{\partial \phi_\Psi}{\partial \theta_L}\right)_\Psi \Delta\theta_L + \left(\frac{\partial \phi_\Psi}{\partial \Psi_L}\right)_\theta \Delta\Psi_L \qquad (4.3\text{-}5)$$

This system (a Jacobian) can be solved for $\Delta\theta_L$ and $\Delta\psi_L$, from which the next trial values of θ_{LR}, ψ_{LR} are found.

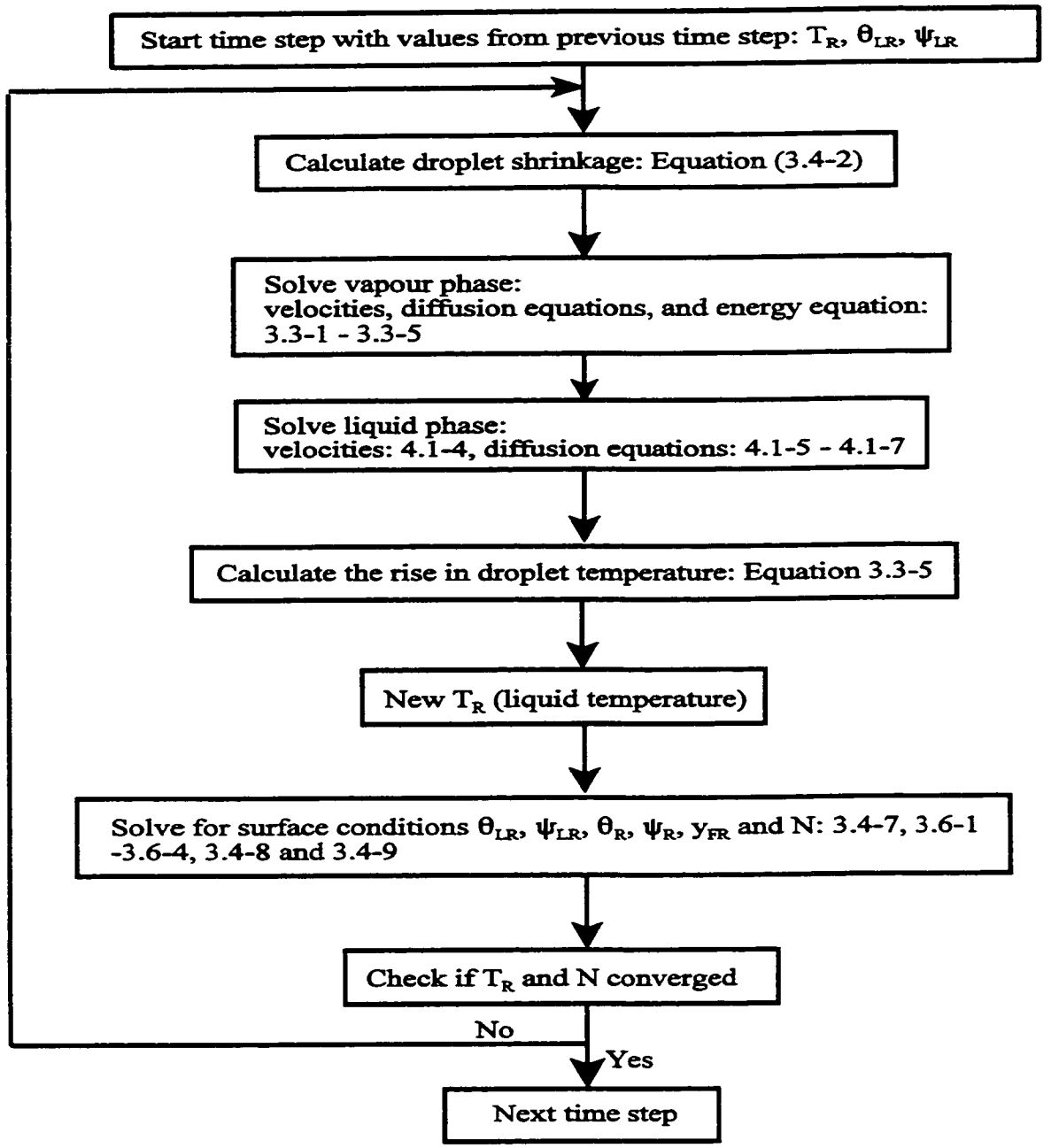

Figure 4.3: Flow chart of computer program

CHAPTER 5: RESULTS AND DISCUSSION

In this chapter sample calculations for vaporizing droplets (no chemical reaction) will be presented in order to demonstrate the capabilities of the theory just developed. All calculations were made for n-paraffin mixtures.

5.1 Selection of Distribution Function

To illustrate the capabilities of the model, a distribution function has to be selected that simulates the commercial fuel chosen: No. 2 Diesel.

The distribution parameters for the initial liquid distribution were determined by continuous thermodynamics simulation of the ASTM D86 distillation test as described by Tamim and Hallett (1995). Mole balances and phase equilibrium relations were numerically integrated to get θ_L, σ_L and the boiling point as functions of the volume evaporated. The distribution parameters were chosen to represent No. 2 Diesel fuel; they give the same θ_L and σ_L as those used by Tamim, but the initial point γ was changed from 0 to 44. The lower bound thus corresponds to molecular weight of propane. The parameters are α_L=11.3, β_L=12.4, γ= 44. Figure 5.1 shows the ASTM curve predicted using continuous thermodynamics and these parameters. The gamma distribution function will be used for the liquid and vapour phase. This distribution is unbounded, and although it can give a very reasonable approximation of distillate fuels from crude petroleum as shown in the ASTM curves, it does give one small discrepancy in the form of a sudden upturn of the curve at the very end (Figure 5.1).

5.2 Program Testing

5.2.1 Comparison with Well-Mixed Model

To test the program, the results from the model developed in chapter 3 with a large mixing factor (χ=100) are compared with results of the well-mixed model developed by Tamim and Hallett (1995) and updated to variable properties by Hallett (1998), using the same initial conditions, initial distribution parameters and initial droplet diameter. The results in Figures 5.2 to 5.5 are plotted for a 0.2 mm diameter droplet with an initial temperature of 25°C evaporating at an ambient temperature of 1000K. Both models used the same grid with 40 grid points in the vapour phase and the same time step of 0.001 sec.

Figures 5.2 - 5.5 show almost identical results for both cases, which means that the program is correct, and the addition of the liquid phase model has not introduced errors. The earlier model was tested by Tamim and Hallett by doing calculations for a pure (single component) fuel, so it can be considered reliable. The fuel droplet reaches a sort of quasi-steady state, during which liquid temperature (Figure 5.2) and liquid molecular mass (Figure 5.3) increase nearly linearly as light components are distilled out. The heat flux to the multi-component droplet can be divided in two parts: one fraction is used to heat up the droplet, the other fraction is used for evaporation. As liquid temperature rises, the vapour fraction starts to form and diffuse in to the surrounding atmosphere (Figure 5.4), resulting an increase in mass evaporated and mass flux outwards from the droplet (Figure 5.5). Near the end of droplet lifetime, only heavy components remain in the liquid, causing the liquid temperature and

molecular mass to increase sharply. The present model with χ=100 stops earlier than the well-mixed model by about 0.01 sec due to convergence problems, leaving 1.2% of the droplet unevaporated. Since the results of both cases are identical for all of the droplet lifetime, this failure to complete the last 1.2% of the calculation is not important.

5.2.2 Selection of Time Step:

To determine the effects of time step on numerical precision, sample calculations were performed for a 0.2 mm droplet using different time steps. Increasing/decreasing the time step will allow the program to show fewer/more time steps during the evaporation process. Figure 5.6 shows the results of multi-component droplet evaporation with the diffusion-limited model (χ=1) to describe the liquid mixing using different time steps. Identical results for three time steps (0.0005sec, 0.001sec and 0.002sec) were obtained, showing that a step of 0.001 sec, or about 0.4% of the droplet lifetime, is short enough.

The selection of the appropriate time step is highly dependent on droplet diameter, the droplet evaporation time varies as a function of squared of droplet diameter (d^2), with larger droplets needing a higher evaporation time. This is a prediction of the "classical" droplet evaporation theory, and it has been found to hold for continuous thermodynamics models too. Earlier work with droplet evaporation (Tamim and Hallett, 1995) showed that the droplet obeys the d^2-law, which means that the square of droplet diameter is proportional to the droplet lifetime. This should be the factor used to scale the time step for smaller or larger droplets.

This idea was also used to reduce the time step as evaporation proceeds: the time step is reduced by a factor of 2 when 80% of the mass has disappeared, by 5 at 90%, by 10 at 95%, by 20 at 99%, and finally cut to 1/50 of its initial value at 99.5% evaporated. This was necessary to ensure convergence of the program near the end of the droplet lifetime. The time step was also reduced by a factor of 5 at the very beginning because of the rapid change taking place then (See Figure 5.6).

5.2.3 Selection of Grid Spacing

Determining the number of grid points that should be used for the vapour and liquid phase depends on how the results are affected by changing the number of grid points. To do that, sample calculations were performed for the 0.2 mm droplet with the number of liquid phase grid points varying from 10 up to 30, while the number of vapour phase grid points was kept constant and equal to 40 grid points (Figure 5.7). The variation in the number of the liquid points hardly affects the results. Based on this, 15 liquid grid points will be a satisfactory choice in order to minimize the calculation time.

For the determination of the vapour grid, another set of calculations were performed for the 0.2 mm droplet with the number of vapour points varying from 20 up to 60, using 15 points for the liquid phase. Figure 5.8 shows that the vapour grids have a larger effect on the results than the liquid grids. This can be explained by the fact that the vapour molar flux is highly dependent upon the gradients of $(y_F\theta)$ and $(y_F\psi)$ at the surface, which in turn is affected by the number of grid points in the vapour phase. As the number of vapour points increases, the

solution is clearly approaching an asymptote. In further calculations 40 vapour points were used.

5.3 Droplet Evaporation-Effect of Liquid Mixing

Sample calculations are presented here for a 0.2 mm droplet of Diesel fuel, represented by a distribution function with initial parameters α_{Lo}=11.3, β_{Lo}=12.4 and γ= 44.0, giving θ_{Lo}=184.12, σ^2_{Lo}=41.7. The droplet diameter of 0.2 mm is considered to be a typical diameter of the largest droplet sizes found in a fuel spray.

The droplet is initially at 300 K and is suddenly exposed to a hot environment at 1000 K. Radiation heat transfer was not included. Calculations were made for mixing factor values χ=1, which represents the pure diffusion-limited model as well as for higher rates of mixing (χ=10 and χ=100). The results for the well-mixed model case were generated using the model described by Tamim and Hallett (1995) updated to include fully variable gas phase properties. The results for the quasi-steady liquid model were generated using the model derived by Law and Law (1981) as adapted to continuous thermodynamics by Hallett (2000).

Figure 5.9 shows that increasing the mixing factor from 1 to 100 does not greatly affect the liquid temperature history. In each case, the droplet liquid temperature rises steadily as lighter components are distilled out. There is a small difference between the diffusion-limited model (χ=1) and the cases with more rapid mixing (χ=10 and χ=100), but there are almost identical results for χ=10 and 100.

As the liquid temperature rises the more volatile components evaporate first and the less volatile components remain in the liquid droplet. Figure 5.10 shows that the mean of the liquid distribution at the droplet surface θ_{LR} increases with time as the concentration of the less volatile components in the mixture rises. Increasing the mixing factor from 1 to 100 yields similar behaviour of the liquid distribution mean with time and the same conclusion that results for χ=10 and χ=100 are very close. It can be noted clearly that the means of the liquid distributions for χ=10 and χ=100 are lower at the surface than that for χ=1 by about 20 kg/kmol on the average. Increasing mixing inside the droplet tends to yield a more homogenous mixture inside the droplet and thus all components will have an almost equal chance to reach the surface, while for the diffusion-limited model, the lighter components are only supplied to the surface very slowly.

The lower value of liquid distribution mean at the droplet surface for χ=10 or 100 will lead to an initial increase in droplet evaporation rate as shown in figure 5.11. This increase in evaporation rate leads later to a small decrease in the droplet heating rate and thus a slightly lower liquid temperature (see figure 5.9) which in turn slightly reduces the droplet evaporation rate for χ=10, 100 after about 60% of droplet life time. The previous conclusion of very similar results for mixing factors 10 and 100 holds.

Figure 5.12 presents the overall fuel vapour mole fraction at the droplet surface with time. The vapour fraction increases sharply in the early droplet lifetime, representing the transient heating period of the droplet, here about 30% of the total droplet lifetime. Then the vapour mole fraction becomes almost constant for mixing factors 10 and 100. Corresponding to the changes in droplet evaporation rate mentioned previously, there is initially a higher vapour

mole fraction for χ=10 and χ=100 than for the diffusion-limited model χ=1, but a lower vapour mole fraction after about 60% of the droplet lifetime. Again the results for χ=10 and χ=100 agree very closely.

For χ=1 near the end of droplet lifetime, the two boundary layers on either side of the droplet join together, and since the concentration of heavy components is much higher in the boundary layers this means that the droplet now has a higher proportion of high boiling components than a well-mixed droplet has. This forces the vapour fraction down (Figure 5.12), resulting in more liquid heating and higher temperatures (See Figure 5.9).

Figure 5.13 shows the liquid distribution standard deviation at the droplet surface σ_{LR} as a function of time for the three mixing factor values 1, 10 and 100. The behaviour of σ_{LR} at χ=10 & 100 is very similar to the well-mixed model: the more volatile components leave the droplet at a fast rate and what is left in the mixture is the less volatile components, which leads to the decrease in σ_{LR} (narrower distribution). For χ=1 the behaviour is different. Since evaporation using the diffusion-limited model assumption (χ=1) will not allow the more volatile components to evaporate as rapidly as in the well-mixed model, the droplet will contain both the more and less volatile components in its mixture. The Diesel distribution at the droplet surface will be shifted from that inside the droplet, so that the concentration of volatile components in the inside distribution is much higher than at the surface. This difference will cause distributions diffusion of lighter species to the surface, making the distribution there broader.

Figures (5.14 - 5.17) compare the diffusion-limited model (χ=1), the well-mixed model, the quasi-steady model and the full model with χ=10. There is very good agreement between the results for χ=10 and the well-mixed model, showing that even at χ=10 the liquid is already close to well-mixed. Also, it can be noticed that the diffusion-limited model and the well-mixed model both have the nearly same behaviour for the liquid temperature, the liquid distribution mean, the mass percent evaporated and the vapour mole fraction histories. Based on that, we can say that the liquid mixing model has a very little effect on the progress of the evaporation of the multi-component droplet, except at the very end of the droplet lifetime, where the behaviour of the diffusion-limited case deviates somewhat from the others. It can also be noted that the full transient liquid diffusion model did not confirm the results of the quasi-steady liquid model of Law & Law; on the contrary, there can be seen to be a very large difference in behaviour between the quasi-steady model and the full numerical model. Figure 5.14 shows an increase in droplet liquid temperature for the quasi-steady model only during the initial transient period, after which temperature reaches an almost constant steady value. Also, Figure 5.15 shows a large initial drop in the liquid distribution mean at the droplet surface in the transient period and then a constant mean for the rest of the droplet lifetime, very different from the behaviour of the other models. Figures 5.16 and 5.17 also show different behaviour for the quasi-steady liquid model in the droplet evaporation rate and vapour mole fraction, corresponding to the variations in liquid temperature and liquid mean distribution. In the initial transient period, although the liquid temperature is higher, the liquid distribution mean is much larger at the surface, therefore the vapour fraction is very small and the evaporation rate lags behind that of the other models. Later, after about 30%

of droplet lifetime, a steady state is achieved, with a nearly constant liquid distribution mean at the surface. The vapour fraction y_{FR} is higher, resulting in a faster evaporation.

Figure 5.18 presents the liquid distribution mean profile inside the droplet at different times for the diffusion-limited model and for χ = 10. The characteristic rise in the liquid distribution mean near to the surface for the diffusion-limited model is caused by preferential evaporation of light components from the surface layer. For the diffusion-limited model (χ=1), a well-defined concentration boundary layer is evident, which slowly spreads into the interior of the droplet, while for χ=10 profiles are produced which are already close to being well-mixed. Even with molecular diffusion alone (χ=1), the differences between the composition at the surface and the interior are not large, which is the main reason why changing the mixing factor (χ) has so little effect.

Figures 5.19 & 5.20 present the profile of the liquid distribution mean at different times for χ=1 and the quasi-steady liquid model. If the quasi-steady model assumption is correct, these two should be nearly identical, because the quasi-steady liquid model also represents a liquid with χ=1. In the early droplet lifetime (see figure 5.19) both models show a uniform behaviour inside the droplet, and the change in concentration takes place only in a boundary layer near to the surface. As time proceeds (see figure 5.20), the thickness of the boundary layer for the diffusion-limited model increases, but that for the quasi-steady model remains nearly constant. The boundary layer profile predicted by the quasi-steady liquid model depends on the initial value of the liquid distribution mean at the center, which is assumed constant by Law and Law (1981), while the value of the liquid distribution mean at the center

changes from one time step to another in the full diffusion-limited model. From the above discussion, it appears that the quasi-steady state postulated in the Law and Law (1981) model does not exist, the liquid in fact being in a continually transient state. This is to be expected: the characteristic time for diffusion in the droplet is R^2/D_L, which for a 200μm droplet with a typical D_L of 5.10^{-9} m^2/s gives 2.0 sec, or about eight times the droplet lifetime; hence transients will dominate the liquid phase throughout. Also, the quasi-steady model did not obey a component mass balance, which makes this model questionable.

Other sample calculations were performed using different droplet diameters (a very large droplet with diameter = 2 mm which is representative of the droplet sizes used for some laboratory experiments on single droplets, and a very small droplet with diameter = 0.02 mm which is representative of the smaller sizes of droplets in a spray). Time steps for the 2 mm and 0.02 mm droplets were scaled as mentioned in section 5.2.2, and the droplet lifetimes can be seen to scale with the d^2 law. Results obtained using 2mm & 20μm droplets are shown in Figures 5.21 - 5.26. The shapes of curves are the same for all droplet sizes, the effects of changing the mixing factor value are also the same, and the evaporation behaviour is the same too. The quasi-steady liquid model behaviour is also the same, so that this model is equally invalid for all droplet sizes.

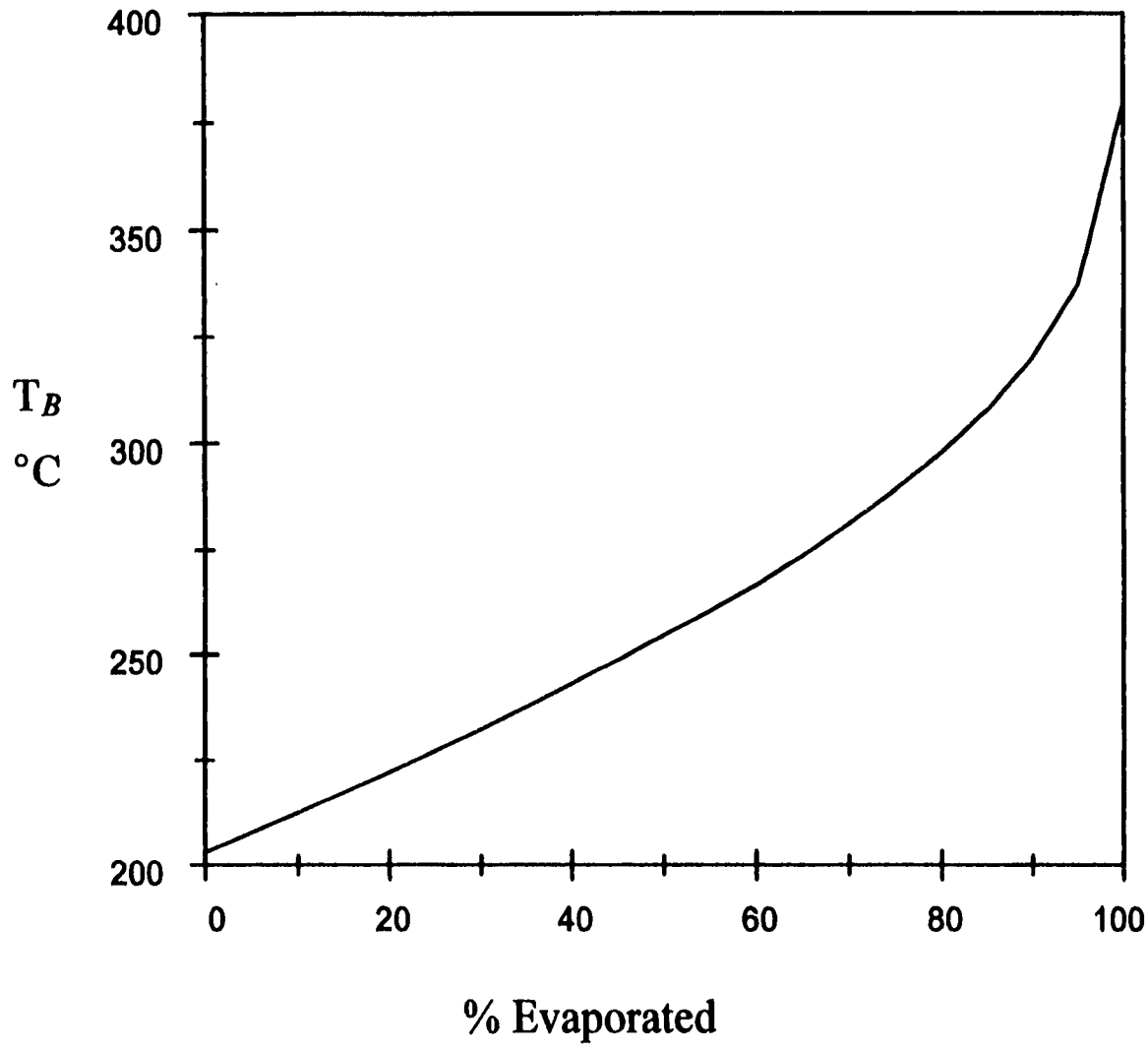

Figure 5.1: ASTM D86 curve predicted using continuous thermodynamics for No. 2 Diesel using $\alpha_L = 11.3$, $\beta_L = 12.4$ and $\gamma = 44$.

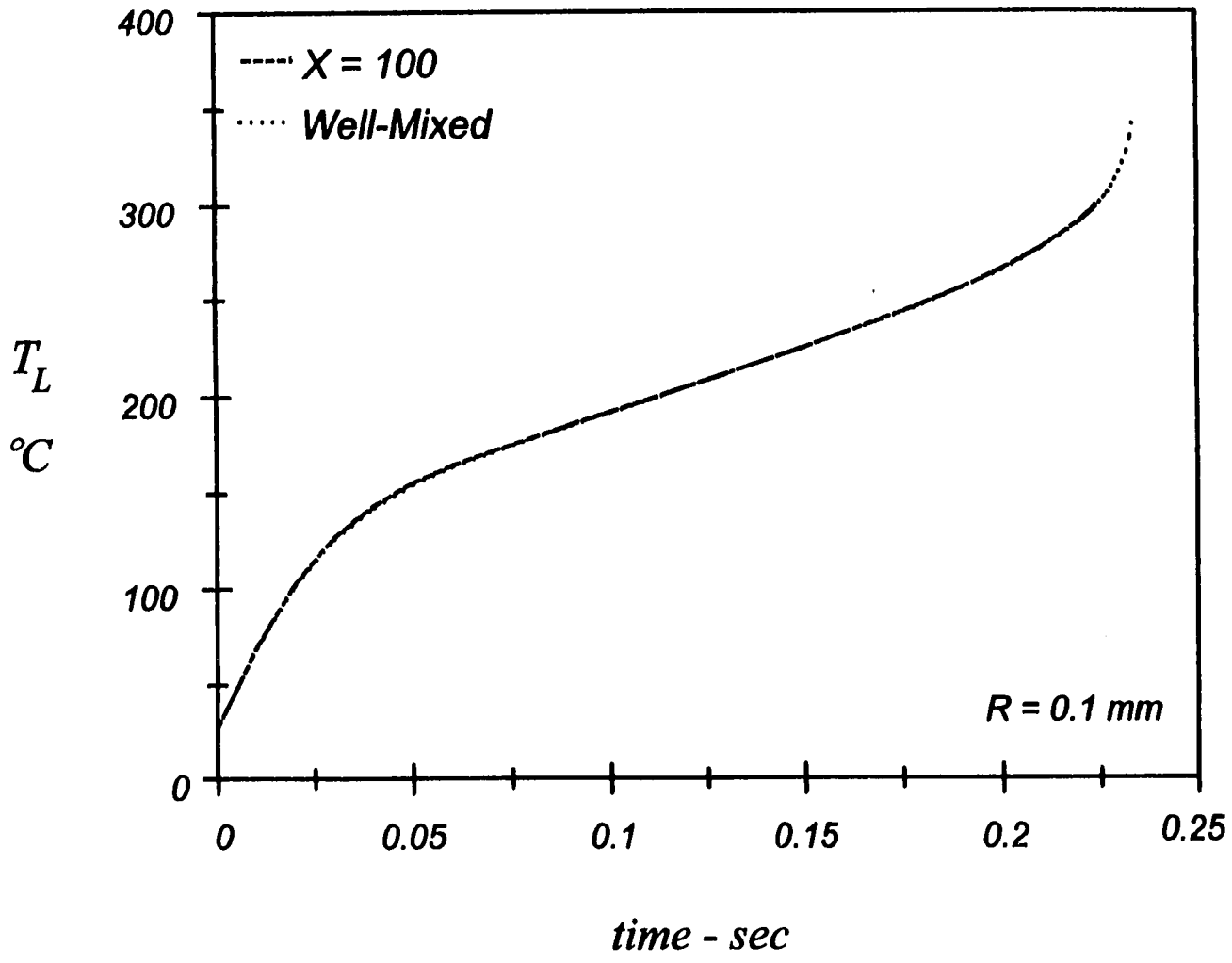

Figure 5.2: Droplet liquid temperature versus time for 200 μm Diesel droplet vaporizing at 1000 K, initial temperature 300 K: Comparison between the well-mixed model and the full model with $\chi = 100$.

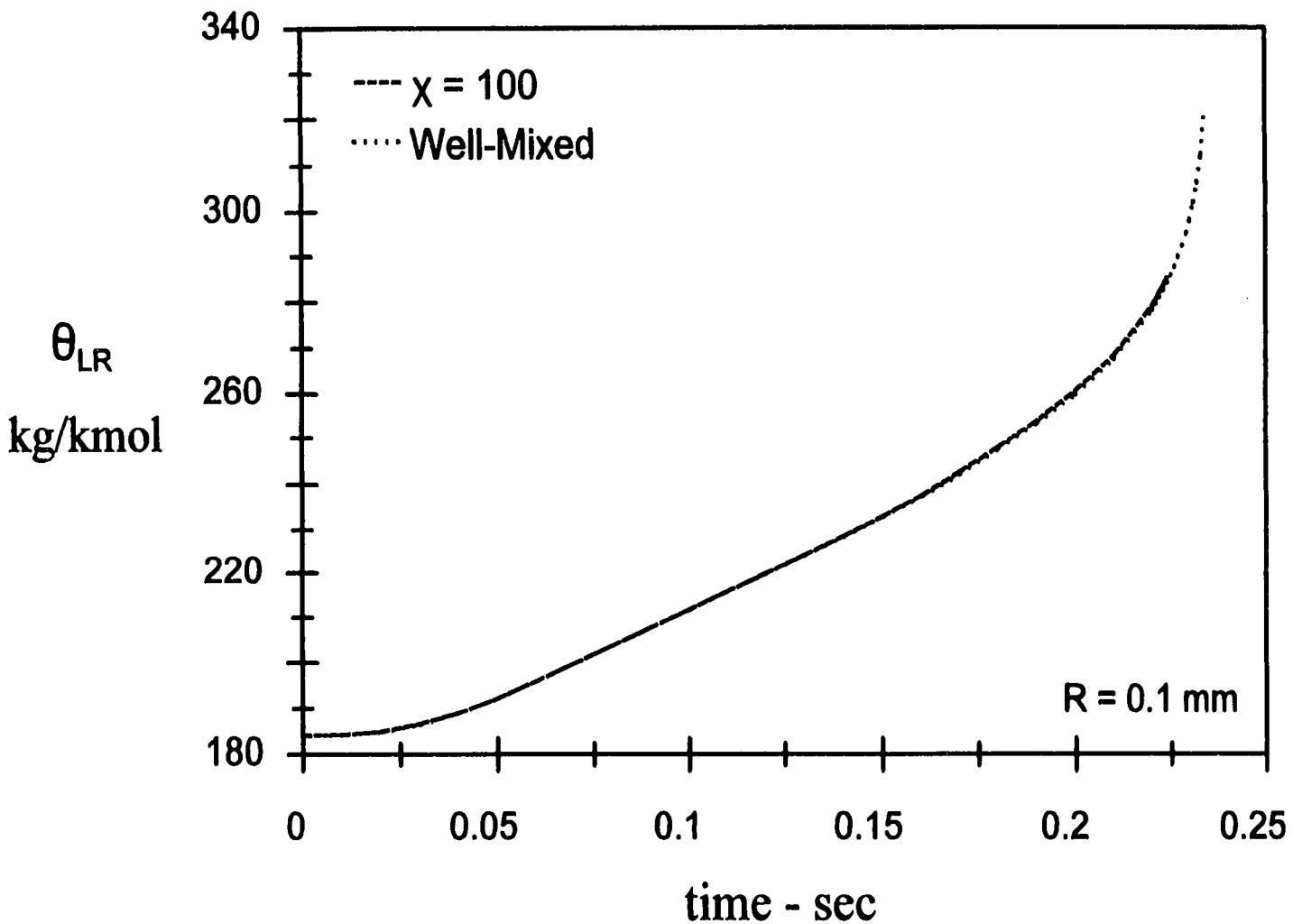

Figure 5.3 Mean of liquid distribution at droplet surface versus time for a 200 μm Diesel droplet vaporizing at 1000 K, initial temperature 300 K: Comparison between the well-mixed model and the full model with $\chi = 100$.

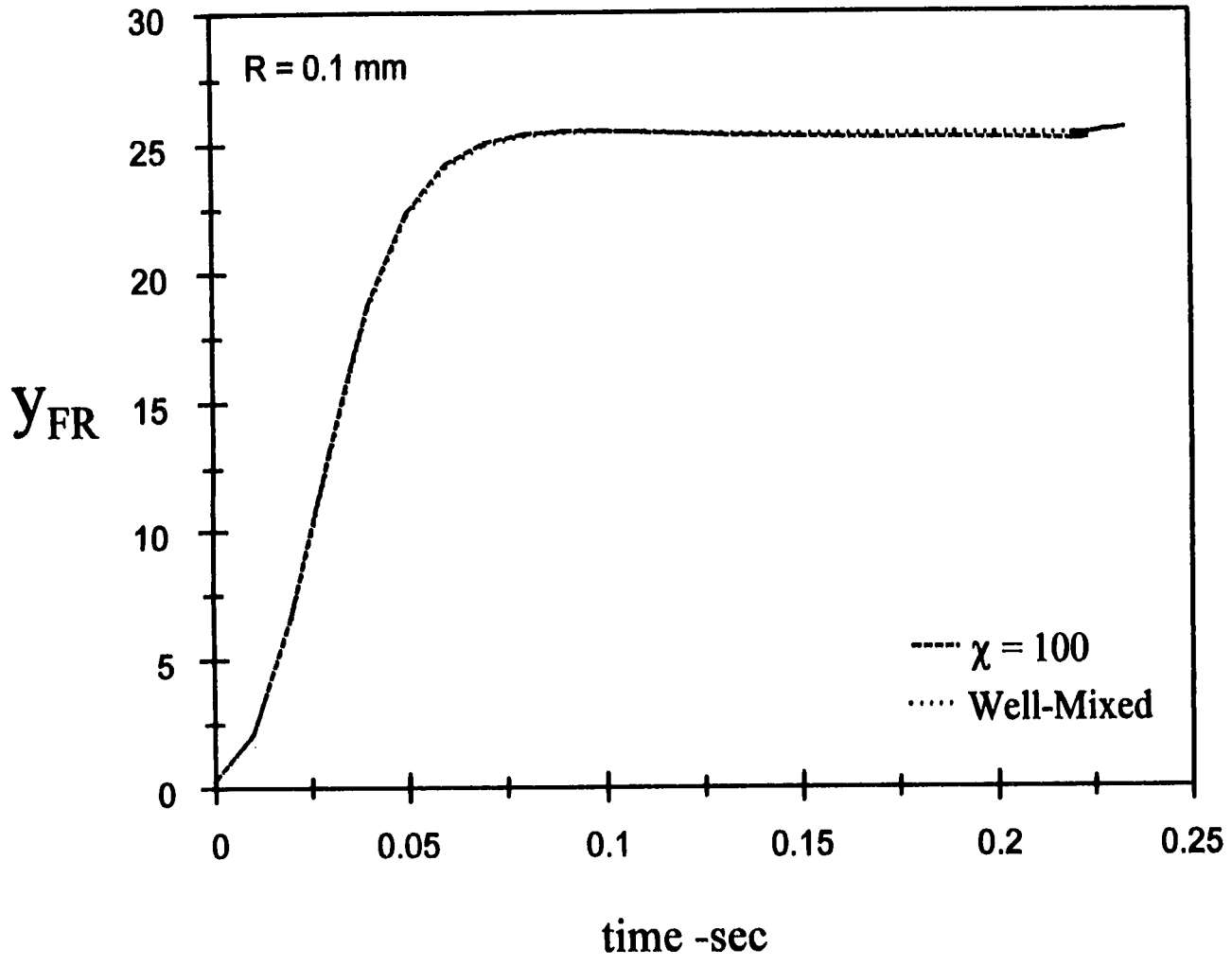

Figure 5.4: Vapour mole fraction at the surface versus time for a 200 μm Diesel droplet vaporizing at 1000 K, initial temperature 300 K: Comparison between the well-mixed model and the full model with $\chi = 100$.

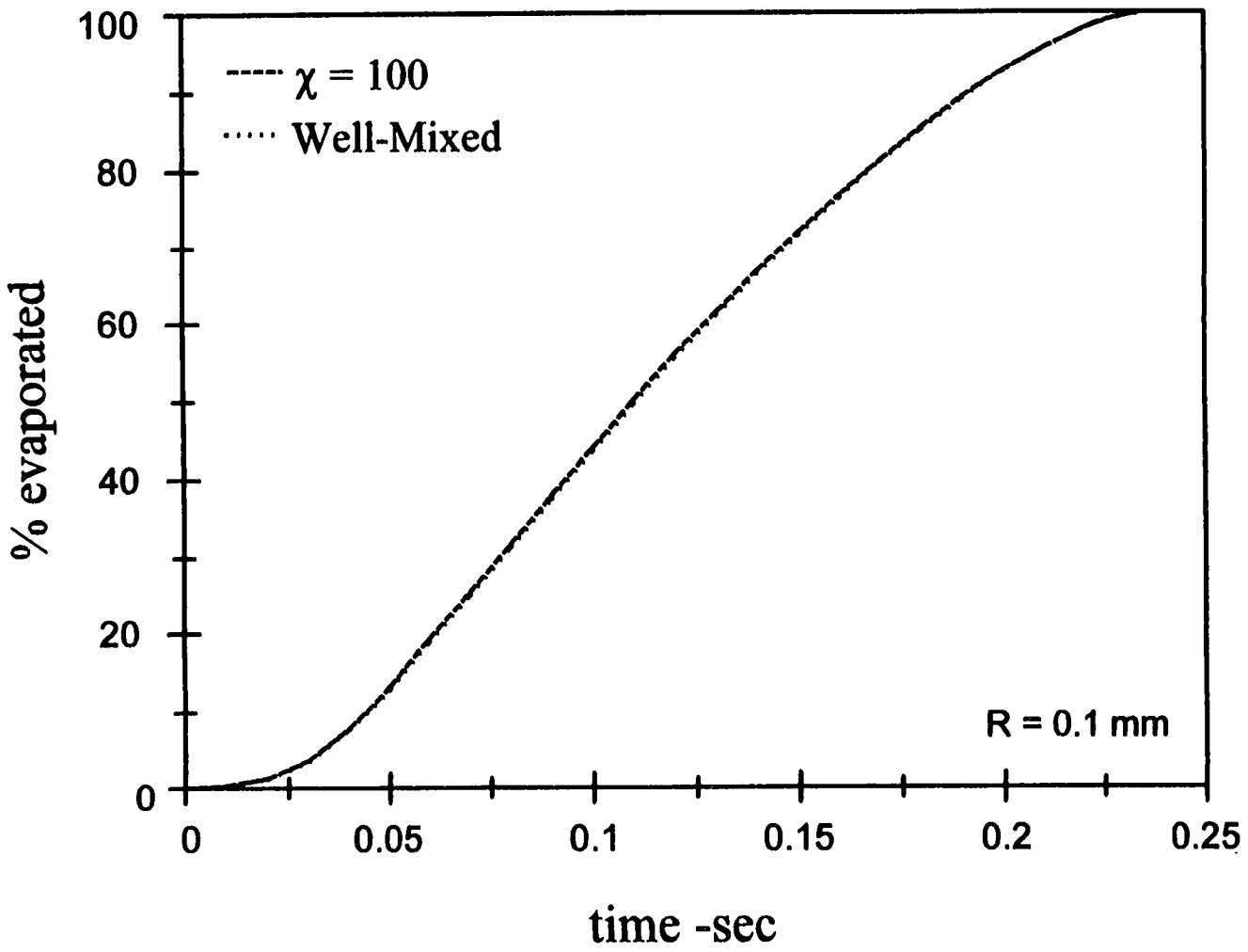

Figure 5.5: Droplet mass percent evaporated versus time for a 200 μm Diesel droplet vaporizing at 1000 K, initial temperature 300 K: Comparison between the well-mixed model and the full model with $\chi = 100$.

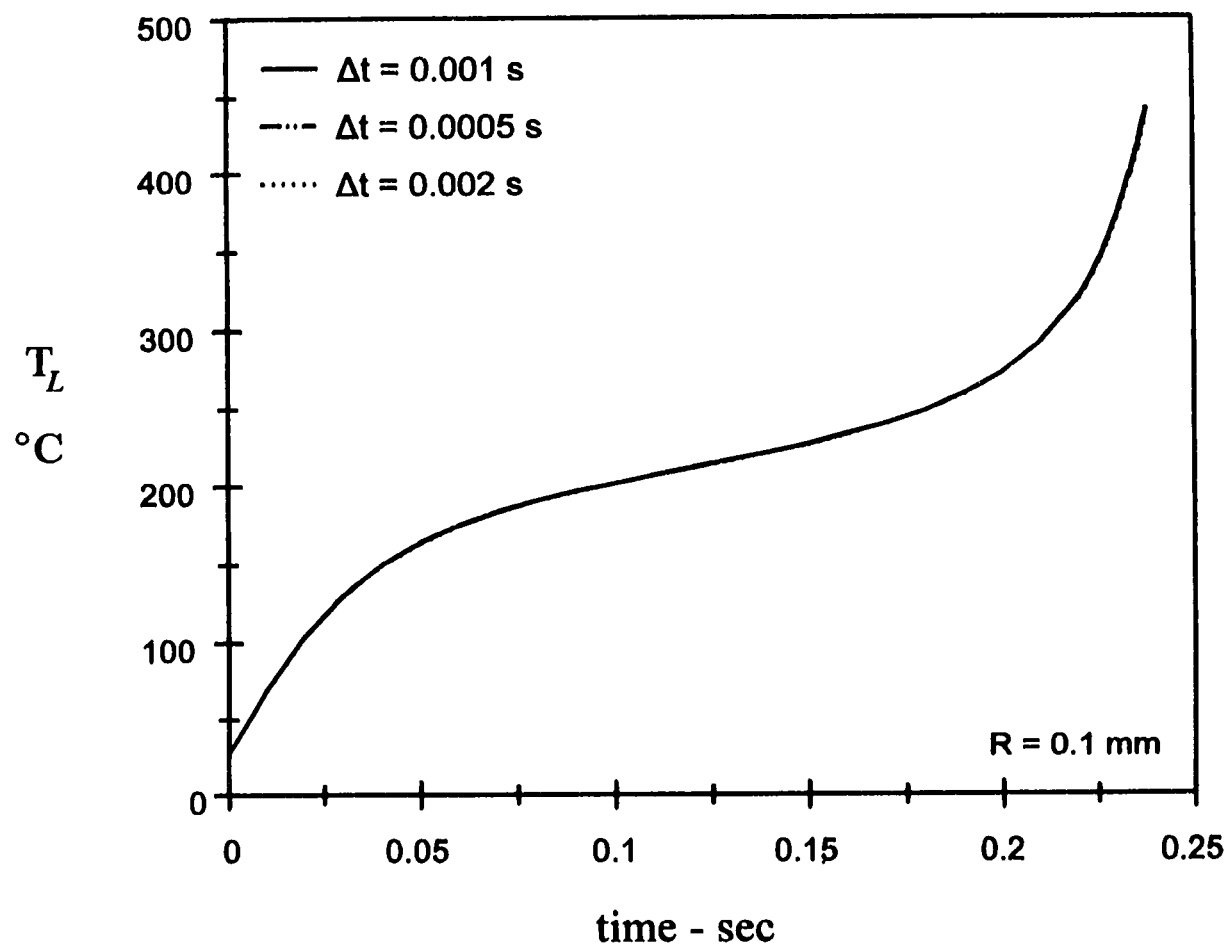

Figure 5.6: Droplet liquid temperature versus time for a 200 μm Diesel droplet vaporizing at 1000 K, initial temperature 300 K: Comparison between different time steps (Δt = 0.001s, 0.0005 s and 0.002 s) applied for the diffusion-limited model (χ=1).

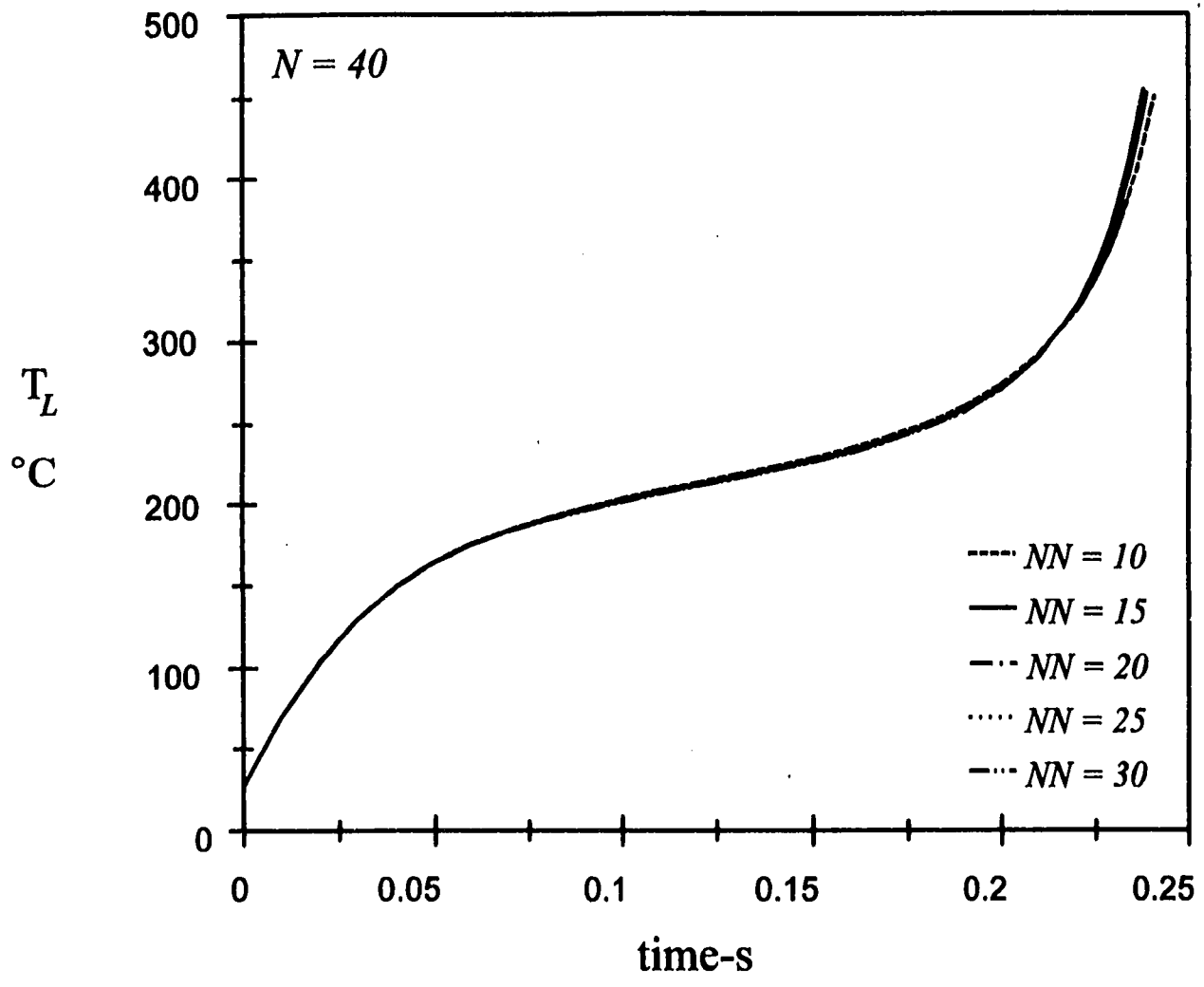

Figure 5.7: Droplet liquid temperature versus time for a 200 μm Diesel droplet vaporizing at 1000 K, initial temperature 300 K: Comparison between different liquid grid points (NN = 10, 15, 20, 25 & 30) applied with 40 vapour grid points.

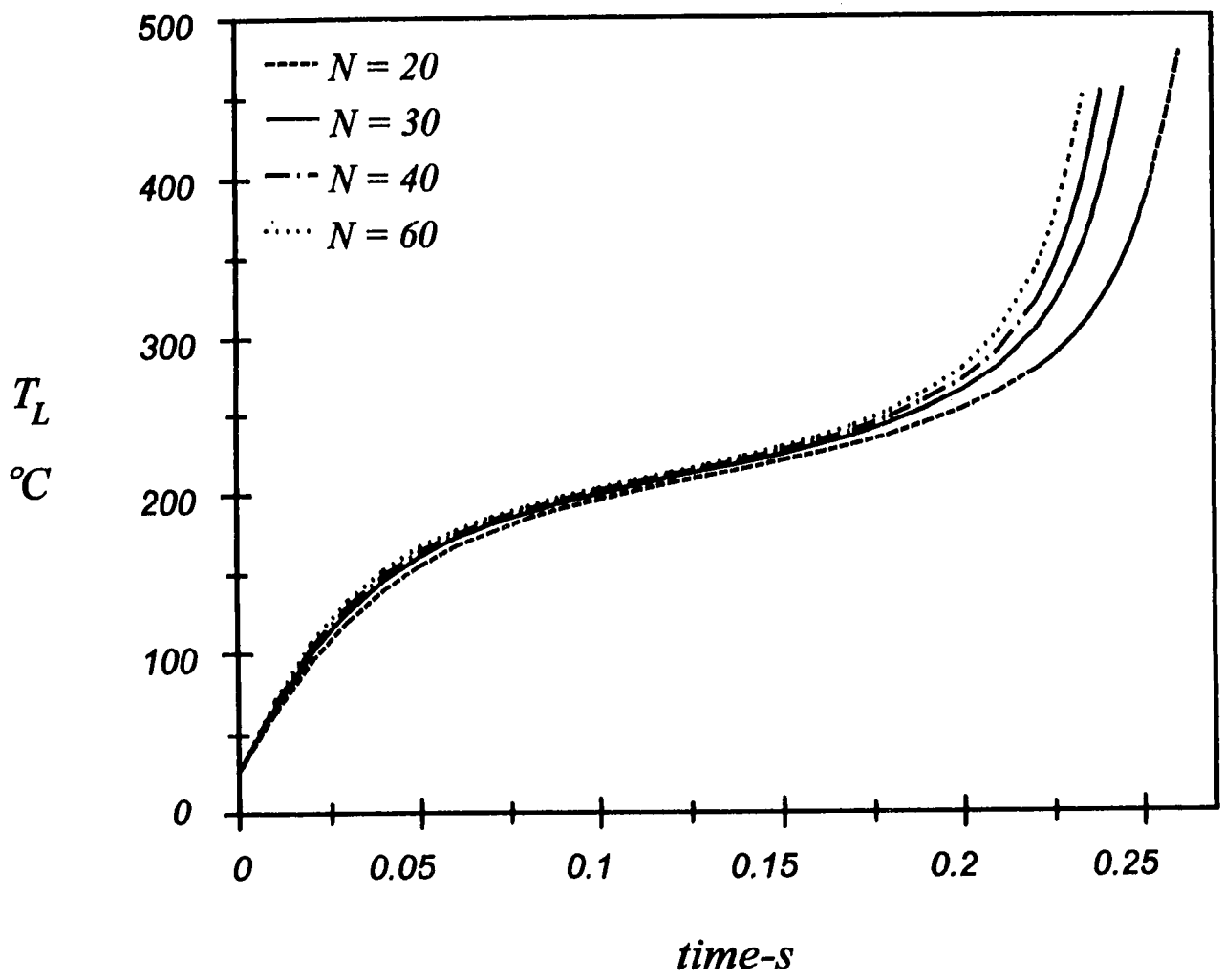

Figure 5.8: Droplet liquid temperature versus time for a 200 μm Diesel droplet vaporizing at 1000 K, initial temperature 300 K: Comparison between different vapour grid points (N = 20, 30, 40 & 60) applied with 15 liquid grid points.

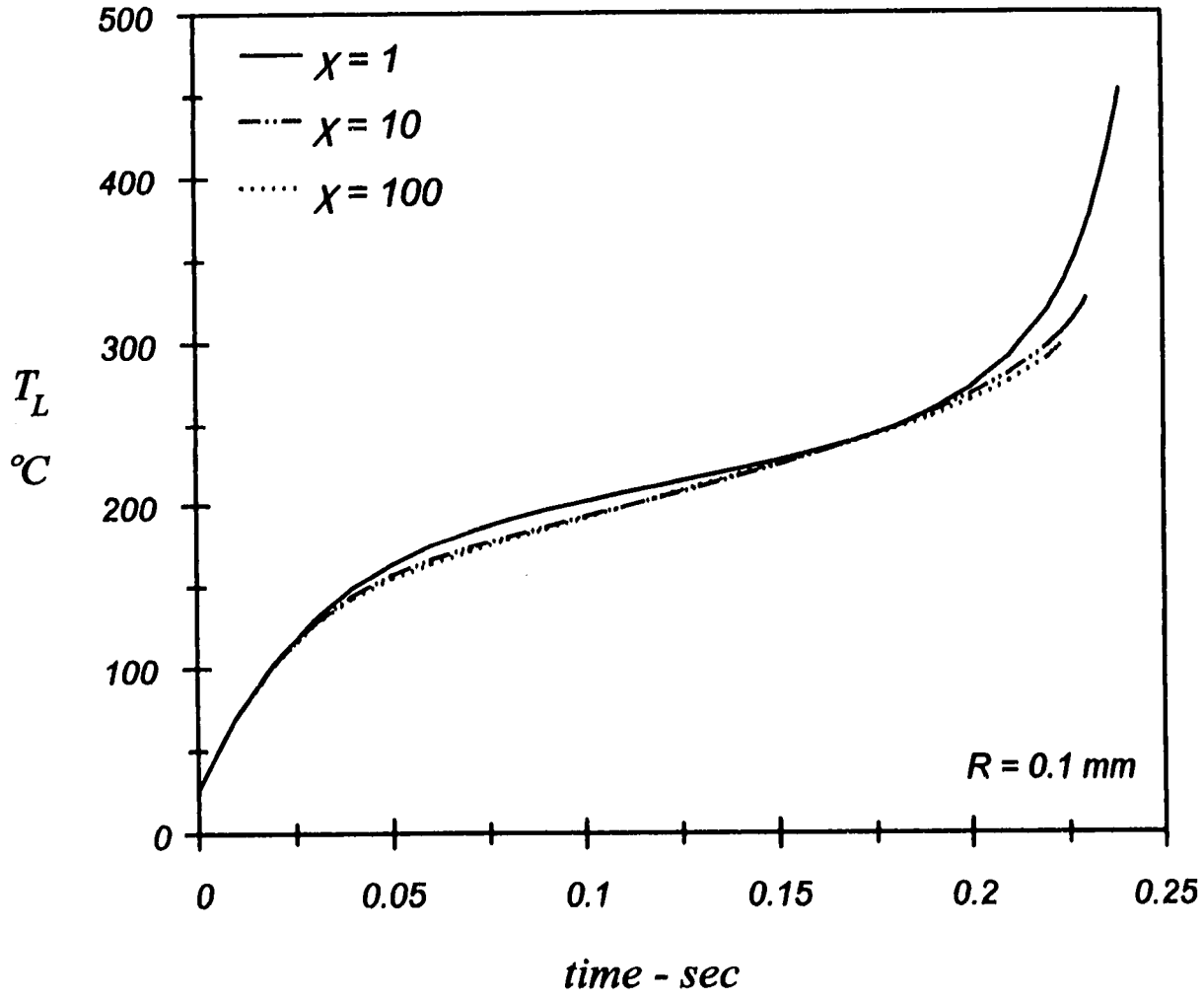

Figure 5.9: Droplet liquid temperature versus time for a 200μm Diesel droplet vaporizing at 1000 K, initial temperature 300 K: Comparison between three mixing factor values ($\chi = 1$, $\chi = 10$ and $\chi = 100$).

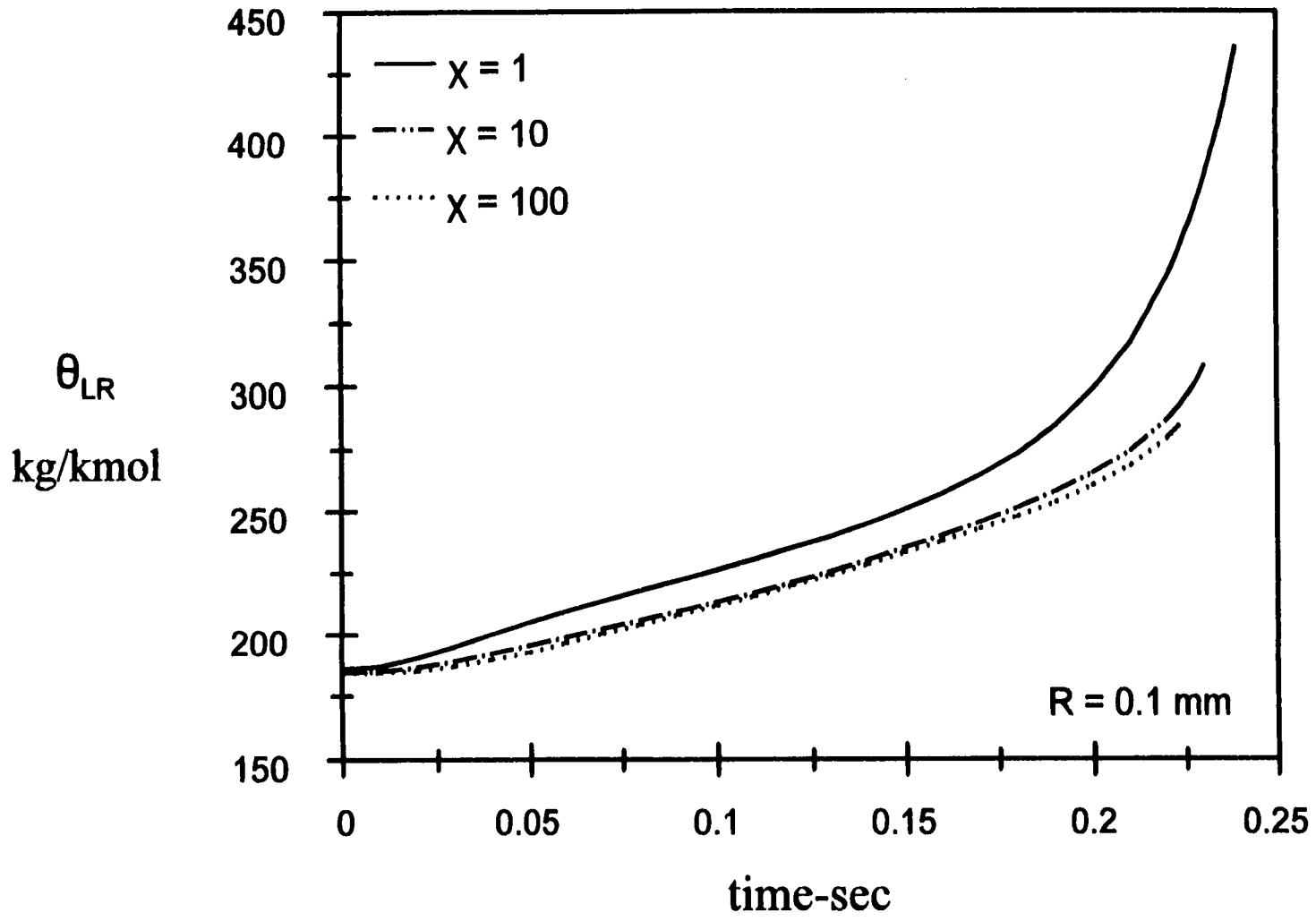

Figure 5.10: Mean of liquid distribution at droplet surface versus time for a 200μm Diesel droplet vaporizing at 1000 K, initial temperature 300 K: Comparison between three mixing factor values ($\chi = 1$, $\chi = 10$ and $\chi = 100$).

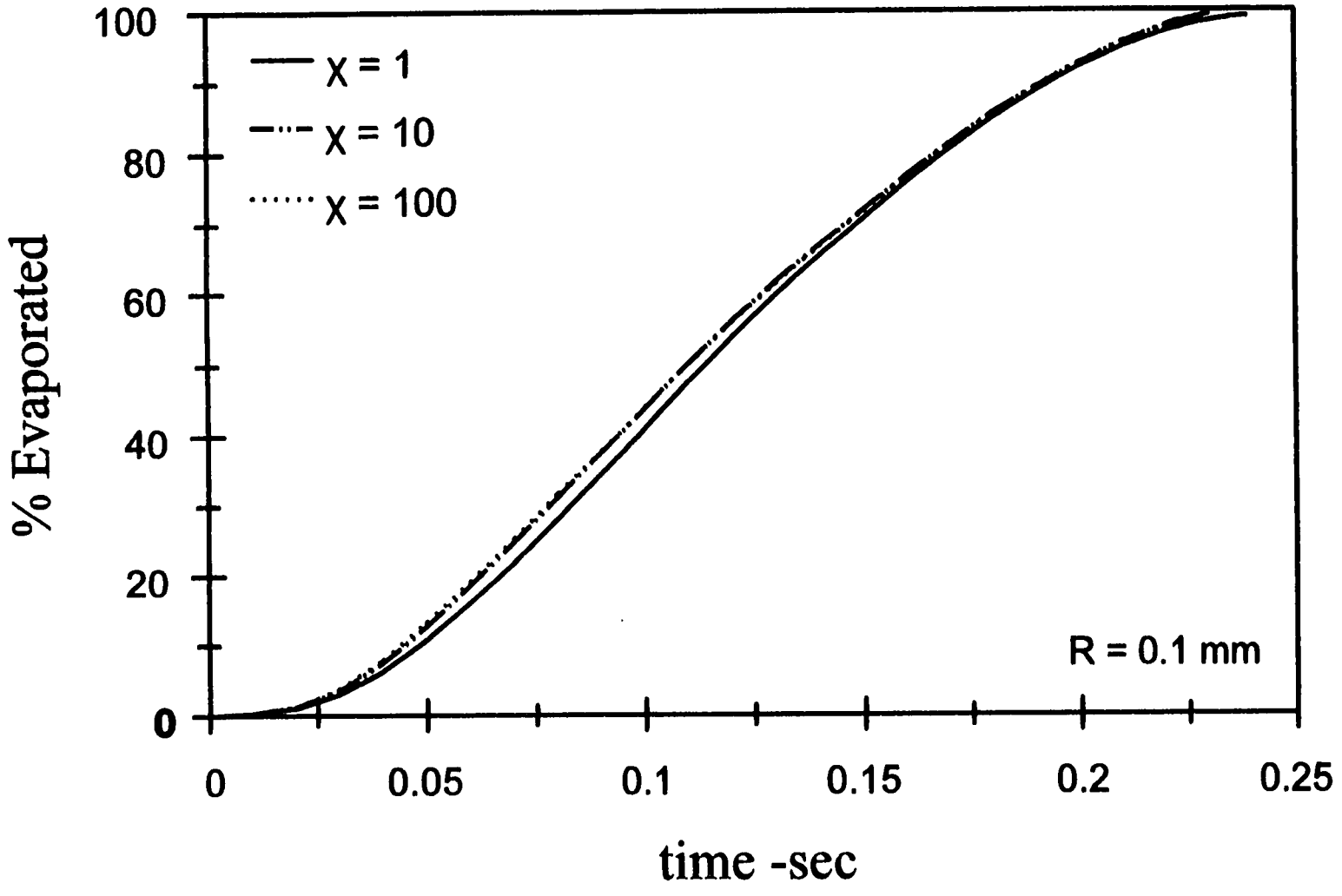

Figure 5.11 Droplet mass percent evaporated versus time for a 200μm Diesel droplet vaporizing at 1000 K, initial temperature 300 K: Comparison between three mixing factor values ($\chi = 1$, $\chi = 10$ and $\chi = 100$).

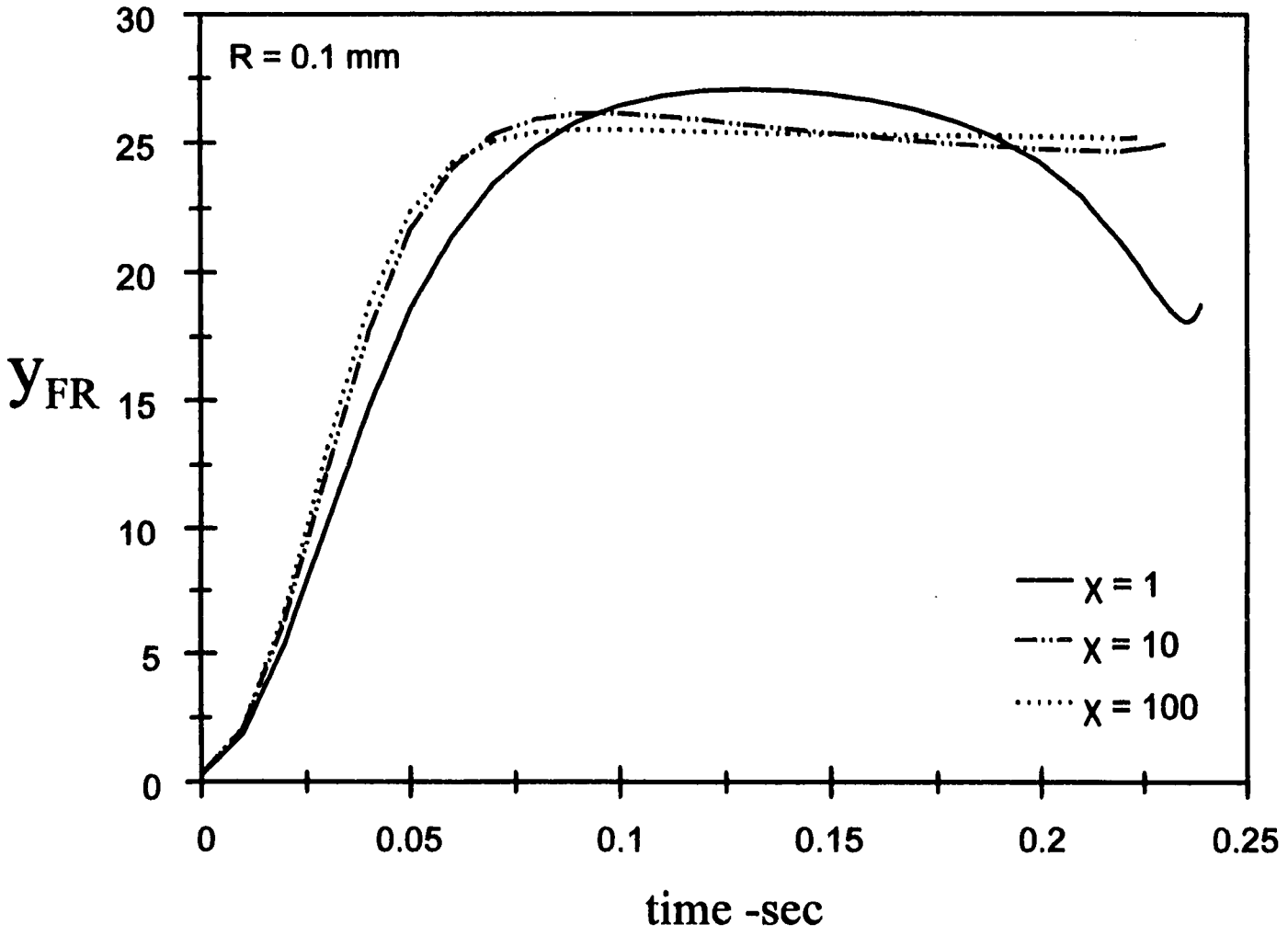

Figure 5.12 Vapour mole fraction at the surface versus time for a 200μm Diesel droplet vaporizing at 1000 K, initial temperature 300 K: Comparison between three mixing factor values (χ = 1, χ = 10 and χ = 100).

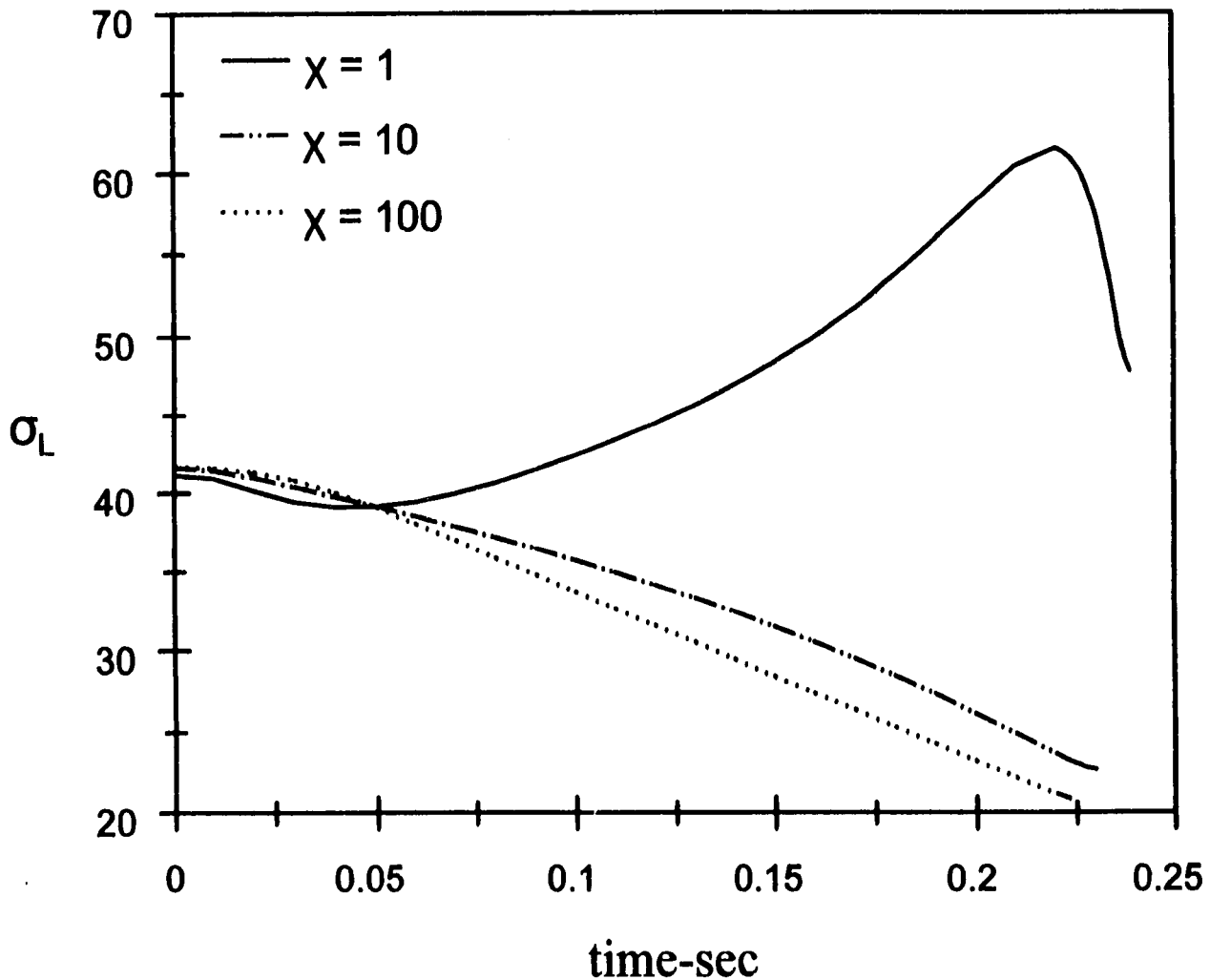

Figure 5.13 Standard deviation of liquid distribution at the surface versus time for a 200μm Diesel droplet vaporizing at 1000 K, initial temperature 300 K: Comparison between three mixing factor values ($\chi = 1$, $\chi = 10$ and $\chi = 100$).

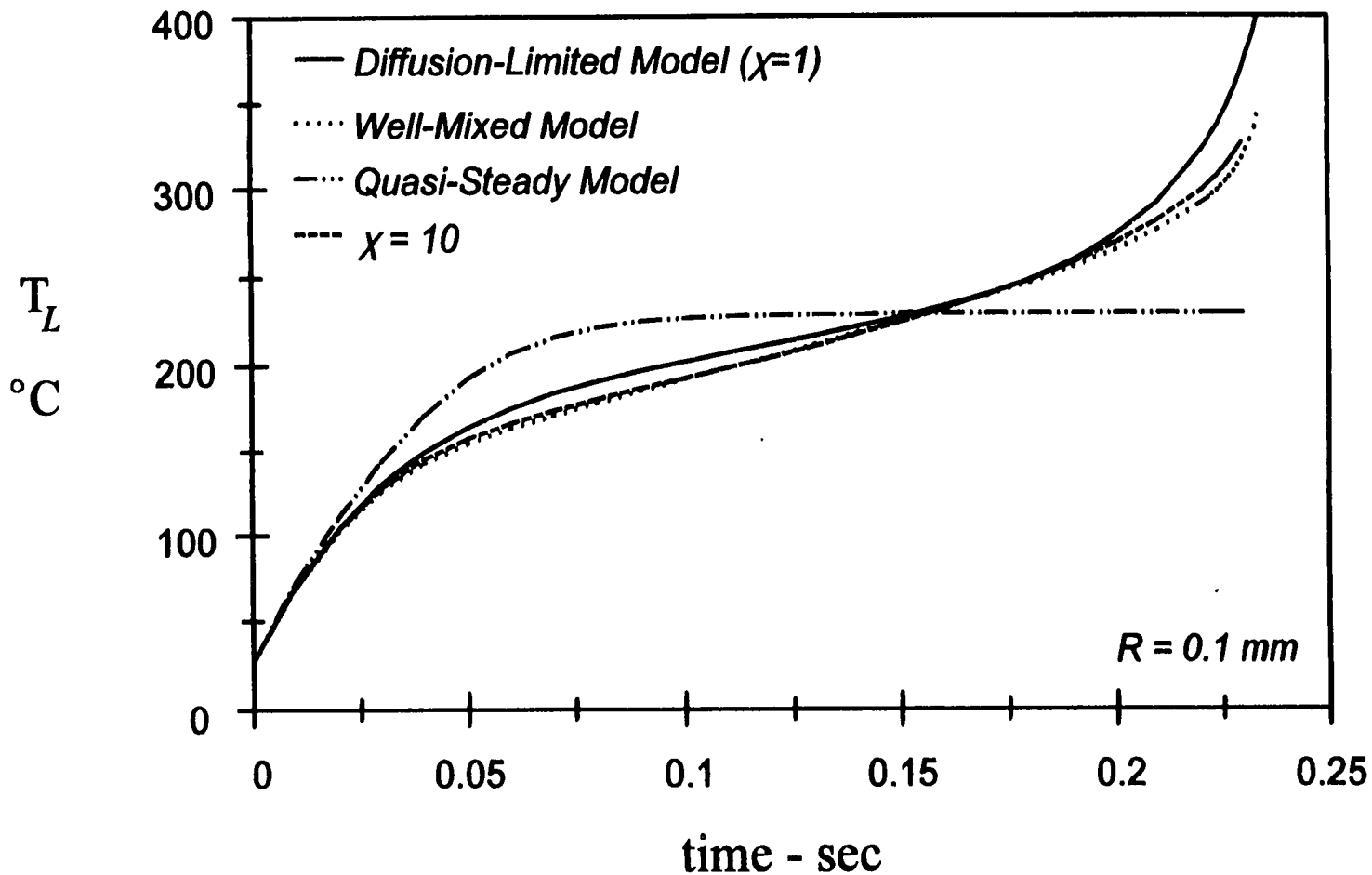

Figure 5.14 Droplet liquid temperature versus time for a 200μm Diesel droplet vaporizing at 1000 K, initial temperature 300 K: Comparison between two limiting mixing models (diffusion-limited and well-mixed models), the quasi-steady model and the full model with $\chi = 10$.

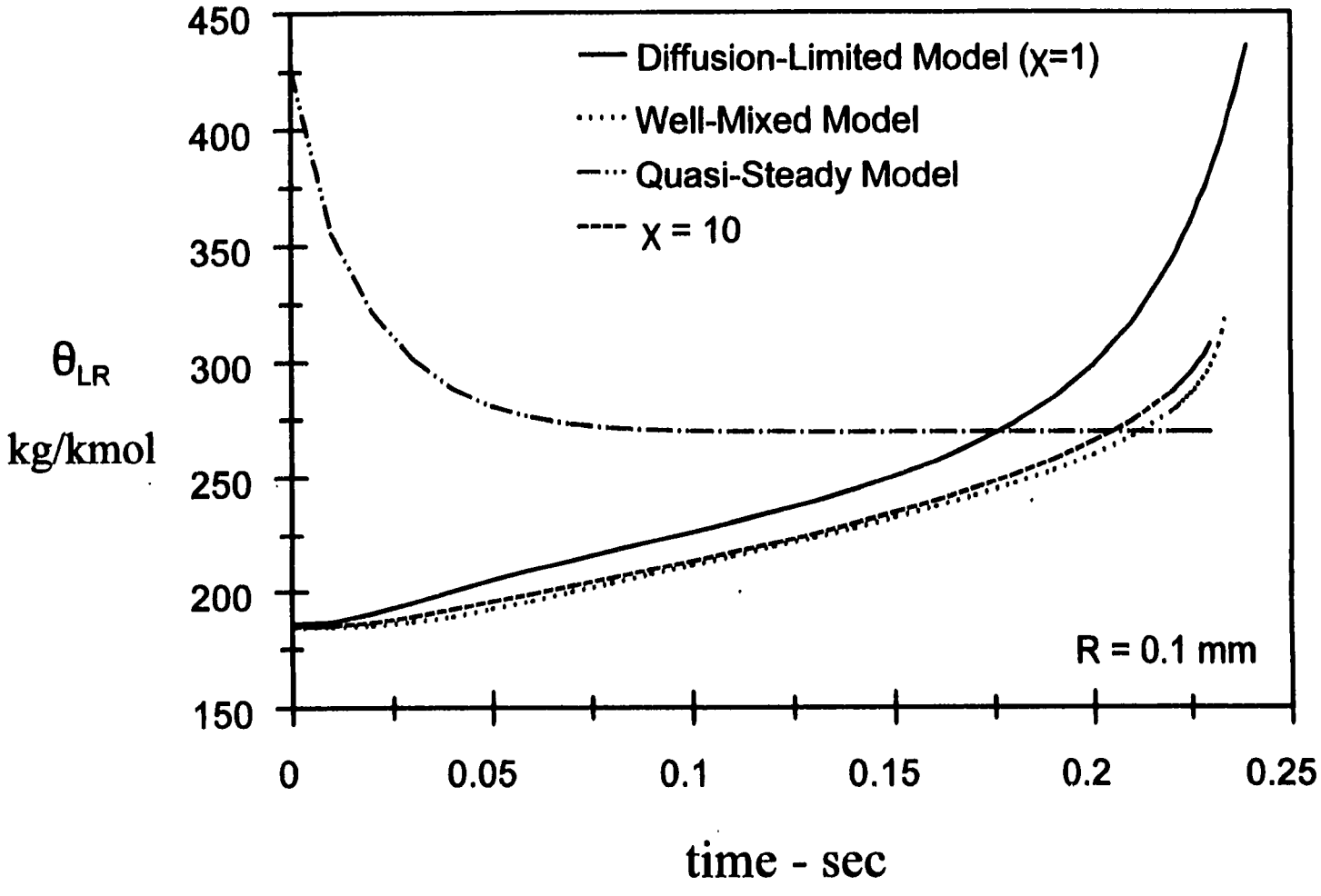

Figure 5.15 Mean of liquid distribution at droplet surface versus time for a 200μm Diesel droplet vaporizing at 1000 K, initial temperature 300 K: Comparison between two limiting mixing models (diffusion-limited and well-mixed models), the quasi-steady model and the full model with χ=10.

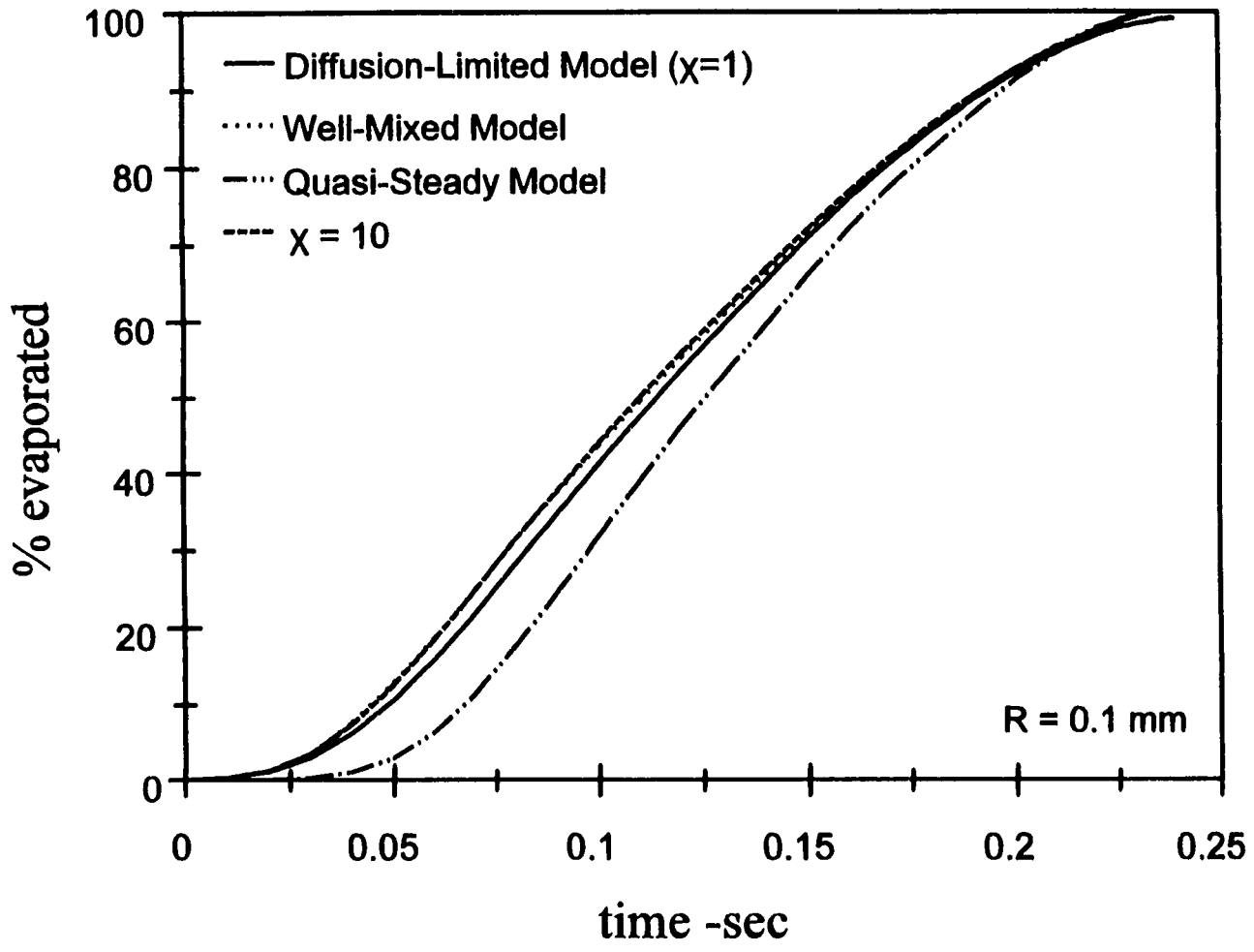

Figure 5.16 Droplet mass percent evaporated versus time for a 200μm Diesel droplet vaporizing at 1000 K, initial temperature 300 K: Comparison between two limiting mixing models (diffusion-limited and well-mixed models), the quasi-steady model and the full model with $\chi = 10$.

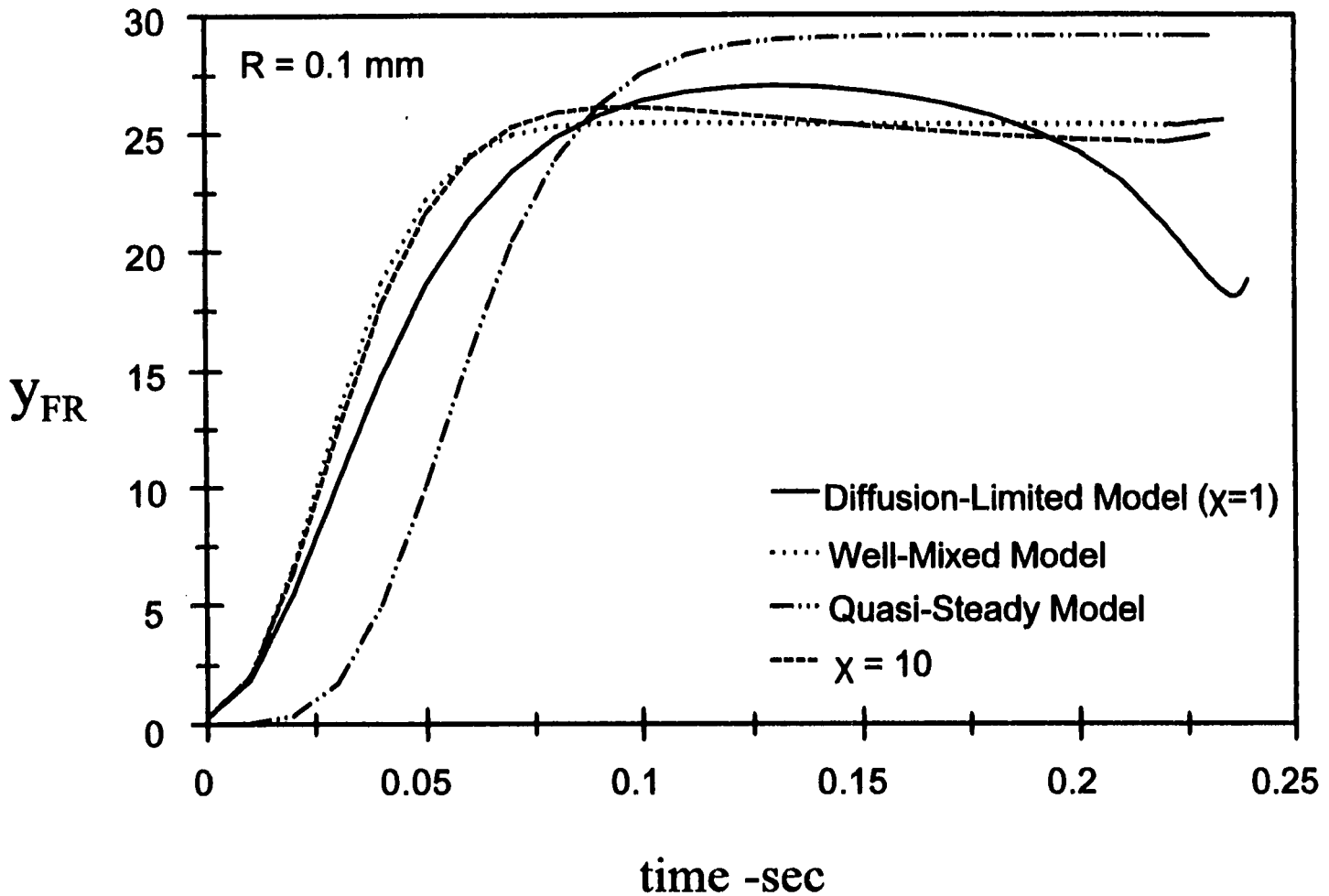

Figure 5.17 Vapour mole fraction at the surface versus time for a 200μm Diesel droplet vaporizing at 1000 K, initial temperature 300 K: Comparison between two limiting mixing models (diffusion-limited and well-mixed models), the quasi-steady model and the full model with $\chi = 10$.

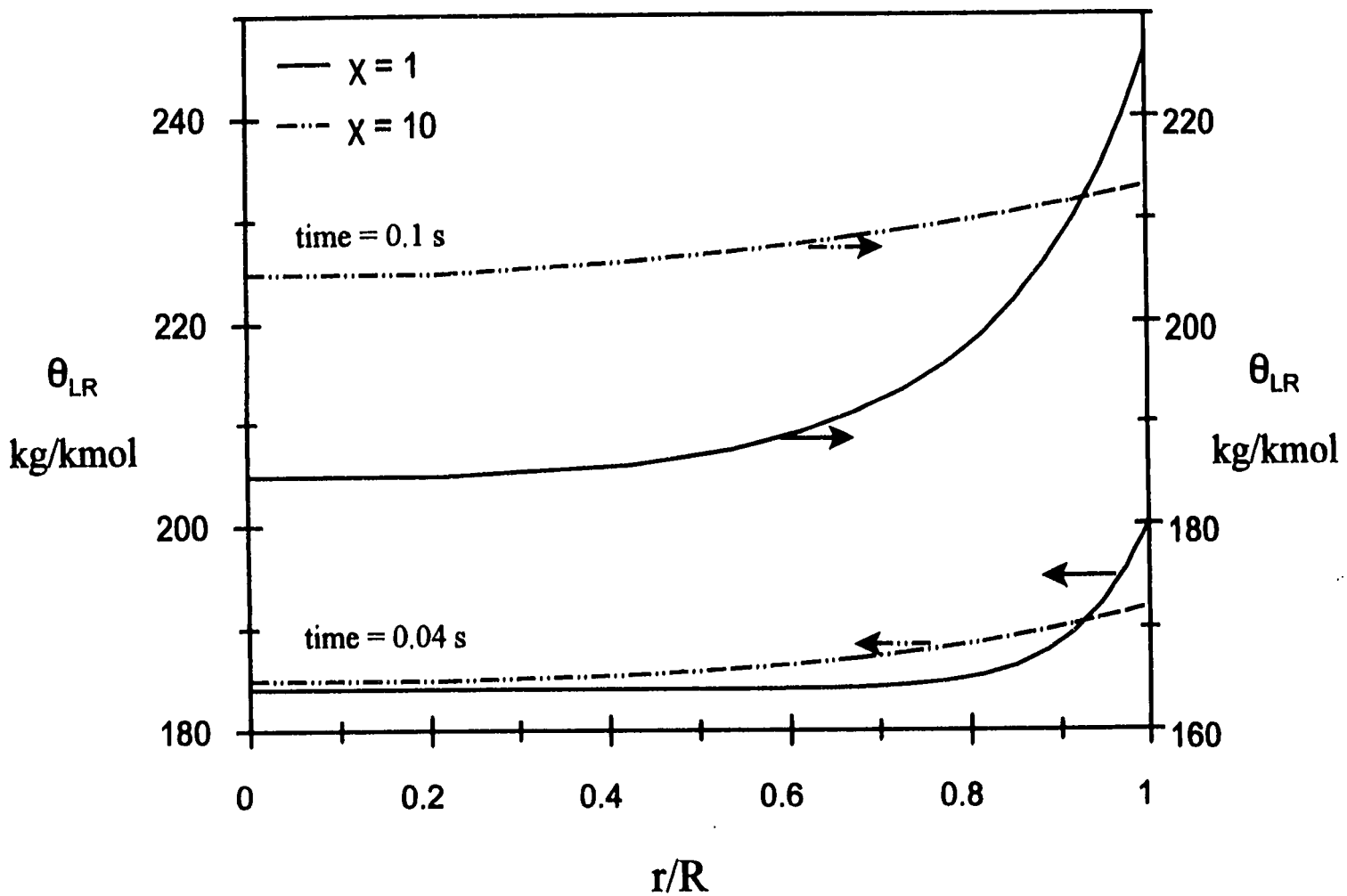

Figure 5.18 Profile of mean of liquid distribution inside droplet at two different time steps: t = 0.04 sec and t = 0.1 sec, for a 200μm Diesel droplet vaporizing at 1000 K, initial temperature 300 K: Comparison between the diffusion-limited model and the full model with $\chi = 10$.

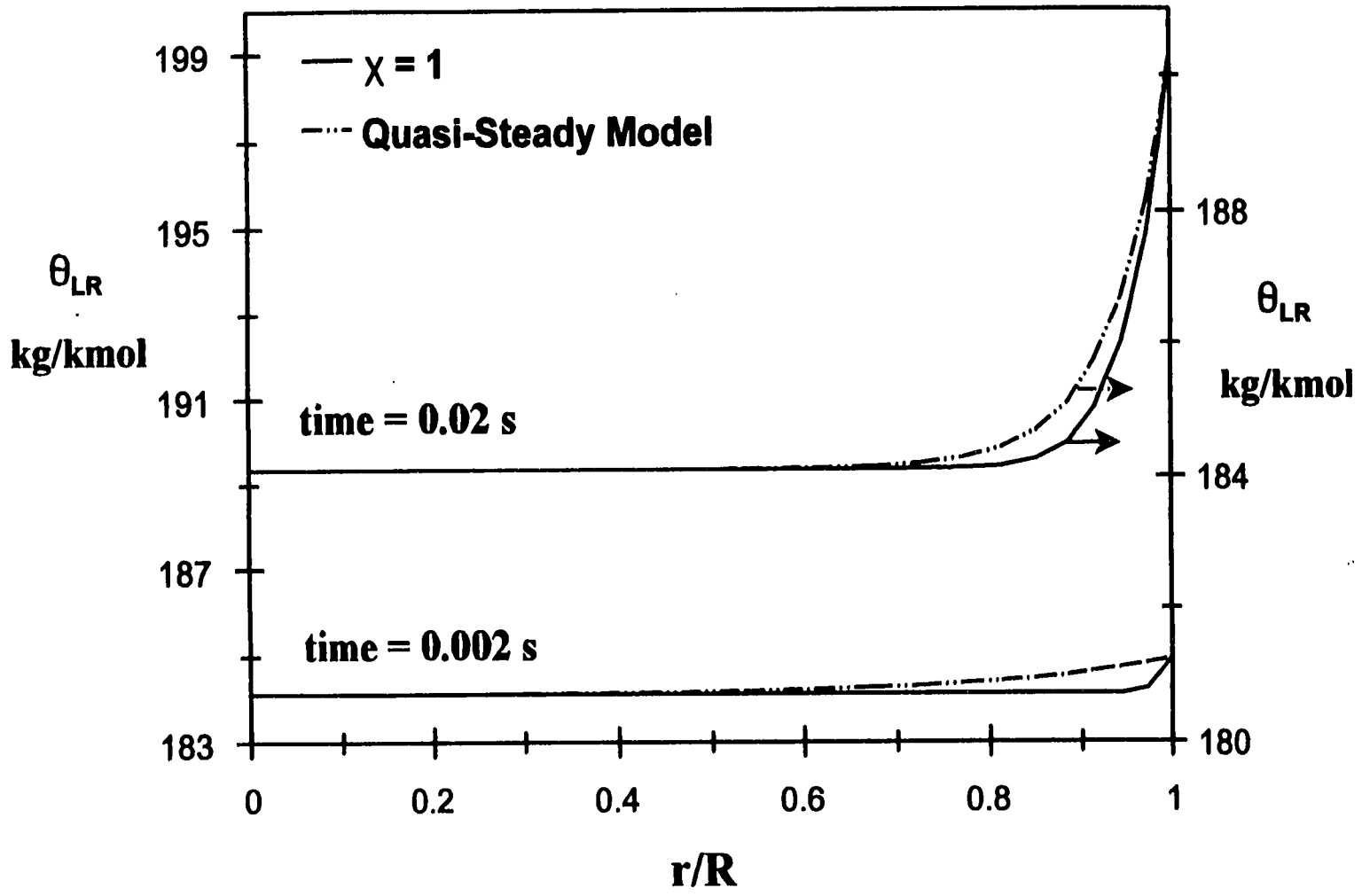

Figure 5.19 Profile of mean of liquid distribution inside droplet at two different time steps: t = 0.002 sec and t = 0.02 sec, for a 200μm Diesel droplet vaporizing at 1000 K, initial temperature 300 K: Comparison between the diffusion-limited model and the quasi-steady model.

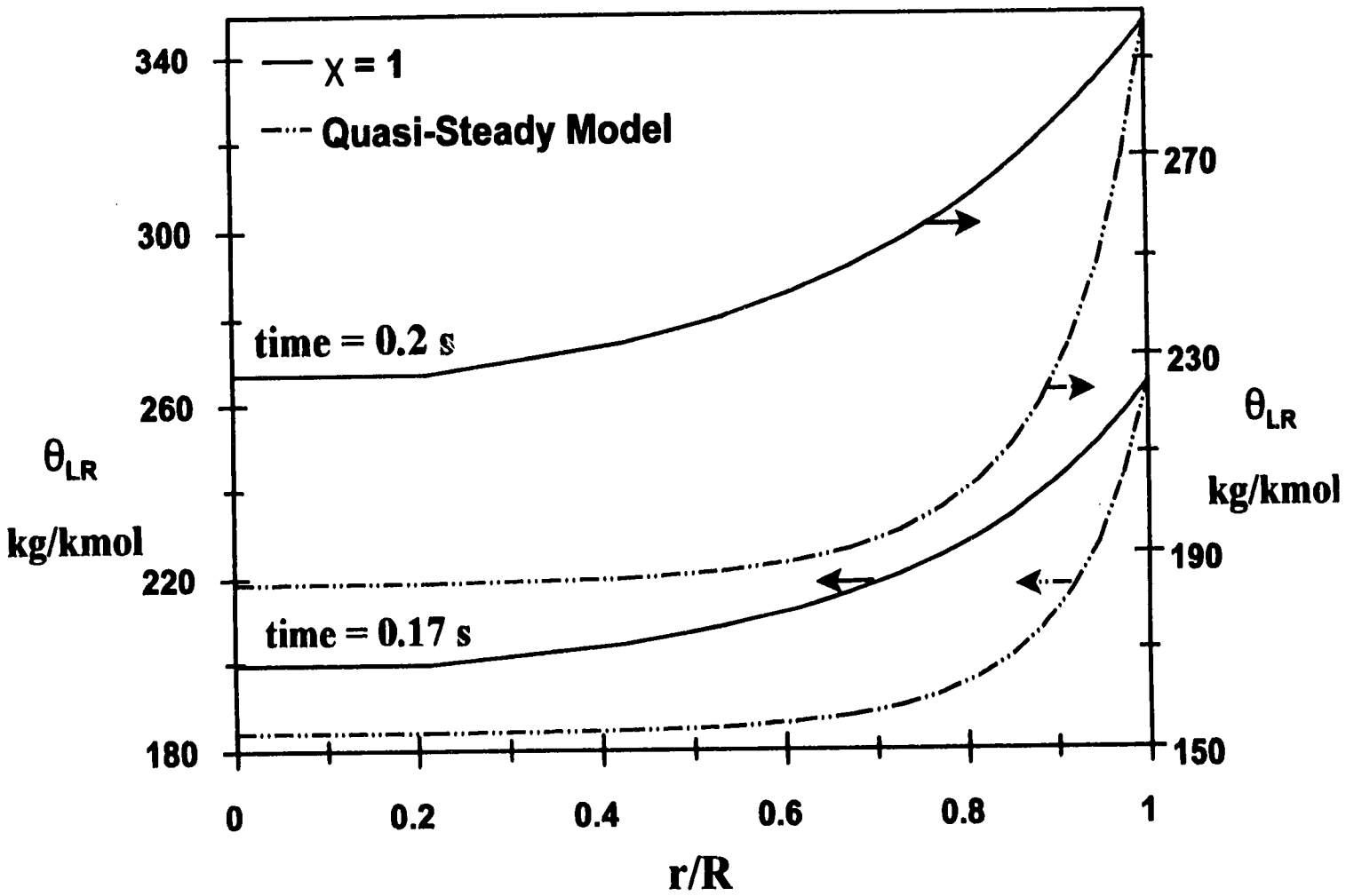

Figure 5.20 Profile of mean of liquid distribution inside droplet at two different time steps: t = 0.17 sec and t = 0.2 sec, for a 200μm Diesel droplet vaporizing at 1000 K, initial temperature 300 K: Comparison between the diffusion-limited model and the quasi-steady model.

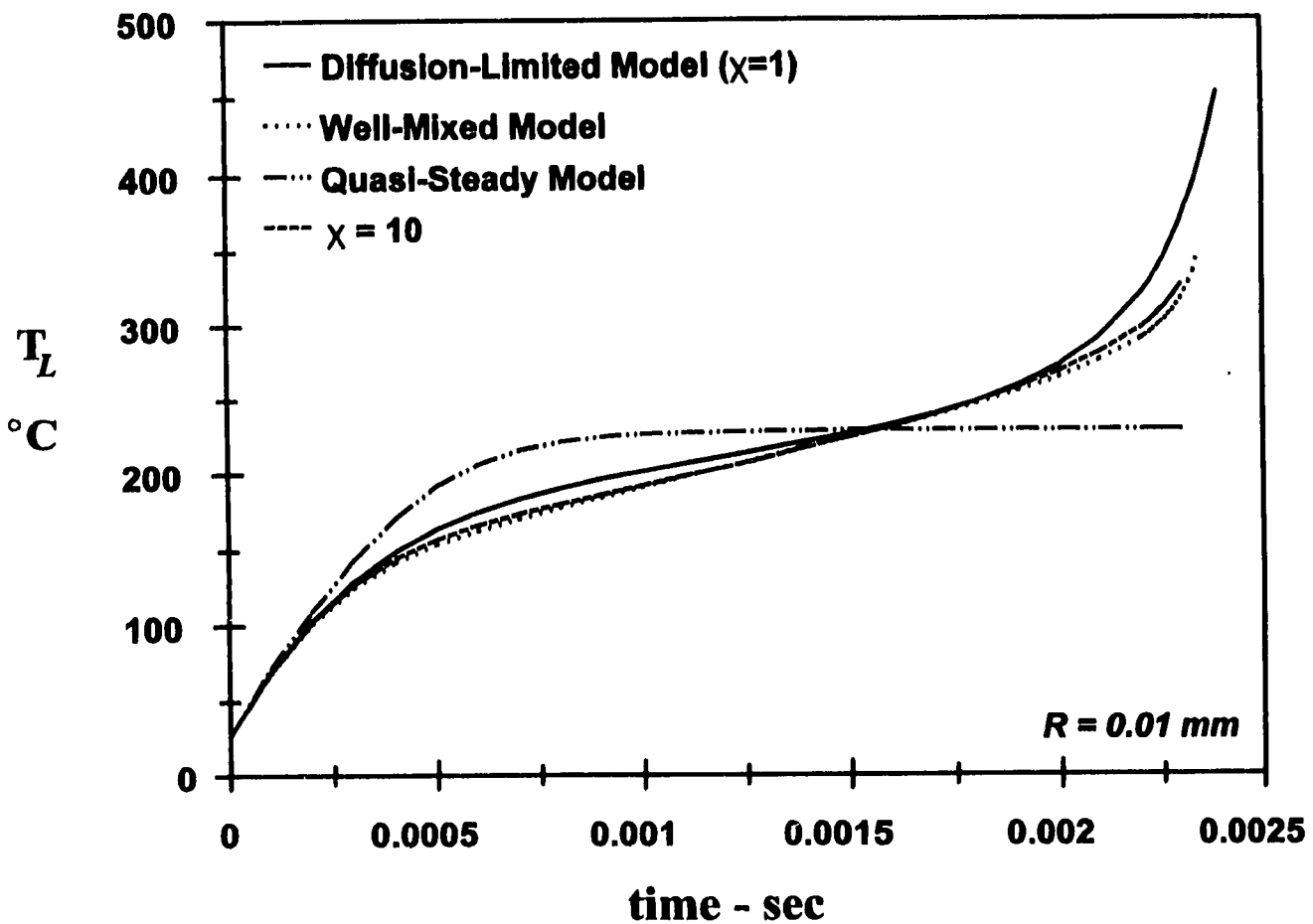

Figure 5.21 Droplet liquid temperature versus time for a 20μm Diesel droplet vaporizing at 1000 K, initial temperature 300 K: Comparison between two limiting mixing models (diffusion-limited and well-mixed models), the quasi-steady model and the full model with $\chi = 10$.

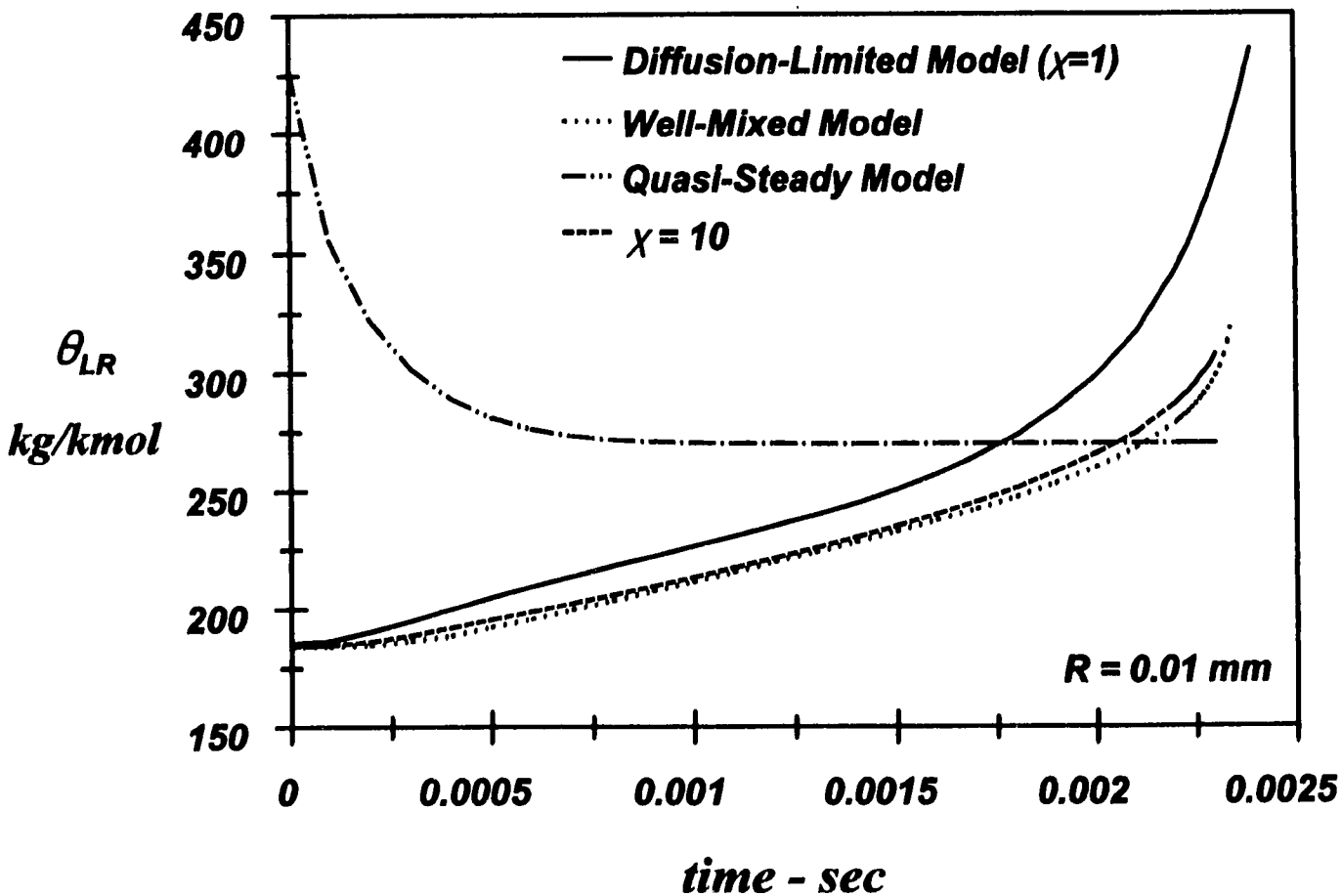

Figure 5.22 Mean of liquid distribution at droplet surface versus time for a 20μm Diesel droplet vaporizing at 1000 K, initial temperature 300 K: Comparison between two limiting mixing models (diffusion-limited and well-mixed models), the quasi-steady model and the full model with χ=10.

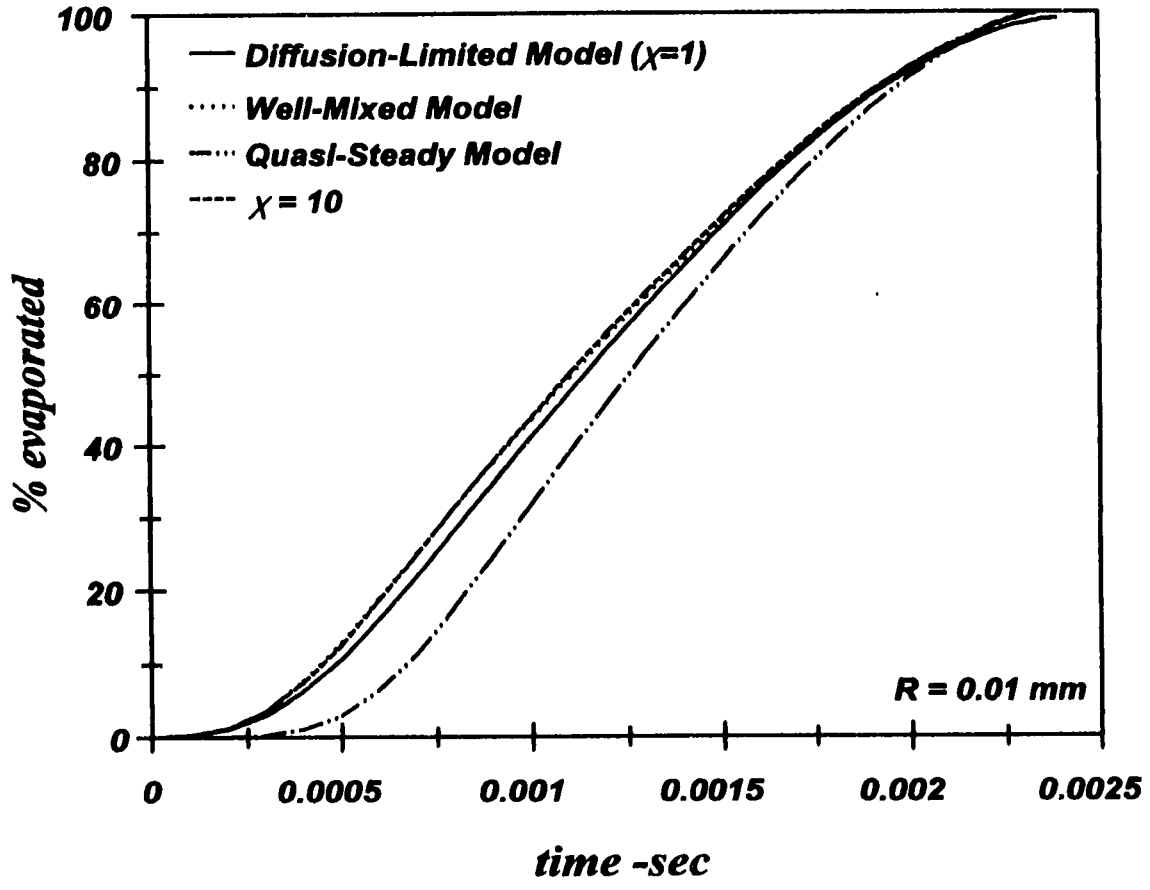

Figure 5.23 Droplet mass percent evaporated versus time for a 20μm Diesel droplet vaporizing at 1000 K, initial temperature 300 K: Comparison between two limiting mixing models (diffusion-limited and well-mixed models), the quasi-steady model and the full model with $\chi = 10$.

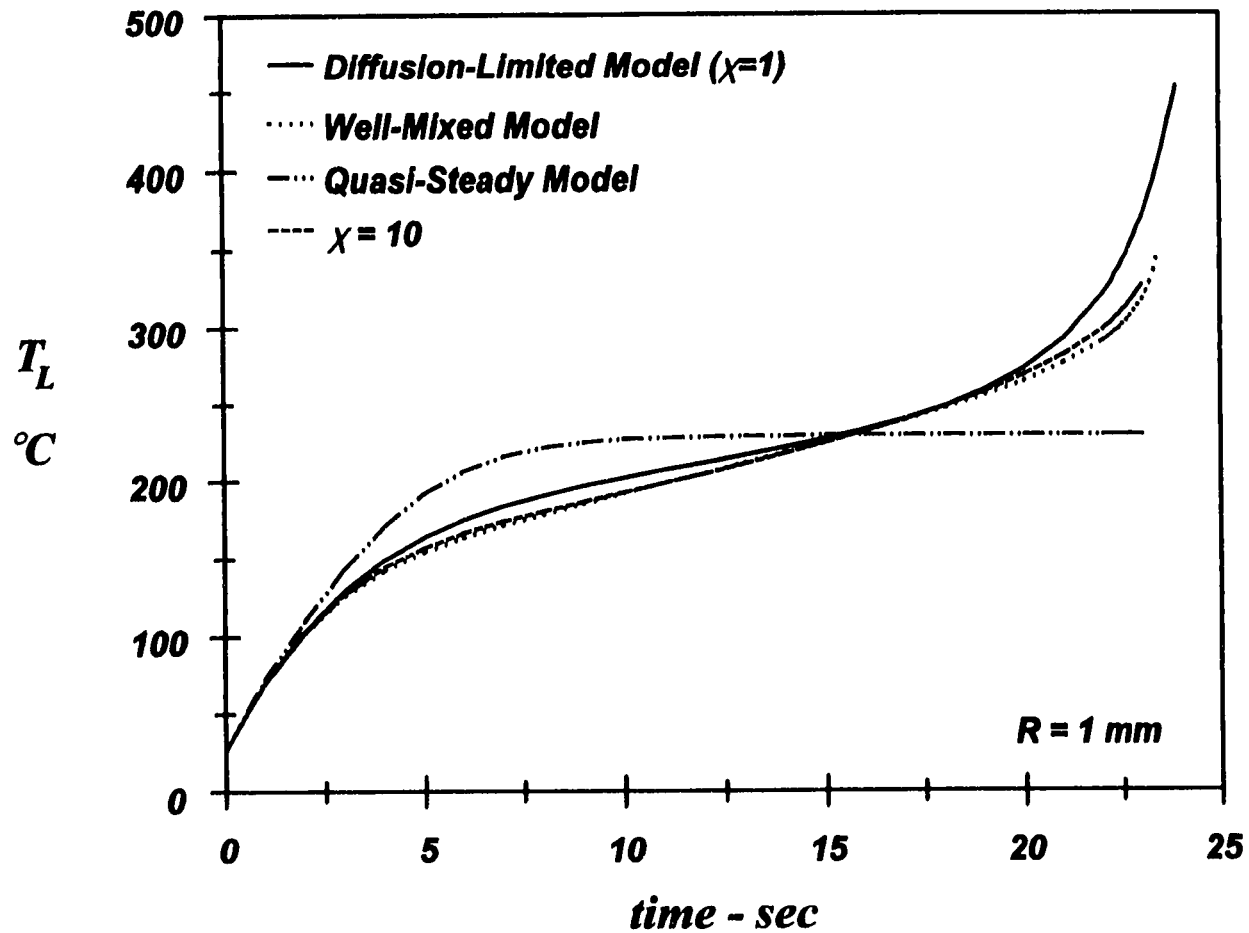

Figure 5.24 Droplet liquid temperature versus time for a 2000μm Diesel droplet vaporizing at 1000 K, initial temperature 300 K: Comparison between two limiting mixing models (diffusion-limited and well-mixed models), the quasi-steady model and the full model with $\chi = 10$.

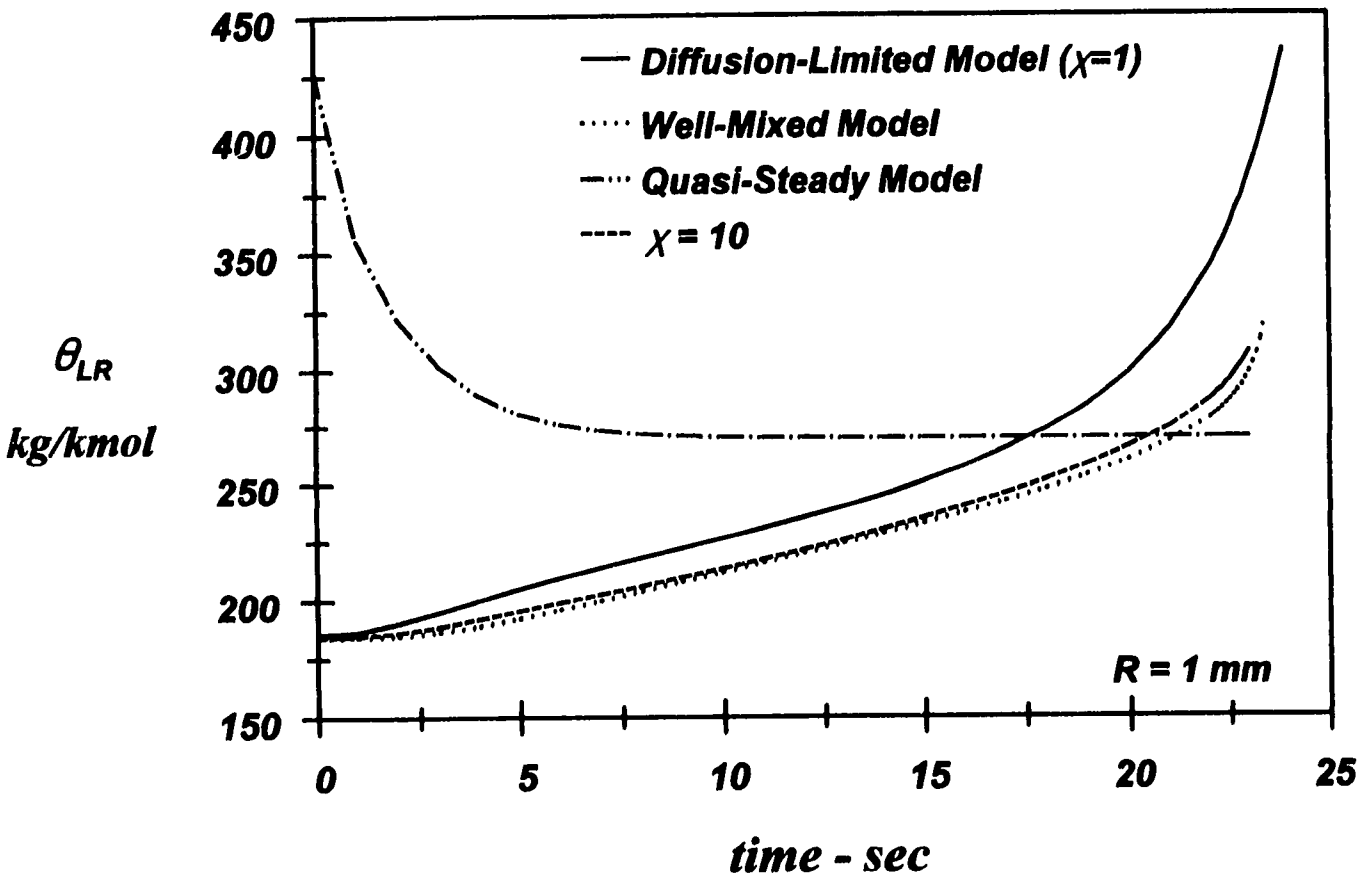

Figure 5.25 Mean of liquid distribution at droplet surface versus time for a 2000μm Diesel droplet vaporizing at 1000 K, initial temperature 300 K: Comparison between two limiting mixing models (diffusion-limited and well-mixed models), the quasi-steady model and the full model with $\chi = 10$.

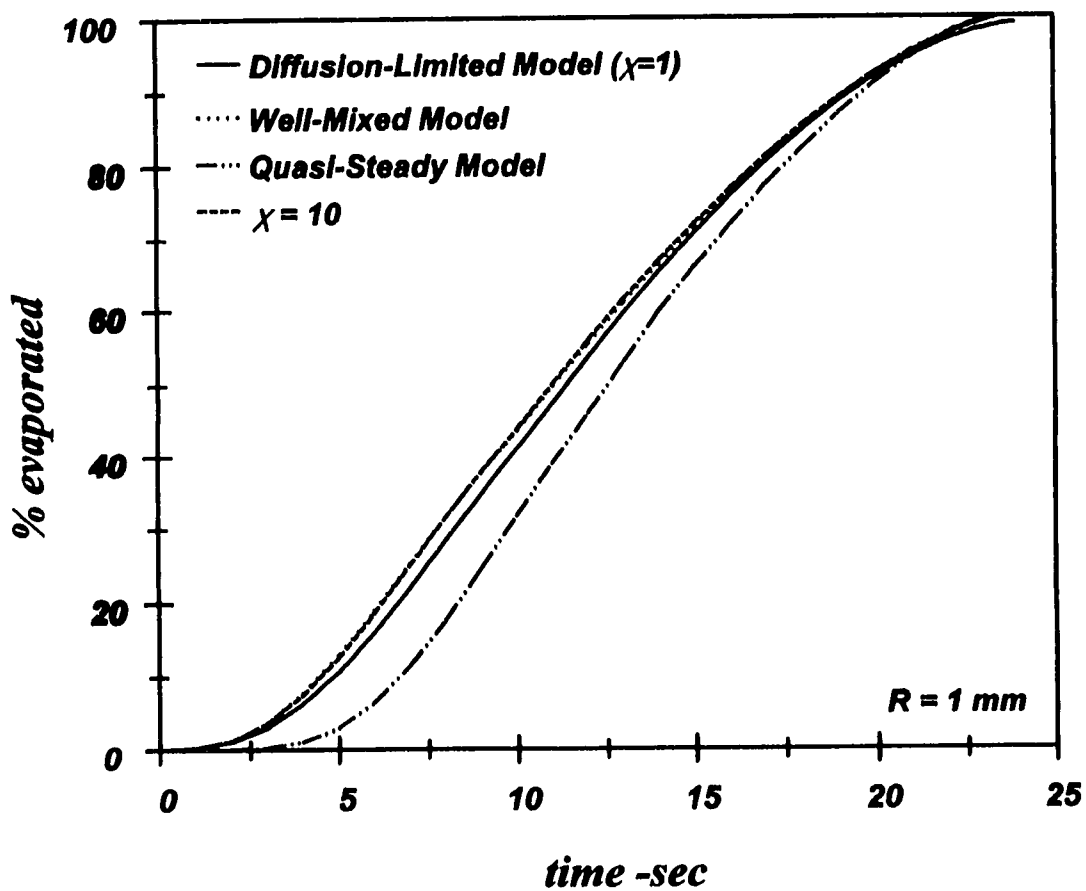

Figure 5.26 Droplet mass percent evaporated versus time for a 2000μm Diesel droplet vaporizing at 1000 K, initial temperature 300 K: Comparison between two limiting mixing models (diffusion-limited and well-mixed models), the quasi-steady model and the full model with $\chi = 10$.

CHAPTER 6: MULTIPLE DISTRIBUTIONS

6.1 Introduction

Most models developed using continuous thermodynamics have used only one distribution function to describe the fuel mixture either in the vapour or in the liquid phase. For fuel mixtures containing different groups of components (e.g., n-paraffins, aromatics, etc.) multiple distribution functions have been suggested , where each distribution can describe one group in the fuel mixture (see figure 6.1). Use of more than one distribution to characterize the fuel can be useful for:

- Representing fuels which are a mixture of n-paraffins, aromatics, etc.
- Representing fuels which are mixtures of very light and very heavy components.
- Representing single discrete components.

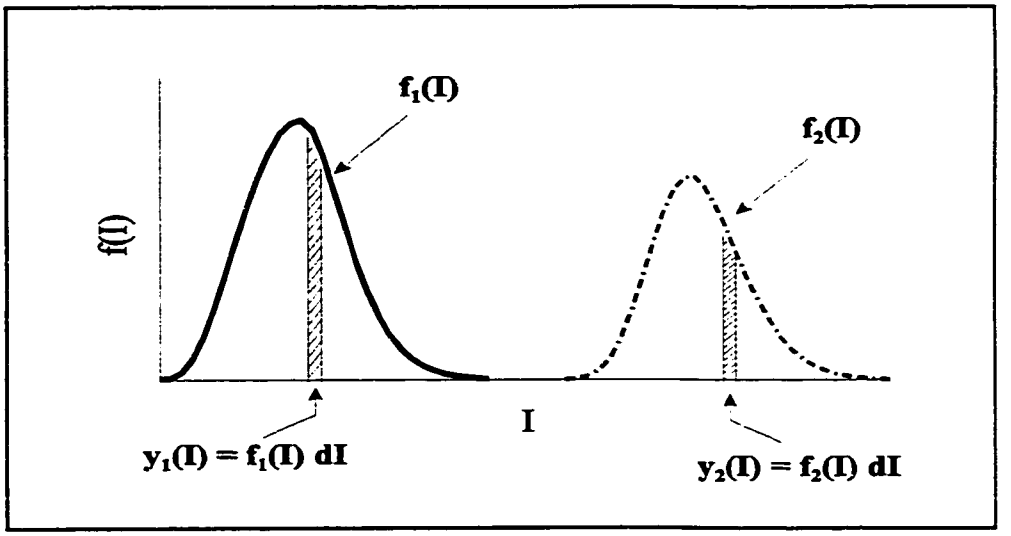

Figure 6.1: Multiple distribution functions to describe fuel mixture.

For this thesis, a multiple distribution model is used to assess the effects of liquid-phase mixing on the evaporation of a droplet with two components or distributions with very different boiling characteristics. The results of the model so far have indicated that liquid-phase mixing is unimportant; however, the literature survey showed that mixing can affect two-component droplets if the components have widely different boiling points. In this work, the multiple distribution model will be used to see if such effects occur for continuous mixtures.

The multiple distributions principle will be applied first to the well-mixed model of droplet evaporation developed by Tamim and Hallett (1995) and will then be expanded to include liquid phase diffusion.

We assume that the vapour phase is described by a number of distributions

$$f_1(I),\ f_2(I),\ \ldots,\ f_j(I)$$

while the liquid phase is given by:

$$f_{L1}(I),\ f_{L2}(I),\ \ldots,\ f_{Lj}(I)$$

The overall concentration of each distribution is given in the vapour phase by

$$y_{F1},\ y_{F2},\ \ldots,\ y_{Fj}$$

and in the liquid phase by

$$x_{F1},\ x_{F2},\ \ldots,\ x_{Fj}$$

6.2 Vapour Phase Equations

The vapour phase equations are exactly the same as (3.3-1) - (3.3-5) except that y_{F1}, y_{F2}, etc. replace y_F , and there will be different diffusivities $c\overline{D}_1, c\overline{D}_2$, etc. for each distribution. However, c and cv* are still for the whole mixture. There will be one set of these equations - i.e. one each for y_{Fj}, θ_j, ψ_j - for each distribution.

6.3 Well-Mixed Liquid-Liquid Balances

Equations for a well-mixed liquid phase will be developed first, since a well-mixed model will be required to compare to results with liquid phase diffusion. Here θ_L, ψ_L are uniform over the whole droplet. The overall balance equations are the same as equations (3.4-1) and (3.4-2). Equating liquid and vapour fluxes at the surface for a single discrete component gives (Tamim and Hallett, 1995)

$$Nx_{FjR}f_{LjR}(I)dI - \frac{c_L R}{3}\frac{d}{dt}\left(x_{FjR}f_{LjR}(I)dI\right)$$

$$= Ny_{FjR}f_{jR}(I)dI - cD_j(I)\frac{\partial}{\partial r}\left[y_{FjR}f_j(I)dI\right]_R \quad (6.3\text{-}1)$$

Integrating over I ($0 \rightarrow \infty$) and simplifying with assumptions as for the earlier transport equations yields:

$$\frac{dx_{Fj}}{dt} = \frac{3}{c_L R}\left[N\left(x_{Fj} - y_{Fj}\right) + c\overline{D}_j \frac{\partial y_{Fj}}{\partial r} \right]_R \qquad (6.3\text{-}2)$$

Multiplying equation (6.3-1) by I and integrating over I yields

$$\frac{d\left(x_F\theta_L\right)_j}{dt} = \frac{3}{c_L R}\left[N\left(\left(x_F\theta_L\right)_{jR} - \left(y_F\theta\right)_{jR}\right) + c\widetilde{D}_j \frac{\partial\left(y_F\theta\right)_j}{\partial r}\bigg|_R \right] \qquad (6.3\text{-}3)$$

Similarly, multiplying equation (6.3-1) by I^2 then integrating over I yields:

$$\frac{d\left(x_F\Psi_L\right)_j}{dt} = \frac{3}{c_L R}\left[N\left(\left(x_F\Psi_L\right)_j - \left(y_F\Psi\right)_j\right) + c\hat{D}_j \frac{\partial\left(y_F\Psi\right)_j}{\partial r}\bigg|_R \right] \qquad (6.3\text{-}4)$$

Summing equation (6.3-2) over all j, and assuming $\sum x_{Fj} = 1$ (no air dissolved in the liquid) yields

$$N\left(1 - \sum_j y_{Fj}\right) = \sum_j -c\overline{D}_j \frac{\partial y_{Fj}}{\partial r}\bigg|_R \qquad (6.3\text{-}7)$$

where the sum of the vapour mole fractions for all distributions is

$$\sum_{j=1}^{JN} y_{Fj} = y_F \qquad (6.3\text{-}8)$$

Equation (6.3-7) can be used to calculate the molar flux, N, after which equations (6.3-2) and (6.3-3) are applied to the liquid phase to find the change in liquid composition.

6.4 Energy Equation

Tamim and Hallett (1995) have used the vapour phase energy equation given here as (3.3-5) for a single distribution. This equation will be used for multiple distribution with modification of the interdiffusion term (the last term) by summing over all the distributions. The final expression for the interdiffusion term is

$$\sum_j \left\{ \left[\left(a_{Cj} - C_{PA} \right) c\overline{D}_j + b_{Cj}\theta_j c\widetilde{D}_j \right] \nabla y_{Fj} \right\} \nabla T \qquad (6.4\text{-}1)$$

6.5 Vapour-Liquid Equilibrium

The same equations for vapour-liquid equilibrium were used as for the single distribution model, except that a separate vapour-liquid equilibrium calculation now has to be made for each distribution.

6.6 Enthalpy of Vaporization

The enthalpy of vaporization is the sum of those for individual components weighted by their mole fluxes. The expression given by Tamim and Hallett (1995) requires modifications for multiple distributions. Using the vapour phase flux expression for one component (equation (6.3-1)) and integrating yields

$$Nh_{fg} = \sum_j \left\{ \left[\int_0^\infty Ny_{Fj} f_j(I) - cD_j(I) \frac{\partial}{\partial r}\left(y_{Fj} f_j(I)\right) \right]_R h_{fgj}(I) dI \right\} \qquad (6.6\text{-}1)$$

where the component enthalpy of vaporization is correlated with I as

$$h_{fgj}(I) = \left[a_{Hj} + b_{Hj} I\right] \Phi_{Hj} \qquad (6.6\text{-}2)$$

Values of a_H, b_H and Φ for n-paraffins are given by Tamim and Hallett (1995). Integrating equation (6.6-1) over I and neglecting terms with gradients of $D_j(I)$ yields

$$Nh_{fg} = \sum_j \Phi_{Hj} \left\{ a_{Hj} \left[Ny_{Fj} - c\overline{D}_j \frac{\partial y_{Fj}}{\partial r} \right]_R \right.$$

$$\left. + b_{Hj} \left[Ny_{Fj}\theta_j - c\widetilde{D}_j \frac{\hat{o}}{\partial r}\left(y_{Fj}\theta_j\right) \right]_R \right\} \qquad (6.6\text{-}3)$$

It should be noted that for one distribution, the first term simplifies to N.

6.7 Multiple Distributions with Diffusion-Limited Liquid Phase

Equations for the multi-distribution model with liquid phase diffusion can now be developed. The liquid phase transport equations are same as (3.2-19) - (3.2-21), for one distribution, except that x_F, θ_L, ψ_L, and D_L becomes x_{Fj}, θ_{Lj}, ψ_{Lj} and D_{Lj}. Three transport equations must be solved for each distribution.

6.7.1 Flux Relations at Droplet Surface

For multiple distributions, the vaporizing molar flux N is obtained by matching the component fluxes at the surface. Similar relations will be obtained as equations (3.4-7), (3.4-8) and (3.4-9):

$$N\left(x_{FjR} - y_{FjR}\right) = c_L \chi \overline{D}_{Lj} \left.\frac{\partial x_{Fj}}{\partial r}\right|_R - c\overline{D}_j \left.\frac{\partial y_{Fj}}{\partial r}\right|_R \tag{6.7-4}$$

$$N\left(x_{FjR}\theta_{LjR} - y_{FjR}\theta_{jR}\right) = c_L \chi \tilde{D}_{Lj} \left.\frac{\partial\left(x_{Fj}\theta_{Lj}\right)}{\partial r}\right|_R - c\tilde{D}_j \left.\frac{\partial\left(y_{Fj}\theta_j\right)}{\partial r}\right|_R \tag{6.7-5}$$

$$N\left(x_{FjR}\Psi_{LjR} - y_{FjR}\Psi_{jR}\right) = c_L \chi \hat{D}_{Lj} \left.\frac{\partial\left(x_{Fj}\Psi_{Lj}\right)}{\partial r}\right|_R - c\hat{D}_j \left.\frac{\partial\left(y_{Fj}\Psi_j\right)}{\partial r}\right|_R \tag{6.7-6}$$

Also, assuming that there is no air penetration into the droplet surface, the sum of the molar fractions of all distributions is

$$\sum_j x_{FjR} = 1 \qquad (6.7\text{-}7)$$

6.8 Results and Discussion of Results

In this chapter calculations for vaporizing droplets (no chemical reaction) will be presented to demonstrate the capabilities of the theory just developed. All calculations were made for n-paraffin mixtures.

6.8.1 Initial Parameters

All calculations were made for the same conditions as in chapter 5: an 0.2 mm diameter droplet initially at 300K, suddenly exposed to a hot environment at 1000K. 20 grid points were assumed in the vapour phase and 15 grid points in the liquid phase. Although it was proved in section 5.2.3 that the use of more grid points in the vapour phase will increase the precision of the results, 20 grid points still gives acceptable results, while reducing the run time, which was longer with the multiple distribution than for the single distribution. Also, the precision of the results is not of great concern at this stage, because all that is needed is to compare general behaviour.

The following results compare mixtures of different pure fuel components and Diesel fuel. The base case for comparison was the same "Diesel" n-paraffin mixture as in chapter 5 with an initial liquid distribution function of θ_L=184.12, σ_L= 41.5, γ = 44 (α_L = 11.3, β_L=12.4). A "kerosine" was also used for comparison purposes with initial distribution parameters of θ_L=115.5, σ_L= 35.8, γ = 30 (α_L =5.7, β_L=15). Pure fuels such as n-heptane, n-octane and n-hexadecane were represented by a very narrow distribution with a mean θ_L equal to the component molecular weight, a gamma value less than the distribution mean by 4 and a very small standard deviation (σ_L= 2).

To demonstrate the difference in volatility between pure fuels and Diesel, Figure 6.1 shows the distributions for these fuels. It can be noticed that n-heptane falls right at the edge of the Diesel distribution with a much lower boiling point than Diesel, which simulates a volatile additive to a Diesel fuel. The difference in volatility becomes less for Diesel/n-octane and reverses for Diesel/n-hexadecane.

6.8.2 Program Testing

To test the programs, a comparison between results developed using the single distribution was made with those of the multiple distribution model using two identical distributions and the same initial conditions. Different proportions of the two distributions were applied, such as 50%/50%, 80%/20%, 90%/10% and 60%/40%. Applying Diesel fuel to both distributions using same initial distribution parameters yields identical results for both the single and the multiple distribution programs. All transport properties of the single distribution model can

be reproduced using the multiple distribution model by using either model to describe the liquid phase internal mixing. This indicates that the programs are correct.

6.8.3 Droplet Evaporation-Effect of Liquid Mixing

To study the effect of liquid phase internal mixing upon fuel mixture with a highly volatile additive, an equimolar mixture of Diesel/n-heptane was applied for the multiple distribution programs using both models to describe the liquid phase internal mixing (the well-mixed and the diffusion-limited). Results of diesel/n-heptane mixture evaporation are plotted in Figures 6.2 - 6.4.

The rate at which the two fuels are produced is influenced to some degree by transport processes in the liquid phase. Liquid phase diffusion alone (χ=1) is very slow, so that diffusion is the only transport process in the droplet, the light component (n-heptane) in a layer near the surface becomes quickly depleted, and further production of light component is limited by diffusion into this surface layer. Using the well-mixed model will speed up transport of the light component to the surface. Figure 6.2 shows that liquid mixing does not greatly affect the liquid temperature history in the very early droplet life time. In each case, the droplet liquid temperature rises as lighter component (n-heptane) is distilled out. Since the well-mixed model will speed up the rate at which the more volatile component can reach the surface, this leads to a larger vapour mole fraction of n-heptane and thus a higher rate of evaporation of n-heptane compared with the diffusion-limited model (see Figure 6.3). For the well-mixed model, the liquid temperature rises more slowly during the period in which

the n-heptane vapour fraction reaches a maximum. Most of the n-heptane is evaporated during this time, and most of the heat supplied will be used for droplet evaporation only. This behaviour in liquid temperature is not shown for the diffusion-limited model because the rate of n-heptane evaporation is not as high as that for the well-mixed model. As the liquid temperature rises, the well-mixed model will allow more evaporation of n-heptane and less evaporation of diesel. Figure 6.4 shows the mean of the liquid distribution at the droplet surface θ_{LR} as a function of time. The behaviour achieved by the Diesel fuel is the same as for the single distribution model: θ_{LR} increases with time as the concentration of the less volatile components (Diesel) in the mixture rises. The θ_{LR} value of Diesel is higher for the diffusion model than that for the well-mixed model due to the lower evaporation of n-heptane because of diffusion effects, and thus more n-heptane in the liquid mixture. After the evaporation of most of the n-heptane for the well-mixed model, the vapour fraction of n-heptane will be decreased, and the Diesel fuel starts to increase in the vapour phase.

To represent the previous results in a simpler way, the mean over the droplet of the liquid mole fraction $\bar{x}_{Fj}$ was calculated for each distribution. Figure 6.5 shows that the decrease of n-heptane content in the droplet described by the well-mixed model is much faster than that described by the diffusion model, which in turn leads to a more rapid increase in the Diesel fraction in the liquid droplet for the well-mixed model than for the diffusion model.

The maximum mass percent evaporated that could be achieved for the Diesel/n-heptane mixture using (χ=1) was about 56%, after which the program refused to converge. This is

much lower than the evaporation achieved by the well-mixed model; however, at the end of this run, there is only about 1% n-heptane left. Because of this, any significant mixing effects will be concentrated near the beginning of the droplet life time, and behaviour at the end of the life time is of less interest.

Using a Diesel/n-octane mixture instead improves convergence and the program can achieve a mass percent evaporated up to 72%. This suggests that the convergence problems are related to the difference in volatility between the components. The same evaporation behaviour is achieved for diesel/n-octane as for the diesel/n-heptane mixture, as shown in Figure 6.6, except that there is less difference between the diffusion-limited and the well-mixed cases. The mean concentration of n-octane in the liquid droplet using the diffusion model is higher than that for the well-mixed model, which agrees with the previous results.

The fuel n-hexadecane has a higher boiling point than Diesel and its molecular weight is only 41 kg/kmol higher than θ_L of the Diesel distribution (See figure 6.1). This mixture reached up to 97.5% evaporation using the diffusion-limited model. Diesel is the first component to show up in the vapour phase since it is the lightest component in the mixture now. The mean concentration of n-hexadecane in the liquid mixture with χ=1 is less than that using the well-mixed model because the n-hexadecane represents the heaviest component in the mixture (see Figure 6.7). The θ_{LR} value for Diesel for a large χ is lower than that for χ=1 (Figure 6.8) because the light components are removed from the surface layer for χ=1, just as was found for the single distribution model. Late in the droplet life time, the rise in θ_L for the Diesel means that the Diesel becomes heavier than hexadecane; thus the concentration of the n-

hexadecane, now the most volatile, starts to decrease rapidly till it is depleted at the end of evaporation (Figure 6.7).

A Diesel/kerosine equimolar mixture was also tested with the multiple distributions program, trying to compare between two distributions of widely differing mean θ_L (see Figure 6.1). Kerosine behaves in a similar way to n-heptane and n-octane. Figure 6.9 shows the change of kerosine and diesel concentration through out the droplet life time using both liquid mixing models.

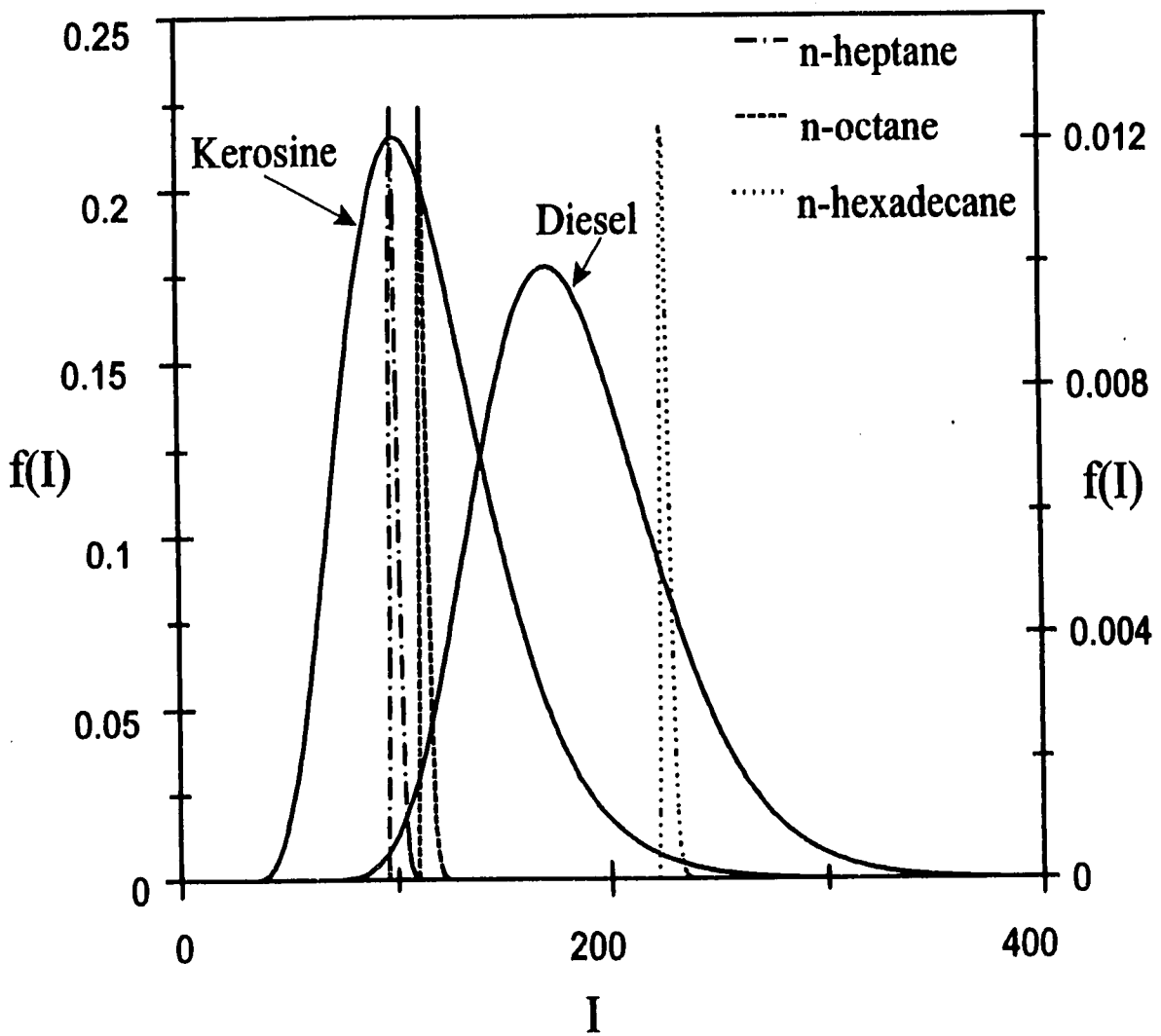

Figure 6.1 Distribution curves for: Diesel, "kerosine", n-heptane, n-octane, n-hexadecane.

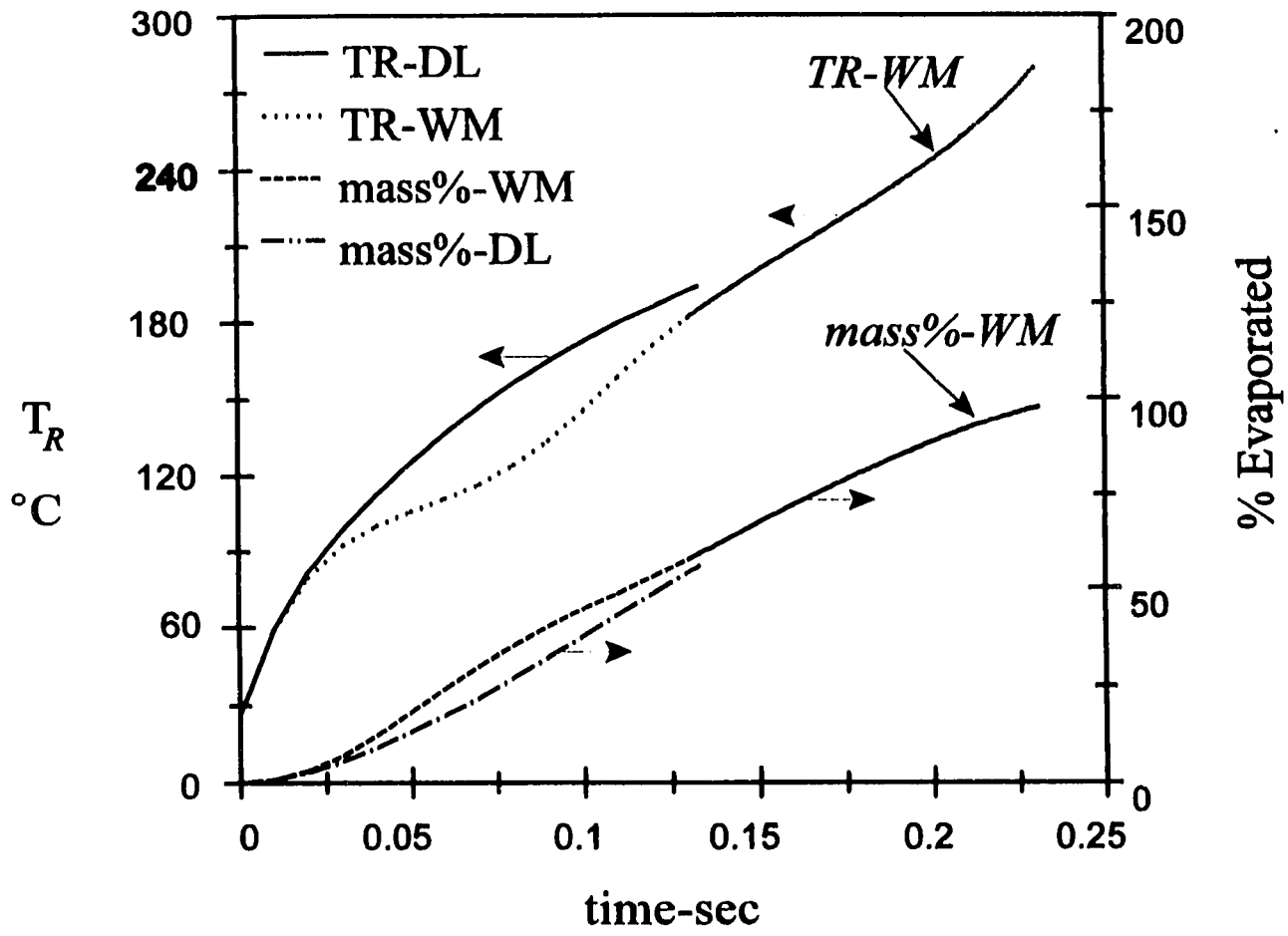

Figure 6.2 Droplet liquid temperature and mass percent evaporated versus time for a 200μm Diesel/n-heptane equimolar droplet mixture vaporizing at 1000 K, initial temperature 300 K: Comparison between the well-mixed model and the diffusion-limited model (χ=1). (Note: For longer times, calculated points are closely spaced and resemble a solid line).

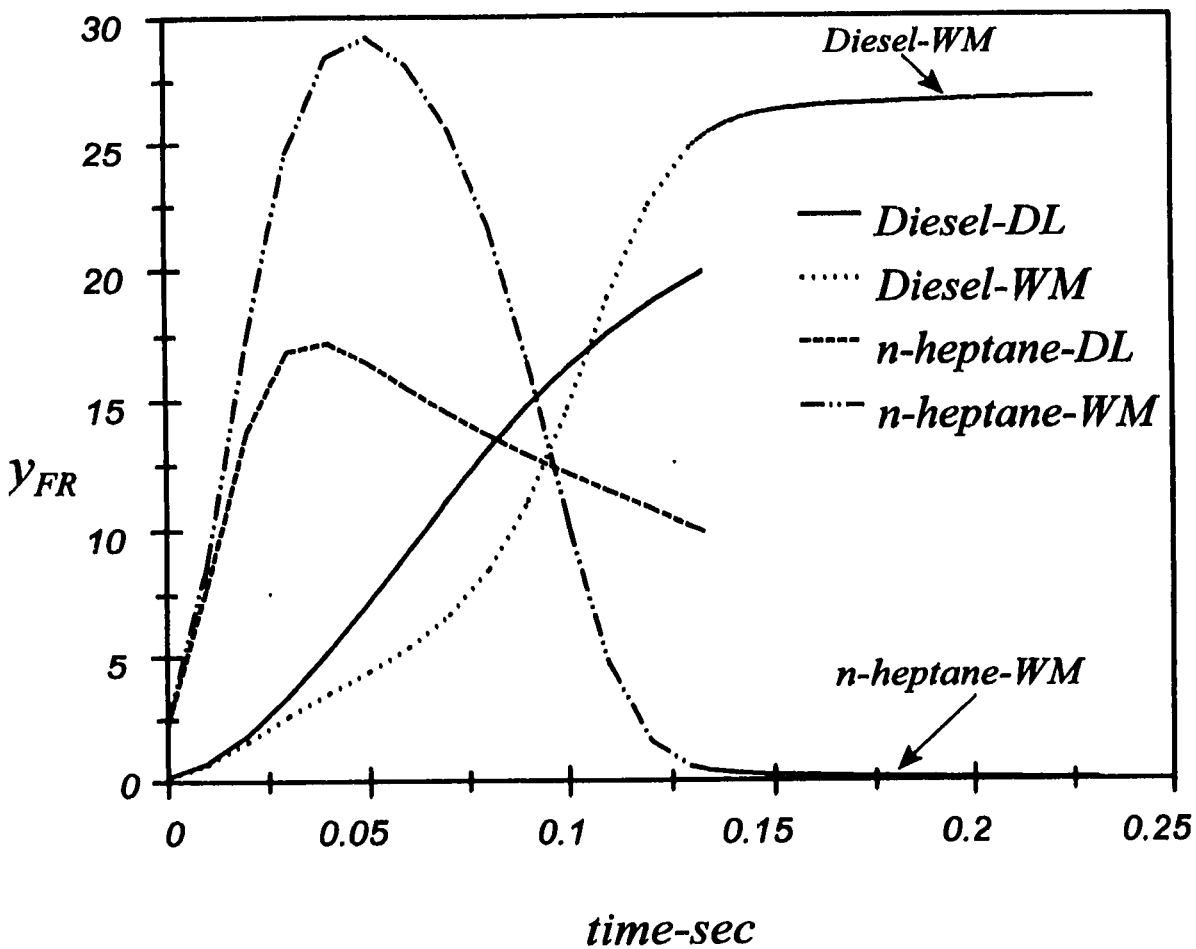

Figure 6.3 Vapour mole fraction at the surface versus time for a 200μm Diesel/n-heptane equimolar droplet mixture vaporizing at 1000 K, initial temperature 300 K: Comparison between the well-mixed model and the diffusion-limited model (χ=1). (Note: For longer times, calculated points are closely spaced and resemble a solid line).

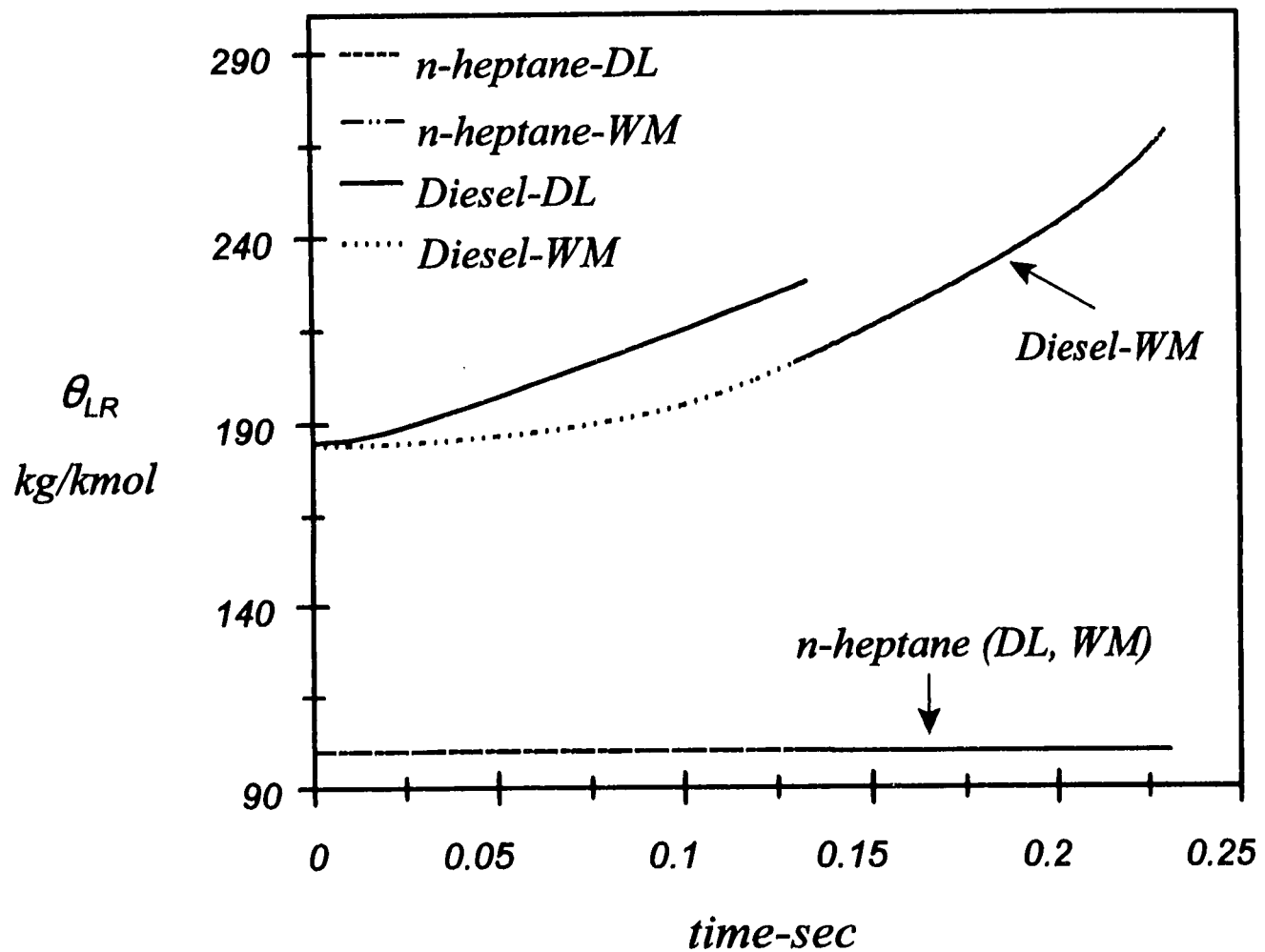

Figure 6.4 Mean of liquid distribution at droplet surface versus time for a 200μm Diesel/n-heptane equimolar droplet mixture vaporizing at 1000 K, initial temperature 300 K: Comparison between the well-mixed model and the diffusion-limited model (χ=1). (Note: For longer times, calculated points are closely spaced and resemble a solid line).

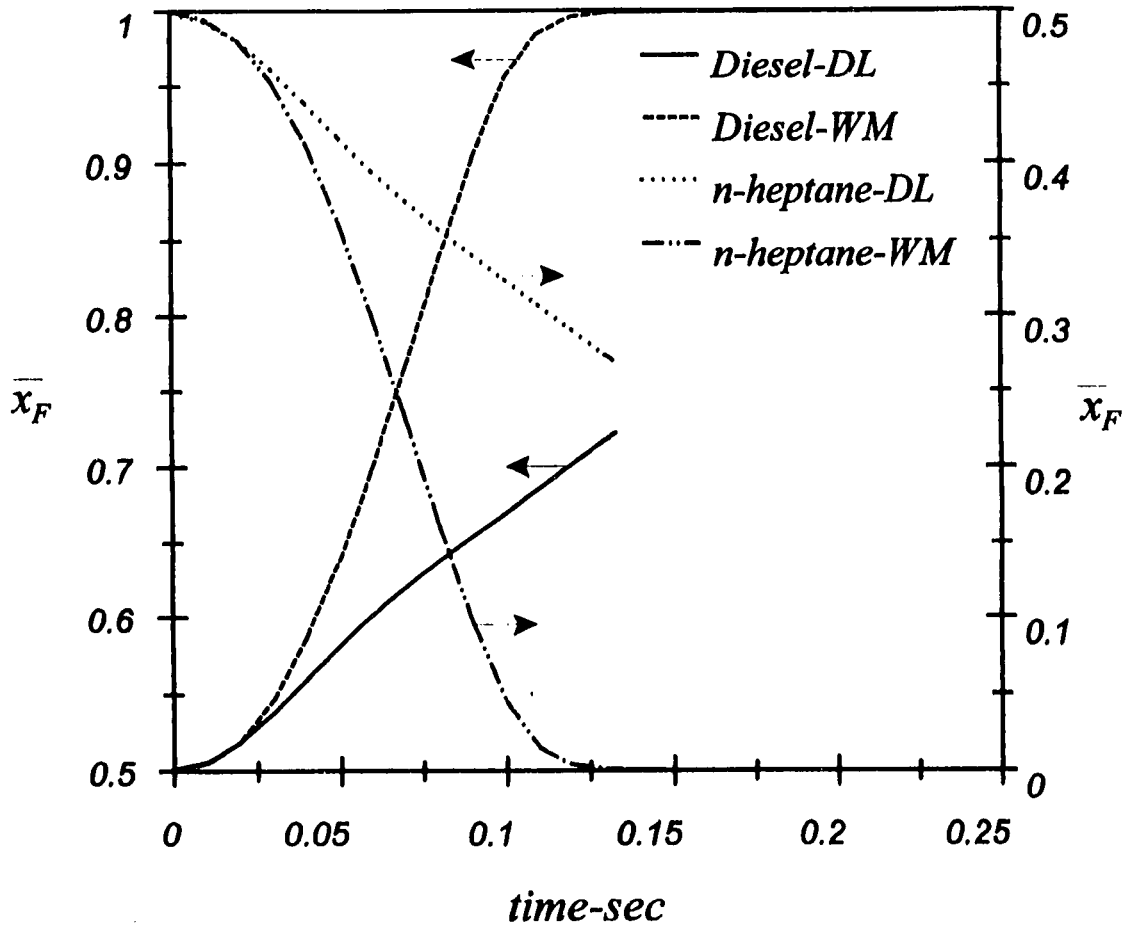

Figure 6.5 Mean of liquid mole fraction at droplet surface versus time for a 200μm Diesel/n-heptane equimolar droplet mixture vaporizing at 1000 K, initial temperature 300 K: Comparison between the well-mixed model and the diffusion-limited model (χ=1).

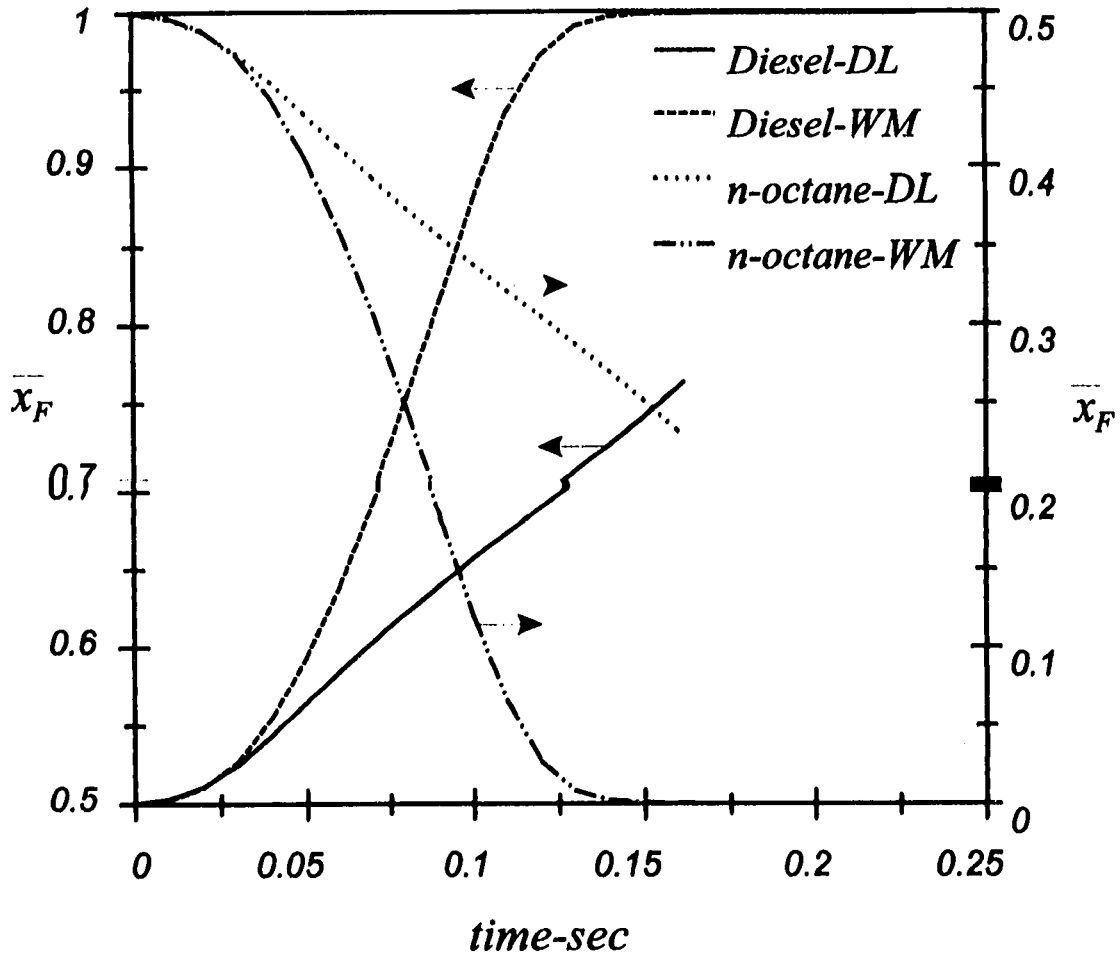

Figure 6.6 Mean of liquid mole fraction at droplet surface versus time for a 200μm Diesel/n-octane equimolar droplet mixture vaporizing at 1000 K, initial temperature 300 K: Comparison between the well-mixed model and the diffusion-limited model (χ=1).

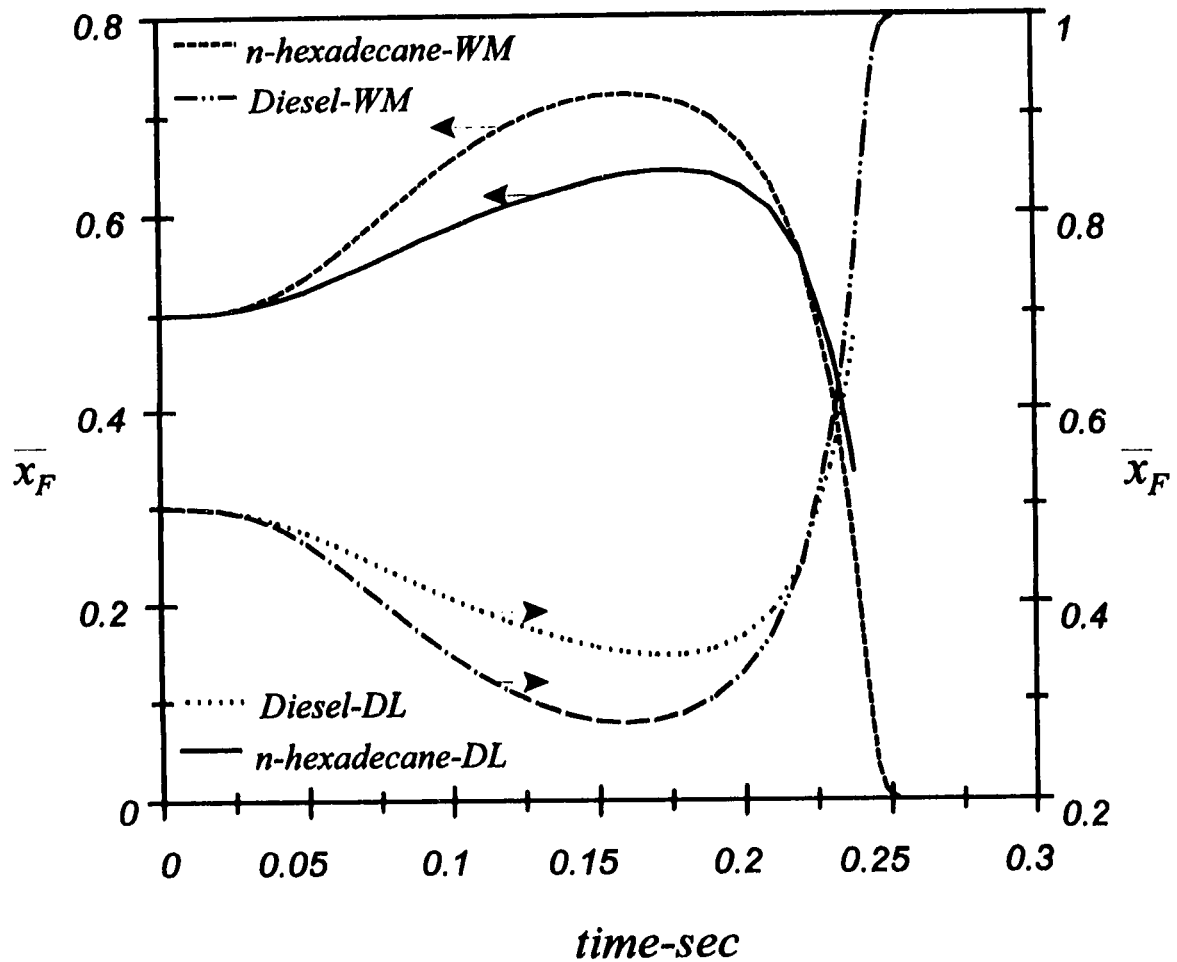

Figure 6.7 Mean of liquid mole fraction at droplet surface versus time for a 200μm Diesel/n-hexadecane equimolar droplet mixture vaporizing at 1000 K, initial temperature 300 K: Comparison between the well-mixed model and the diffusion-limited model (χ=1).

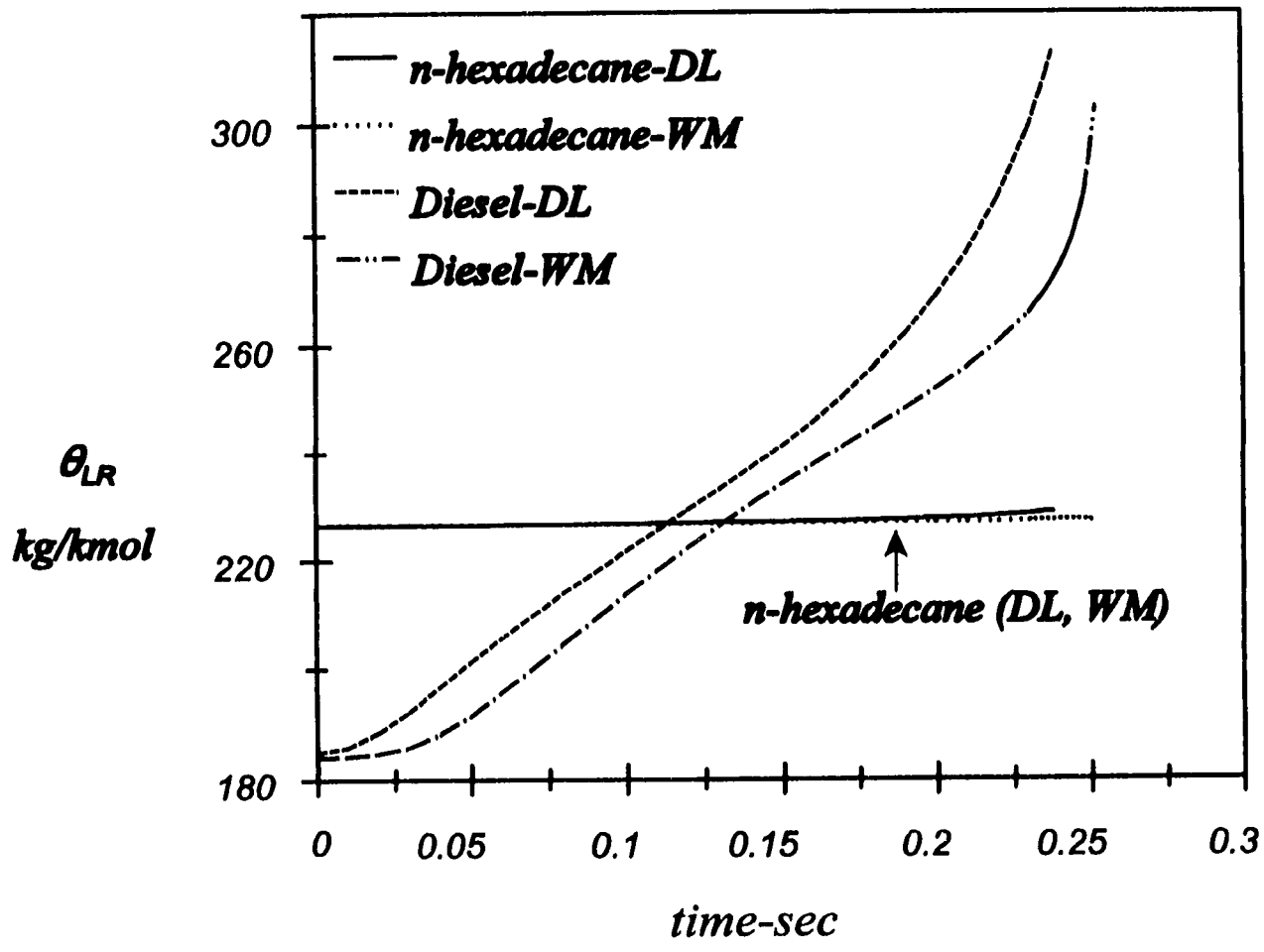

Figure 6.8 Mean of liquid distribution at droplet surface versus time for a 200μm Diesel/n-hexadecane equimolar droplet mixture vaporizing at 1000 K, initial temperature 300 K: Comparison between the well-mixed model and the diffusion-limited model (χ=1).

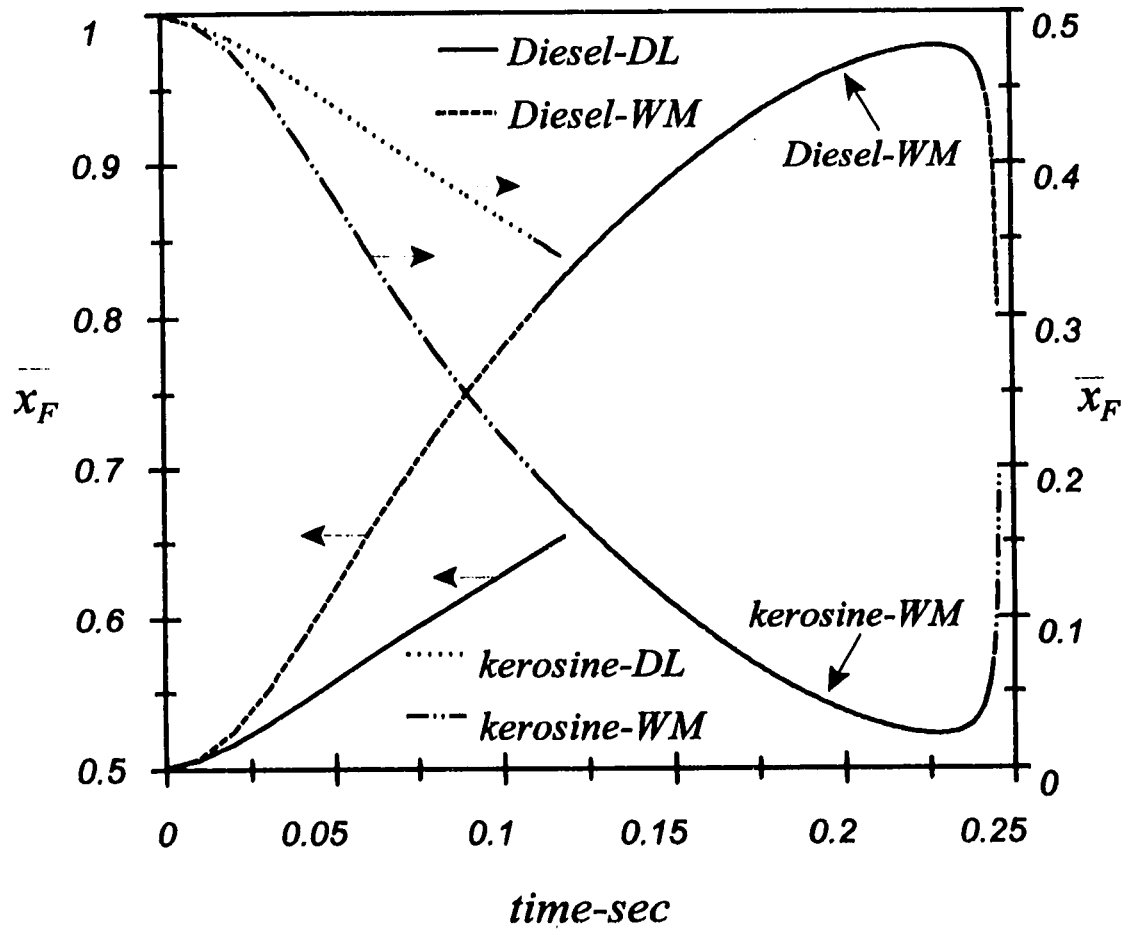

Figure 6.9 Mean of liquid mole fraction at droplet surface versus time for a 200μm Diesel/kerosine equimolar droplet mixture vaporizing at 1000 K, initial temperature 300 K: Comparison between the well-mixed model and the diffusion-limited model (χ=1). (Note: For longer times, calculated points are closely spaced and resemble a solid line).

CHAPTER 7: CONCLUSIONS AND RECOMMENDATIONS

7.1 General Conclusions

This work aims to study the effect of liquid phase internal mixing upon on evaporation process of continuous mixtures. The diffusion-limited and the well-mixed models were the extreme cases which describe liquid droplet internal mixing. The value of liquid diffusivity was multiplied by a mixing factor χ, where pure diffusion was presented using χ=1, while increasing χ to 10 & 100 means higher mixing rate in the droplet. The last part of this work allows the use of a two distributions mixture, which facilitates showing the effect of liquid mixing using wide range of components volatilities. The main conclusions to be drawn from the present work are as follows:

1. The simulation results show that the state of mixing in the liquid phase does not significantly affect the vaporization of a droplet of continuous mixture represented by a single distribution. The droplet temperature and evaporation rates were identical regardless of the state of mixing except at the very end of the process, when a diffusion-limited droplet rises to a higher temperature than a well-mixed one.
2. Relatively small values of the mixing factor χ are required to produce well-mixed behaviour (a factor of 10 for example is sufficient).
3. The well-mixed model can therefore be used for most practical calculations instead of the full diffusion model which will simplify the calculations.
4. The state of mixing in the liquid phase does have some effect on evaporation

behaviour for two distributions of widely differing boiling points or a mixture of fuel with a very volatile additive. The temperature for the diffusion-limited case is higher than that for the well-mixed case, and thus a faster rate of evaporation for the well-mixed over the diffusion model. Liquid mixing effects upon evaporation process showed to be more important for mixtures with large difference in boiling point (large difference in their mean molecular weight, like diesel/n-heptane mixture). As these differences lowered, the liquid mixing becomes less important (like the case of diesel/n-hexadecane mixture).

5. The quasi-steady liquid state assumed by Law and Law does not exist, and thus a quasi-steady model can not be used instead of the full diffusion model for the liquid phase. The liquid phase was shown here to be in a transient state throughout the droplet lifetime.

7.2 Recommendations for Future Work

- Performing of experiments testing the effect of liquid mixing on evaporation process will help verify the model. Liquid droplet evaporation in nitrogen atmosphere will avoid droplet combustion and/or ignition at high atmospheric temperature (1000 K), Liquid temperature of the droplet as well as the droplet shrinkage should be measured as a function of time. Freezing the droplet by liquid nitrogen will allow the analysis of the droplet composition at a certain time.
- The effect of liquid mixing at high pressure should be investigated and compared with those at low or moderate pressure. This will include the effect variation of the liquid mole fraction in space because air will start to diffuse inside the droplet.
- The effect of allowing the liquid droplet temperature to vary spatially inside the droplet should be investigated to investigate the effect of liquid diffusion accompanied with thermal diffusion.
- Investigation the effect of liquid mixing in the case of the presence of a chemical reaction between the fuel and oxygen (combustion and/or ignition).
- Investigation the effect of selection of a distribution function other than the gamma distribution which might help improve the results by avoiding unbounded distribution effects.
- Finally, the effect of heat transferred by radiation should be included in the diffusion-limited case to show its effects upon evaporation process.

LIST OF REFERENCES

Abramovitz, M. and Stegun, I. A., *Handbook of Mathematical Functions,* Dover, NewYork (1970).

Abramzon, B. and Sirignano, W. A., "Droplet vaporization model for spray combustion calculations", *Int. J. Heat Mass Transfer*, **32**, 1605-1618 (1989).

Aggrawal, S. K., "Modeling of a dilute vaporizing mutli-component fuel spray", *Int. J. Heat Transfer*, **30**, 1949-1961 (1987).

Angelos, C. P. and Ewing, R. E., "Continuous thermodynamic correlations for thermal simulations using a cubic equation of state", *AIChE Symposium Series*, **84**, 186-190 (1988).

Behrens, R. A. and Sandler, S. I., "The use of semicontinuous description to model the C_{7+} fraction in equation of state calculations", *SPE Reservoir Engineering*, **3**, 1041-1047, Aug. (1988).

Bergeron, C. A. and Hallett, W. L., "Auto-ignition of single droplets of two component liquid fuels", *Combust. Sci. and Tech.*, **65**, 181-194 (1989a).

Bergeron, C. A. and Hallett, W. L., "Ignition characteristics of liquid hydrocarbon fuels as single droplets", *Can. J. Chem. Eng.*, **67**, 142-149 (1989b).

Bergeron, C. A. and Hallett, W. L., "Ignition of multi-component liquid fuels",*Final Report for the Dept. of National Defence, Defence Research Est. Ottawa*, (1987).

Briano, J. G. and Glandt, E. D., "Molecular thermodynamics of continuous mixtures", *Fluid Phase Equilibria*, **14**, 91-102 (1983).

Browarzik, D., Kowalewski, M. and Kehlen H., "Stability calculations of semicontinuous mixtures based on equation of state", *Fluid Phase Equilibria*, **142**, 149-162 (1998)

Chou, G. F. and Prausnitz, J. M., "Adiabatic flash calculations for continuous or semicontinuous mixtures using an equation of state", *Fluid Phase Equilibria*, **30**, 75-82 (1986).

Cotterman, R. L. and Prausnitz, J. M., "Flash calculations for continuous or semicontinuous mixtures using an equation of state", *Ind. Eng. Chem. Process, Des. Dev.***24**, 433-443 (1985).

Cotterman, R. L. and Prausnitz, J. M., "Application of continuous thermodynamics to natural-gas mixtures", *Revue de l'Institut Français du Pétrole*, **45**, 633-643 (1990)

Cotterman, R. L. and Prausnitz, J. M., "Continuous thermodynamics for phase-equilibrium calculations in chemical process design", *Kinetic and Thermodynamic Lumping of Multi-component Mixtures*, edited by G. Astarita and S. I. Sandler, Elsevier Science Publishers B. V., Amsterdam, 1991- Printed in the Netherlands.

Cotterman, R. L., Bender, R. and Prausnitz, J. M., "Phase equilibria for mixtures containing very many components. Development and application of continuous thermodynamics for chemical process design", *Ind. Eng. Chem. Process Des. Dev.* **24**, 194-203 (1985).

Du, P. C. and Mansoori, G. A., "Phase equilibrium computational algorithms of continuous mixtures", *Fluid Phase Equilibria*, **30**, 57-64 (1986).

El-Wakil, M. M., Priem, R. J., Brikowski, H.J., Myers P.S., and Uyehara O. A., " Experimental and calculated temperature and mass histories of vaporizing fuel drops", NACA TN 3490 (1956).

Faeth, G. M. and Olson, D. R., "The ignition of hydrocarbon fuel droplets in air", *SAE* Paper 680465, 1793-1802 (1968).

Faeth, G. M., "Combustion characteristics of blended monopropellant droplets", *AIAA 8th Aerospace Sciences Meeting*, No. 70-7 (1970).

Gualtieri, J. A., Kincaid, J. M. and Marrison, G., "Phase equilibria in polydisperse fluids", *J. Chem. Phys.*, **77**, 521 (1982).

Hallett, W. L., "Combustion in diffusion systems: Lecture notes for MCG 5192", University of Ottawa, Faculty of Engineering, Mechanical Engineering, Revised (1997).

Hallett, W. L., "Multi-component droplet ignition using continuous thermodynamics", *Combustion Inst. Canadian Section Spring Technical Meeting*, 9-16-9-20 (1998).

Hallett, W. L., "A simple model for the vaporization of droplets with large numbers of components", *Combustion and Flame*, 334-344 (2000).

Hallett, W. L. and Ricard, M. A., "Calculations of the auto-ignition of liquid hydrocarbon mixtures as single droplets", *Fuel*, **71**, 225-229 (1992).

Haywood, R. J., Nafziger, R. and Renksizbulut, M., "A detailed examination of gas and liquid phase transient processes in convective droplet evaporation", *J. Heat Transfer*, **111**, 495-502 (1989).

Hubbard, G. L., Denny, V. E. and Mills, A. F., "Droplet evaporation: effects of transients and variable properties", *Int. J. Heat Mass Transfer*, **18**, 1003-1008 (1975).

Katz, D. L. and Brown, G. G., "Vapour pressure and vaporization of petroleum fractions", *Ind. Eng. Chem.*, **25**, 1373-1384 (1933).

Kanury, A. M., "Introduction to combustion phenomena", Gordon and Breach Science Publishers, New York (1975).

Kehlen, H. and Rätzsch, M. T., "Continuous thermodynamics of multi-component mixtures", *Proceedings Sixth International Conference on Thermodynamics, Merseburg (GDR)*, 41-51 (1980).

Kehlen, H. and Rätzsch, M. T., "Separate treatment of paraffins and aromatics in complex hydrocarbon mixtures by continuous thermodynamics", *Z. Phys. Chem.*, Leipzig, **265**, 1049 (1984)

Kehlen, H., Rätzsch, M. T. and Bergmann, J., "Continuous thermodynamics of multi-component systems", *AIChE J.*, **31**, No. 7, 1136-1148 (1985).

Kehlen, H. and Rätzsch, M. T., "Complex multi-component distillation calculations by continuous thermodynamics", *Chem. Eng. Sci.*, **42**, 221-232 (1987)

Kneer, R., Schneider, M., Noll, B. and Wittig, S., "Diffusion controlled evaporation of a multi-component droplet: theoretical studies on the importance of variable liquid properties", *Int. J. Heat Mass Transfer*, **36**, 2403-2415 (1993a).

Kneer, R., Schneider, M., Noll, B. and Wittig, S., "Effects of variable liquid properties on multi-component droplet vaporization", *Journal of Engineering for Gas Turbines and Power*, **115**, 467-472 (1993b).

Landis, R. B. and Mills, A. F., "Effects of internal diffusional resistance on the evaporation of binary droplets", *Fifth International Heat Transfer Conference*, 345-349 (1974).

Law, C. K., "Multi-component droplet combustion with rapid internal mixing", *Combustion and Flame*, **26**, 219-233 (1976).

Law, C. K., "Recent advances in droplet vaporization and combustion", *Prog. Energy Combust. Sci.*, **8**, 171-201 (1982).

Law, C. K., "Recent advances in multi-component and propellant droplet vaporization and combustion", *The American Society of Mechanical Engineers*, Paper 86-WA/HT-14 (1986).

Law, C. K. and Law, H. K., "A d^2-law for multi-component droplet vaporization and combustion", *AIAA J.*, **20**, 522-527 (1981).

Law, C. K., Prakash, S. and Sirignano, W. A., "Theory of convective, transient, multi-component droplet vaporization", *Sixteenth Symposium (International) on Combustion*, 605-617 (1976).

Lippert, A. M, Stanton, D. W., Reitz, R. D., Rutland, C. J. and Hallett, W. L. H., "Investigating the effect of spray targeting and impingement on diesel engine cold start", *SAE* 2000-01-0269, 1-31 (2000).

Lippert, A. M, Stanton, D. W., Reitz, R. D., Rutland, C. J. and Hallett, W. L. H., "Multidimensional simulation of diesel engine cold start with advanced physical submodels", *Int. J. Engine Research*, **1**, 1-27 (2000).

Lippert, A. M. and Reitz, R. D., "Modelling of multi-component fuels using continuous distributions with application to droplet evaporation and sprays", *Society of Automotive Engineers*, Paper 972882 (1997).

Lippert, A. M., "Modelling of multi-component fuels with application to sprays and simulation of diesel engine cold start", *PhD thesis, Mechanical Engineering, University of Wisconsin-Madison*, (1999).

Mawid, M. and Aggrawal, S. K., "Analysis of transient combustion of a multi-component liquid fuel droplet", *Combustion and Flame*, **84**, 197-209 (1991).

Newbold, F. R. and Amundson, N. R., "A model for evaporation of a multi-component droplet", *AIChE J.*, **19**, 22-30 (1973).

Patankar, S. V., "Numerical Heat Transfer and Fluid Flow", Published by Hemisphere publishing corporation, New York (1980).

Peng, D. Y., Wu, R. S. and Batycky J. P., "Application of continuous thermodynamics to oil reservoir fluid systems using an equation of state", *AOSTRA J. Research*, **3**, 113-122 (1987).

Rätzsch, M. T. and Kehlen, H., "Continuous thermodynamics of complex mixtures", *Fluid Phase Equilibria*, **14**, 225-234 (1983).

Rätzsch, M. T., Kehlen, H. and Schumann, J., "Flash calculations for a crude oil by continuous thermodynamics", *Chem. Eng. Comm.*, **71**, 113-125 (1988).

Rätzsch, M. T., Kehlen, H. and Schumann, J., "Computer simulation of complex multi-component hydrocarbon distillation by continuous thermodynamic", *Fluid Phase Equilibria*, **51**, 133-146 (1989).

Reid, R. C., Prausnitz, J. M. and Poling, B. E., "The properties of gases and liquids, 4th edition, McGraw-Hill, New York (1986).

Renksizbulut, M. and Haywood, R. J., "Transient droplet evaporation with variable properties and internal circulation at intermediate Reynolds numbers", *Int. J. Multiphase Flow*, **14**, 189-202, (1988).

Ruszalo, R., Gibbs, L. A., Burelle, C. A., Dickson, T. E. and Hallett, W. L., "Ignition of liquid fuel droplets at high pressure", *Final Report for the Dept. of National Defence, Mechanical Engineering, University of Ottawa*, (1990).

Shaw, B. D. and Williams, F. A., "Theory of influence of a low-volatility, soluble impurity on spherical-symmetric combustion of fuel droplets", *Int. J. Heat Transfer*, **33**, 301-317 (1990).

Sirignano, W. A. and Law, C. K., "Transient heating and liquid-phase mass diffusion in fuel droplet vaporization", *Evaporation and Combustion of Fuels*, J. F. Zung, editor, Adv. In Chem. **166**, 3 (1978).

Sirignano, W. A. and Law, C. K., "Unsteady droplet combustion with droplet heating-II: conduction limit", *Combustion Flame*, **28**, 175-186 (1976).

Spalding, D. B., "Combustion and mass transfer: a textbook with multiple-choice exercises for engineering students", Pergamon Press (1979) London.

Talley, D. G. and Yao, S. C., "Unsteady droplet vaporization experiments and modelling at intermediate Reynolds numbers", *The American Society of Mechanical Engineers*, Paper 84-WA/HT-19 (1984).

Talley, D. G. and Yao, S. C., "A semi-empirical approach to thermal and composition transients inside vaporizing fuel droplets", *Twenty-first Symposium (International) on Combustion, The Combustion Institute*, 609-616 (1986).

Tamim, J. and Hallett, W. L., "A continuous thermodynamics model for multi-component droplet vaporization", *Chem. Eng. Sci.*, **50**, 2933-2942 (1995).

Tamim, J. and Hallett, W. L., "A continuous thermodynamics model for multi-component droplet vaporization", *M. A. S. Chem. Eng. Dept., University of Ottawa*, (1996).

Tong, A. Y. and Sirignano, W. A., "Multi-component droplet vaporization in a high temperature gas", *The American Society of Mechanical Engineers*, 84-WA/HT-17 (1984).

Wang, C. H., Liu, X. Q. and Law, C. K., "Combustion and micro-explosion of freely falling multi-component droplets", *Combustion and Flame*, **56**, 175-197 (1984).

Willman, B. T. and Teja, A. S., "Continuous thermodynamics of phase equilibria using a multi-variate distribution function and an equation of state", *AIChE J.*, **32**, 2067 (1986).

Willman, B. T. and Teja, A. S., "Prediction of dew points of semicontinuous natural gas and petroleum mixtures: Non-ideal solution calculations", *Ind. Eng. Chem. Res.* **26**, 953-957 (1987).

Wood, B. J., Wise, H., and Inami S. H., "Heterogeneous combustion of multi-component fuels", *Combustion and Flame*, **4**, 235-242 (1960).

APPENDIX A

Elimination of Terms From Transport Equations

The liquid phase equation for overall fuel concentration is

$$\frac{\partial}{\partial t}\left(c_L x_F\right) + \nabla \cdot \left(c_L v_L^* x_F\right) = \nabla \cdot \left\{c_L \chi \overline{D}_L \nabla x_F + x_F \nabla \left(c_L \chi \overline{D}_L\right)\right.$$

$$\left. - x_F \int_0^\infty f_L(I) \nabla \left(c_L D_{Lm}(I) dI\right)\right\}$$

For the radial direction in spherical coordinates, the second term on the right hand side in finite difference formulation gives

$$I_1 = \nabla \cdot \left(x_F \nabla \left(c\chi \overline{D}_L\right)\right) = \nabla \cdot \left[x_F \frac{\left(c\chi \overline{D}_L\right)_{i+1} - \left(c\chi \overline{D}_L\right)_i}{R\left(\xi_{i+1} - \xi_i\right)}\right]$$

$$= \frac{1}{R\left(\xi_{e_i} - \xi_{e_{i-1}}\right)}\left[\frac{x_{F_{i+1}} + x_{F_i}}{2}\left(\frac{\left(c\chi \overline{D}_L\right)_{i+1} - \left(c\chi \overline{D}_L\right)_i}{R\left(\xi_{i+1} - \xi_i\right)}\right)\right.$$

$$\left. - \frac{x_{F_i} + x_{F_{i-1}}}{2}\left(\frac{\left(c_L \chi \overline{D}_L\right)_i - \left(c_L \chi \overline{D}_L\right)_{i-1}}{R\left(\xi_i - \xi_{i-1}\right)}\right)\right] \qquad \text{A-1}$$

where subscripts i+1, i etc. refer to the grid nodes, and "ei" refers to the "east" interface

between nodes (i+1) and i. The last term is

$$I_2 = -\nabla \cdot \left[x_F \int_0^{\infty} f_L(I) \nabla \left(c_L \chi D_L(I) \right) dI \right] \qquad \text{A-2}$$

which can be estimated in finite difference form as follows

$$\nabla \left(c_L \chi D_L(I) \right) = \frac{\left[c_L \chi D_L(I) \right]_{i+1} - \left[c_L \chi D_L(I) \right]_i}{R\left(\xi_{i+1} - \xi_i \right)} \qquad \text{A-3}$$

Integrating:

$$\int_0^{\infty} f_L(I) \nabla \left(c_L \chi D_L(I) \right) dI = \frac{\left(c_L \chi \overline{D}_L \right)_{i+1} - \left(c_L \chi \overline{D}_L \right)_i}{R\left(\xi_{i+1} - \xi_i \right)} \qquad \text{A-4}$$

then

$$I_2 = -\frac{1}{R\left(\xi_{e_i} - \xi_{e_{i-1}} \right)} \left[\frac{x_{F_{i+1}} + x_{F_i}}{2} \left(\frac{\left(c_L \chi \overline{D}_L \right)_{i+1} - \left(c_L \chi \overline{D}_L \right)_i}{R\left(\xi_{i+1} - \xi_i \right)} \right) \right.$$

$$\left. - \frac{x_{F_i} + x_{F_{i-1}}}{2} \left(\frac{\left(c_L \chi \overline{D}_L \right)_i - \left(c_L \chi \overline{D}_L \right)_{i-1}}{R\left(\xi_i - \xi_{i-1} \right)} \right) \right] \qquad \text{A-5}$$

I_1 and I_2 are identical in finite difference form; they cancel each other and can be dropped from the equation. The same calculations apply to equation (3.2-13), (3.2-16) and (3.4-6).

APPENDIX B

Derivation of Finite Volume Equations by Integration of Differential Equations

1-Continuity Equation (eq. 4.1-4)

Integrating equation (4.1-4) over a control volume (CV) (Figure 4.1) from "west" w to "east"e to get $(c_L w_L)_e$ in terms of $(c_L w_L)_w$:

$$\xi^2 \frac{dc_L}{dt} + \frac{1}{R}\frac{\partial}{\partial \xi}\left(\xi^2 c_L w_L^*\right) + \frac{\dot{R}}{R} c_L \frac{\partial}{\partial \xi}\left(\xi^3\right) = 0 \qquad \text{B-1}$$

gives

$$\left(\xi^2 c_L w_L^*\right)_e = \left(\xi^2 c_L w_L^*\right)_w - \left(\xi_e^3 - \xi_w^3\right)\left[\dot{R} c_{LP} + \frac{R}{3\Delta t}\left(c_{LP}^o - c_{LP}\right)\right] \qquad \text{B-2}$$

Starting at the droplet center (node 1, $\xi = 0$), where

$$w_L^* = 0 \qquad \text{B-3}$$

all the other velocities can be found. The velocity in the program is stored as $(\xi_L^2\, c_L w_L^*)_e$ which is the velocity at the east face of cell I.

2-Transport Equation for x_F (eq. 4.1-5)

$$\xi^2 \frac{\partial(c_L x_F)}{\partial t} + \frac{\dot{R}}{R}(c_L x_F)\frac{\partial \xi^3}{\partial \xi} + \frac{1}{R}\frac{\partial}{\partial \xi}\left(\xi^2 c_L w_L^* x_F\right)$$

$$= \frac{1}{R^2}\frac{\partial}{\partial \xi}\left(c_L \chi \overline{D}_L \xi^2 \frac{\partial x_F}{\partial \xi}\right) \qquad \text{B-4}$$

Integrate over CV from w to e and over time t to t+Δt to get x_{FP} in terms of neighbours W and P. The first two terms integrate to

$$\frac{1}{3}\left(\xi_e^3 - \xi_w^3\right)\left(c_{L_P} x_{F_P} - c_{L_P}^o x_{F_P}^o\right) + c_{L_P} x_{F_P} \frac{\dot{R}\Delta t}{R}\left(\xi_e^3 - \xi_w^3\right) \qquad \text{B-5}$$

where the first two terms of equation B-5 represents the transient and moving co-ordinate terms. The last two terms of equation B-4 represent convection and diffusion, and are modelled using the power law hybrid scheme of Patankar(1980). Equation B-5 and the last two terms of equation B-4 will be solved to be in the following form

$$a_P x_P = a_E x_E + a_W x_W + S \qquad \text{B-6}$$

where

$$a_E = D_e A(P_e) + \|-F_e, 0\|$$

$$a_W = D_w A\left(P_w\right) + \left\| -F_w, 0 \right\| \qquad \text{B-7}$$

$$a_P = -a_e - a_w - F_e + F_w$$

D and F represent diffusion and convection respectively

$$D_e = \frac{c_{L_e} \overline{D}_{L_e}}{R^2} \frac{\xi_{L_e}^2 \Delta t}{\left(\xi_{L_E} - \xi_{L_P}\right)} \qquad \text{B-8}$$

$$F_e = \frac{\left(\xi_L^2 c_L w_L^*\right)_e \Delta t}{R} \qquad \text{B-9}$$

$$D_w = \frac{c_{L_w} \overline{D}_{L_w}}{R^2} \frac{\xi_{L_w}^2 \Delta t}{\left(\xi_{L_P} - \xi_{L_W}\right)} \qquad \text{B-10}$$

$$F_w = \frac{\left(\xi_L^2 c_L w_L^*\right)_w \Delta t}{R} \qquad \text{B-11}$$

S is the source term and it is calculated as

$$S = \frac{1}{3}\left(\xi_{L_e}^3 - \xi_{L_w}^3\right) c_{L_P}^o x_{F_P}^o \qquad \text{B-12}$$

and P is the Peclet number

$$P = F / D \qquad \text{B-13}$$

and the function A(P) is given by

$$A(P) = \left\| 0, \left(1 - 0.1|P|^5\right) \right\| \qquad \text{B-14}$$

where the brackets ‖...‖means "the greatest of".

Implementing this solution will lead to $x_F = 1$ everywhere in the program.

3-Transport Equation for ($x_F\theta_L$) (eq. 4.1-6)

$$\xi^2 \frac{\partial\left(c_L x_F \theta_L\right)}{\partial t} + \frac{\dot{R}}{R}\left(c_L x_F \theta_L\right)\frac{\partial \xi^3}{\partial \xi} + \frac{1}{R}\frac{\partial}{\partial \xi}\left(\xi^2 c_L w_L^*\left(x_F \theta_L\right)\right)$$

$$= \frac{1}{R^2}\frac{\partial}{\partial \xi}\left(c_L \chi \widetilde{D}_L \xi^2 \frac{\partial\left(x_F \theta_L\right)}{\partial \xi}\right) \qquad \text{B-15}$$

The first two terms integrated over the CV from w to e and over time t to t+Δt give

$$\frac{1}{3}\left(\xi_e^3 - \xi_w^3\right)\left(\left(c_L x_F \theta_L\right)_P - \left(c_L^o x_F^o \theta_L^o\right)\right) + \left(c_L x_F \theta_L\right)_P \frac{\dot{R}\Delta t}{R}\left(\xi_e^3 - \xi_w^3\right) \qquad \text{B-16}$$

The last two terms of equation B-15 represents the convection and diffusion respectively of

the mean of the distribution, and are again modelled using the power-law hybrid scheme. The expressions are the same as for the x_F equation except for the diffusion coefficient and the source term. The equation is solved for $(x_F\theta_L)$, the value of θ_L at each node then being obtained by dividing by x_F:

$$D_e = \frac{c_{L_e}\widetilde{D}_{L_e}}{R^2}\frac{\xi_e^2\Delta t}{\left(\xi_E - \xi_P\right)} \qquad \text{B-17}$$

$$F_e = \frac{\left(\xi^2 c_L w_L^*\right)_e \Delta t}{R} \qquad \text{B-18}$$

$$D_w = \frac{c_{L_w}\widetilde{D}_{L_w}}{R^2}\frac{\xi_w^2\Delta t}{\left(\xi_P - \xi_W\right)} \qquad \text{B-19}$$

$$F_w = \frac{\left(\xi^2 c_L w_L^*\right)_w \Delta t}{R} \qquad \text{B-20}$$

S is the source term and it is calculated as

$$S = \frac{1}{3}\left(\xi_e^3 - \xi_w^3\right)\left(c_L^o x_F^o \theta_L^o\right)_P \qquad \text{B-21}$$

4-Transport Equation for ($x_F\psi_L$) (eq. 4.1-7)

$$\xi^2 \frac{\partial\left(c_L x_F \Psi_L\right)}{\partial t} + \frac{\dot{R}}{R}\left(c_L x_F \Psi_L\right)\frac{\partial \xi^3}{\partial \xi} + \frac{1}{R}\frac{\partial}{\partial \xi}\left(\xi^2 c_L w_L^*\left(x_F \Psi_L\right)\right)$$

$$= \frac{1}{R^2}\frac{\partial}{\partial \xi}\left(c_L \chi \hat{D}_L \xi^2 \frac{\partial\left(x_F \Psi_L\right)}{\partial \xi}\right) \quad \text{B-22}$$

The first two terms integrated over the CV from w to e and over time t to t+Δt give

$$\frac{1}{3}\left(\xi_e^3 - \xi_w^3\right)\left(\left(c_L x_F \Psi_L\right)_P - \left(c_L^o x_F^o \Psi_L^o\right)\right) + \left(c_L x_F \Psi_L\right)_P \frac{\dot{R}\Delta t}{R}\left(\xi_e^3 - \xi_w^3\right) \quad \text{B-23}$$

The last two terms of equation B-15 represents the convection and diffusion respectively of the mean of the distribution, and are again modelled using the power-law hybrid scheme. The expressions are the same as for the diffusion equation except for the diffusion coefficient, the source term and the equation is solved for ($x_F\psi_L$), the value of ψ_L at each node then being obtained by dividing by x_F:

$$D_e = \frac{c_{L_e}\hat{D}_{L_e}}{R^2}\frac{\xi_e^2 \Delta t}{\left(\xi_E - \xi_P\right)} \quad \text{B-24}$$

$$F_e = \frac{\left(\xi^2 c_L w_L^*\right)_e \Delta t}{R} \qquad \text{B-25}$$

$$D_w = \frac{c_{L_w} \hat{D}_{L_w}}{R^2} \frac{\xi_w^2 \Delta t}{\left(\xi_P - \xi_W\right)} \qquad \text{B-26}$$

$$F_w = \frac{\left(\xi^2 c_L w_L^*\right)_w \Delta t}{R} \qquad \text{B-27}$$

S is the source term and it is calculated as

$$S = \frac{1}{3}\left(\xi_e^3 - \xi_w^3\right)\left(c_L^o x_F^o \Psi_L^o\right)_P \qquad \text{B-28}$$

APPENDIX C

Balances on Liquid Phase Distribution Parameters

1- <u>Mean Liquid Properties</u>

The number of moles of species i in the liquid droplet is

$$n_i = 4\pi \int_0^R c_L x_i r^2 dr = \frac{4}{3}\pi R^3 \bar{c}_L \bar{x}_i \qquad \text{C-1}$$

where $\bar{c}_L$, $\bar{x}_i$ are quantities averaged over the liquid volume. Converting to continuous thermodynamics:

$$\bar{x}_F \bar{c}_L \bar{f}_L(I) dI = 3\int_0^1 c_L x_F f_L(I) dI \xi^2 d\xi \qquad \text{C-2}$$

where $\xi = r/R$. This defines $\bar{f}_L(I)$ as an average distribution function for the whole droplet.

Integrating over I and setting $x_F = 1$ yields

$$\bar{c}_L = 3\int_0^1 c_L \xi^2 d\xi \qquad \text{C-3}$$

Multiplying equation (C-2) by I and integrating over I yields

$$\bar{c}_L \bar{\theta}_L = 3\int_0^1 c_L \theta_L \xi^2 d\xi \qquad \text{C-4}$$

or

$$\bar{\theta}_L = \frac{\bar{\rho}_L}{\bar{c}_L} \qquad \text{C-5}$$

which defines the average over the droplet of the mean molecular weight. Multiplying equation (C-2) by I^2 and integrating over I yields:

$$\bar{c}_L \overline{\Psi}_L = 3\int_0^1 c_L \Psi_L \xi^2 d\xi \qquad \text{C-6}$$

2- Balance on Droplet

From equation (3.4-1), the molar flux of species i from the surface can be described as

$$N_i = \frac{-1}{A}\frac{d}{dt}\left(\bar{x}_i \bar{c}_L V\right) = \bar{x}_i N - \bar{c}_L \frac{R}{3}\frac{d\bar{x}_i}{dt} \qquad \text{C-7}$$

where V is the droplet volume and A is the droplet surface area. The vapour flux composition can be described by a distribution $f_N(I)$, which is defined by

$$N_i = N f_N(I) dI \qquad \text{C-8}$$

Substituting this and $\bar{f}_L(I)$ into equation (C-7) yields

$$Nf_N(I)dI = N\overline{f}_L(I)dI - \overline{c}_L \frac{R}{3}\frac{d}{dt}\left[\overline{f}_L(I)dI\right] \qquad \text{C-9}$$

Multiplying equation (C-9) by I and integrating over I yields:

$$\frac{d\overline{\theta}_L}{dt} = \frac{3N}{\overline{c}_L R}\left(\overline{\theta}_L - \theta_N\right) \qquad \text{C-10}$$

Multiplying equation (C-9) by I^2 and integrating over I yields:

$$\frac{d\overline{\Psi}_L}{dt} = \frac{3N}{\overline{c}_L R}\left(\overline{\Psi}_L - \Psi_N\right) \qquad \text{C-11}$$

3- Vapour Flux Distribution $f_N(I)$

The parameters θ_N and ψ_N of the vapour molar flux distribution can be obtained from the flux of i either on the vapour or on the liquid phase side:

From Vapour Side:

For discrete component i, the vapour molar flux can be described as:

$$N_i = Ny_{iR} - cD_i \left.\frac{\partial y_i}{\partial r}\right|_R \qquad \text{3.4-4}$$

Introducing the distribution $f_N(I)$ and f(I), multiplying by I and integrating over I yields

$$N\theta_N = Ny_{FR}\theta_R - c\tilde{D}\frac{\partial}{\partial r}\left(y_F\theta\right)\Big|_R \qquad \text{C-13}$$

Multiplying equation (3.4-4) by I^2 and integrating over I yields

$$N\Psi_N = Ny_{FR}\Psi_R - c\hat{D}\frac{\partial}{\partial r}\left(y_F\Psi\right)\Big|_R \qquad \text{C-14}$$

Values of y_{FR}, θ_R and ψ_R are known from the vapour phase solution; hence θ_N and ψ_N can be found. The same procedure can be followed on the liquid side of the surface to give

$$N\theta_N = N\theta_{LR} - c_L\chi\tilde{D}_L\frac{\partial}{\partial r}\left(\theta_L\right)\Big|_R \qquad \text{C-15}$$

and

$$N\Psi_N = N\Psi_{LR} - c_L\chi\hat{D}_L\frac{\partial}{\partial r}\left(\Psi_L\right)\Big|_R \qquad \text{C-16}$$

APPENDIX D

```
************************************************************************
*   PROGRAMME MDCTLD ("MULTIPLE DISTRIBUTION CONTINUOUS
*   THERMODYNAMICS WITH LIQUID DIFFUSION")
*   LAST MODIFIED 11 SEPTEMBER 2000
*   DEVELOPED FROM WELL-MIXED MODEL (MODELCTV.FOR) WITH THE
*   FOLLOWING MODIFICATIONS:
*  - SUBROUTINE XCONC ADDED TO SOLVE LIQUID DIFFUSION EQUATIONS
*    INSIDE DROPLET. LIQUID GRID SYSTEM ADDED WITH NN GRID POINTS.
*    THIS ALLOWS LIQUID PHASE DISTRIBUTION PROPERTIES "THETAL",
*    "VARRL" & "PSIL" TO CHANGE IN SPACE AS WELL AS IN TIME.
*  - VAPOR LIQUID EQUILIBRIUM MOVED TO SEPARATE FUNCTION
*    CALLED "PVAP".
*  - PARABOLIC INTERPOLATION MOVED TO SEPARATE FUNCTION
*    CALLED "PARAB2".
*  - SUBROUTINE "PROPS" SPLIT INTO THREE SEPARATE SUBROUTINES AS
*    FOLLOWS:
*      - SUBROUTINE SPECHT : TO CALCULATE VAPOR & LIQUID SPECIFIC
*        HEAT.
*      - SUBROUTINE VDIF : TO CALCULATE VAPOR PHASE DIFFUSIVITIES.
*      - SUBROUTINE CONDK : TO CALCULATE VAPOR PHASE THERMAL
*        CONDUCTIVITY.
*  - SUBROUTINE LDIF ADDED TO CALCULATE LIQUID PHASE
*    DIFFUSIVITIES WHICH CHANGE IN SPACE & TIME.
*  - FACTOR "FAC" ADDED IN LDIF SUBROUTINE AS MULTIPLIER FOR THE
*    DIFFUSIVITY VALUES. ALLOWS MOVING FROM DIFFUSION-LIMITED
*    MODEL (FAC = 1) TO COMPLETE MIXING (LARGE FAC).
*  - SUBROUTINE DENSIT CHANGED ITS NAME TO VDENSIT.
*  - SUBROUTINE LIQDENSIT ADDED TO CALCULATE THE LIQUID MOLAR
*    DENSITY "RHOL(I)" WHICH VARIES IN SPACE AND TIME.
*  - SUBROUTINES "CONC" & "CONCI" RENAMED "YCONC" & "YCONCI"
*  - SUBROUTINE "LQMIXVIS" ADDED TO CALCULATE LIQUID MIXTURE
*    VISCOSITY.
*  - FUNCTION "GAMMA" ADDED TO CALCULATE GAMMA(ALPHAL) FOR
*    VISCOSITY.
*  - SUBROUTINE "THTJACB" ADDED TO SOLVE FOR "THETAL(NN)" &
*    "PSIL(NN)" AT SURFACE FROM VLE AND FLUX RELATIONS USING 2D
*    NEWTON METHOD
*  - DOUBLE PRECISION USED INSTEAD OF SINGLE PRECISION.
*  - VELOCITY IN LIQUID PHASE "VELL(I)" ADDED, VARIES IN SPACE AS
*    WELL AS IN TIME.
*  - ALL REFERENCES TO CHEMICAL REACTION HAS BEEN REMOVED.
*  - MEAN THETAL VALUE "THETLM" CALCULATED IN LIQDENSIT
*    SUBROUTINE USED FOR LIQUID SPECIFIC HEAT AND CRITICAL TEMP.
*  - EXTRA GRID POINT ADDED MIDWAY BETWEEN DROPLET CENTER AND
*    SECOND POINT GENERATED BY CUBIC EQUATION IN ORDER TO
```

```
*     INCREASE THE ACCURACY OF THE CALCULATION NEAR THE DROPLET
*     CENTER.
*   - NO. OF INTEGRATION STEPS FOR LQMIXVIS  AND LDIF SUBROUTINES:
*       IF(FAC.EQ.1)THEN  I=600
*       IF(FAC.GT.1)THEN  I=400
*   - SUBROUTINE NEWTONIAN ADDED FOR TWO-DISTRIBUTION MODEL TO
*     SOLVE FOR SURFACE VALUE OF XF(J)
**********************************************************************
      IMPLICIT DOUBLE PRECISION (A-H,O-Z)
      DOUBLE PRECISION MASS,MASSEV,MASSP
      INTEGER CNTTEM
      DIMENSION      SUMTHETAL(60),HFGR(5),AH(5),BH(5),FUEL(5),RHOLI1(5),
     1AA(5),BB(5),SIGL(5),SIGR(5),SUMRDTWIDL(60),SUMRDHAT(60),
     1SUMRDTWIDLL(60),SUMRDHATL(60),XFMI(5)

      CHARACTER*23 FUEL
*
      COMMON/AREA1/N,NN,JN,R
      COMMON/AREA2/TC(5),PC,W,CPVAPA,CPVAPB,CPVAPC,CPVAPD,AL,BL,
     1CL,DL,CONDK(0:60),PCF
      COMMON/AREA3/CP(60),CPF(60),CPL,CPAIR(60),AO,A1,A2,A3,BO,B1,B2,B3
      COMMON/AREA4/TIME,DTIME,G0,VEL(60),RDOT,GTRR,DTLDT,DTR,TBOIL
      COMMON/AREA5/MA,PRES,RUGC,SM(60),PATM,AVGM
      COMMON/AREA6/YOAMB,YNAMB,YF(60,5),YO(60),YN(60),YMF(60,5),
     1YMO(60),YFR(5),YFTHET(60,5),YFPSI(60,5),YFOLD(60,5),YFTHOLD(60,5),
     1YFPSOLD(60,5),SUMYF(60)
      COMMON/AREA8/RDBAR(0:60,5),RDTWIDL(0:60,5),RDHAT(0:60,5),D0(60),DIF(60)
      COMMON/AREA9/ZETA(60),ZETAE(60),ZE2DZ(60),ZE3(60),ZE3D(60),ZETAD(60)
      COMMON/AREA10/RHO(60),RHOOLD(60)
      COMMON/AREA11/RHOL(60),RHOLOLD(60),RHOLM,RHOLI,DIFLL(60),XFBAR(5)
      COMMON/AREA12/TR,T(60),TOLD(60)
      COMMON/AREA13/ALPHAV(5),BETAV(5),THETA(60,5),VAR(60,5),VARM2(60,5)
      COMMON/AREA14/THETLM,AMEANL(5),VARL(5),VARLM2(5),ALPHAL(60,5),
     1BETAL(60,5),VLGAMA(5),THETAL(60,5),VARRL(60,5),PSIL(60,5),PSILM
      COMMON/AREA16/RDBARL(60,5),RDTWIDLL(60,5),RDHATL(60,5),FAC,
     1DBARL(60,5),DTWIDLL(60,5),DHATL(60,5)
      COMMON/AREA17/A(5),B(5),SFGR
      COMMON/AREA18/VISCA,VISCF,CVA,CVF,DP,AAF,AFA,AT,BT,CT,AP,BP
      COMMON/AREA19/XF(60,5),XFTHET(60,5),XFPSI(60,5),XFOLD(60,5),
     1XFTHOLD(60,5),XFPSOLD(60,5),XFI(5),SUMXFTHET(60),SUMXFPSI(60)
      COMMON/AREA20/ZETAL(60),ZETALE(60),ZLE2DZ(60),ZLE3(60),ZLE3D(60),
     1ZETALD(60),ZLE2(60),VELL(60)
      COMMON/AREA21/AD,BD,BPHI
      COMMON/AREA22/VISMIX(60),GML(60,5)
      COMMON/AREA23/YFINF(5),YFTHIN(5),YFPSIN(5),PTOT,XFR(5),DXFDR(5)
     1,DYFDR(5),DXFTHDR(5),DXFPSDR(5),DYFTHDR(5),DYFPSDR(5),THLRPF(4),
     1PSLRPF(4)
```

```
      COMMON/AREA24/SUMYFR

      OPEN(1,FILE='C:\COMBF\OUT\ERRORS.PLT')
      OPEN(2,FILE='C:\COMBF\DATA\CTLD1.DAT')
      OPEN(3,FILE='C:\COMBF\DATA\CTLD2.DAT')
      OPEN(4,FILE='C:\COMBF\DATA\CTFUEL1.DAT')
      OPEN(5,FILE='C:\COMBF\DATA\CTFUEL2.DAT')
      OPEN(10,FILE='C:\COMBF\OUT\CTLD0.PLT')
      OPEN(11,FILE='C:\COMBF\OUT\CTLD1.PLT')
      OPEN(12,FILE='C:\COMBF\OUT\CTLD2.PLT')
      OPEN(21,FILE='C:\COMBF\OUT\CTLD3.PLT')
      OPEN(22,FILE='C:\COMBF\OUT\CTLD4.PLT')
      OPEN(31,FILE='C:\COMBF\OUT\CTLD5.PLT')
      OPEN(32,FILE='C:\COMBF\OUT\CTLD6.PLT')
      OPEN(41,FILE='C:\COMBF\OUT\CTLD7.PLT')
      OPEN(42,FILE='C:\COMBF\OUT\CTLD8.PLT')
      OPEN(90,FILE='C:\COMBF\OUT\CTLDCHK1.CHK')
      OPEN(91,FILE='C:\COMBF\OUT\CTLDCHK2.CHK')
*************************************************************************
*    INPUT INITIAL VALUES:
*************************************************************************
      JN = 2

      DO 65 J=1,JN
      READ(J+1,*)
      READ(J+1,*)
      READ(J+1,*)N,ZETAN,W,A(J),B(J),SFG
      READ(J+1,*)
      READ(J+1,*)
      READ(J+1,*)BH(J),AH(J)
      READ(J+1,*)
      READ(J+1,*)AT,BT,AP,BP
      READ(J+1,*)
      READ(J+1,*)AO,A1,A2,A3
      READ(J+1,*)BO,B1,B2,B3
      READ(J+1,*)
      READ(J+1,*)AD,BD,BPHI
*
       WRITE(J+89,*)N,ZETAN,W,A(J),B(J),SFG
      WRITE(J+89,*)BH(J),AH(J),AD,BD,BPHI
      WRITE(J+89,*)AT,BT,AP,BP
      WRITE(J+89,701)AO,A1,A2,A3
701   FORMAT('AO=',2X,E12.5,2X,'A1=',2X,E12.5,/, 'A2=',2X,E12.5,2X,'A3=',2X,
     1E12.5)
      WRITE(J+89,702)BO,B1,B2,B3
702   FORMAT('BO=',2X,E12.5,2X,'B1=',2X,E12.5,/,
     1'B2=',2X,E12.5,2X,'B3=',2X,E12.5)
```

```
65    CONTINUE
*
      DO 66 J=1,JN
      READ(J+3,*)
      READ(J+3,503)FUEL(J)
      READ(J+3,*)
      READ(J+3,*)XFI(J)
      READ(J+3,*)
      RE AD(J+3,*)ALPHAL(1,J),BETAL(1,J),VLGAMA(J),RHOLI1(J)
      READ(J+3,*)
      READ(J+3,*)TDROP,TFURN,RDROP,TEND,DTIME0,TIMELIM,IRAD,FAC
      READ(J+3,*)
      READ(J+3,*)YFINF(J),YFTHIN(J),YFPSIN(J)
503   FORMAT(A23)
66    CONTINUE
*  ************************************************************************
*    PRINT OUT CONDITIONS FOR CALCULATIONS
************************************************************************
      DO 86 J=1,JN
      WRITE(*,*) 'PARAMETERS OF DIST. #',J
      WRITE(J+10,*) 'PARAMETERS OF DIST. #',J
      WRITE(*,504)FUEL(J),XFI(J),ALPHAL(1,J),BETAL(1,J),VLGAMA(J)
      WRITE(J+10,504)FUEL(J),XFI(J),ALPHAL(1,J),BETAL(1,J),VLGAMA(J)
504   FORMAT(1X,'FUEL TYPE: ',A23,/,1X,'XFI=',F8.5,'ALPHAL= ',F5.1,/,1X,
     1'BETAL = ',F5.1,/,1X,'GAMMA = ',F5.1)
86    CONTINUE

      WRITE(10,110)TFURN,TDROP,RDROP*2000.,DTIME0
110   FORMAT(1X,'AMBIENT TEMP. ',F5.0,'K; INITIAL LIQUID TEMP. ',F4.0,
     1' K',/,1X,'DROPLET DIAM. ',F7.4,' MM, DT ',F6.4,' S')
*
      DO 84 J=1,JN
      WRITE(J+10,113)
84    CONTINUE

      DO 10 J=1,JN
      WRITE(J+10,114)J,XFI(J),J,ALPHAL(1,J),J,BETAL(1,J),J,VLGAMA(J)
114   FORMAT(1X,'XFI(',I2,')=',F8.5,'  ALPHAL(',I2,')=',F7.3,'  BETAL(',I2,')=',F7.3,'
      GAMMA(',I2,')=',F7.3,/)
10    CONTINUE
*  ************************************************************************
*    SET CONSTANTS, DEFINE COMPUTATIONAL GRID
*  ************************************************************************
C
C     PHYSICAL CONSTANTS, BOUNDARY CONDITIONS
C
```

```
      NLP = 0
      NJ=2
      NN=15
      MA=2.897D1
      PATM=1.0D0
      PAMB=PATM*7.60D2
      PRES=1.013D2*PATM
      RUGC=8.314D0
      SFGR=SFG/RUGC
      YOAMB=0.21D0
      YNAMB=0.79D0
      SIGMA=5.669D-8
C
C   PROGRAMME CONTROL VARIABLES
C
      NPRINT=10
      TIMEPRT=NPRINT*DTIME0

*  SET CONVERGENCE CRITERION FOR MASS FLUX (CRITG, RELATIVE
*  ERROR) AND TEMP (CRITT IN K) AND RELAXATION FACTOR FOR
* VELOCITY AND TEMP.

      CRITG = 1.0D-6
      CRITT = 1.0D-6
      RELAX = 5.0D-1

      IF(IRAD.EQ.0) THEN
      WRITE(10,112)
112   FORMAT(1X,'*******NO RADIATION HEAT TRANSFER**********',/)
      ELSE
      WRITE(10,111)
111   FORMAT(1X,'********RADIANT HEAT TRANSFER INCLUDED******',/)
      ENDIF

      WRITE(*,201)
      WRITE(10,101)
201   FORMAT(4X,'TIME',2X,'TR',2X,'D2',2X,'%EVAP',2X,'TBOIL')
101   FORMAT(4X,'TIME',2X,'TR',2X,'%EVAP',2X,'TBOIL',2X,'THETLM',4X,'D2')

      DO 873 J=1,JN
      WRITE(10+J,*) 'LIQUID PHASE PROPERTIES'
      WRITE(10+J,997)
997   FORMAT(4X,'TIME',4X,'XF',4X,'THETAL(NN)')
      WRITE(20+J,*) 'VAPOR PHASE PROPERTIES'
      WRITE(20+J,994)
994   FORMAT(4X,'TIME',4X,'YFR',4X,'THETA(1)',3X,'SIGR')
873   CONTINUE
```

```
      WRITE(11,997)
997   FORMAT(4X,'XFBAR1',4X,'XF1',4X,'THETAL(NN,1)',3X,'YFR1',4X,'XFBAR'
     1,4X,'XF2',4X,'THETAL(NN,2)',3X,'YFR2')

      IFLAGT=0
      NITER=0
*************************************************************************
*   GEOMETRY OF GRID OUTSIDE THE DROPLET:
*************************************************************************
      ZETA(N)=ZETAN
      DZ=DLOG(ZETA(N))/(N-1)
      DO 11 I=1,N
      ZETA(I)=DEXP(DZ*(I-1))
      IF (I.EQ.1) GOTO 11
      ZETAE(I-1)=(ZETA(I-1)+ZETA(I))/2.D0
      ZE3(I-1)=ZETAE(I-1)**3
11    CONTINUE
      DO 12 I=1,N-1
      ZE2DZ(I)=ZETAE(I)**2/(ZETA(I+1)-ZETA(I))
12    CONTINUE
      DO 13 I=2,N-1
      ZE3D(I)=ZE3(I)-ZE3(I-1)
13    CONTINUE
*************************************************************************
*  GEOMETRY OF GRID INSIDE THE DROPLET:
*************************************************************************
      DO 14 I=2,NN-1
      ZETAL(I+1)=((I-1.D0)/(NN-2.D0))**(1.D0/3.D0)
14    CONTINUE
      ZETAL(1) = 0.0
      ZETAL(2) = ZETAL(3)/2.D0
      DO 15 I=1,NN-1
      ZETALE(I)=(ZETAL(I)+ZETAL(I+1))/2.D0
      ZLE3(I)=(ZETALE(I))**3
      ZLE2(I)=(ZETALE(I))**2
      ZETALD(I)=ZETAL(I+1) - ZETAL(I)
      ZLE2DZ(I)=ZLE2(I)/ZETALD(I)
15    CONTINUE
      DO 16 I=2,NN-1
      ZLE3D(I)=ZLE3(I)-ZLE3(I-1)
16    CONTINUE
*
      TRAD=TFURN-2.0D1
```

```
************************************************************************
*    INITIALIZE QUANTITIES FOR FIRST TIME STEP:
************************************************************************
3000 TIME = 0.0D0
      TR = TDROP
      TROLD = TR
      R = RDROP
      ROLD = R
      PTOT = PATM
      T(1)=TR
      DO 17 I=2,N
      T(I) = TFURN
17    CONTINUE

      DO 31 J = 1,JN
      XFR(J) = XFI(J)
31    CONTINUE
************************************************************************
*    INITIAL LIQUID PROPERTIES AND CONCENTRATION PROFILES:
************************************************************************
      SUMXFAML = 0.0
      DO 33 J=1,JN
      AMEANL(J) = ALPHAL(1,J)*BETAL(1,J)+VLGAMA(J)
      VARL(J) = ALPHAL(1,J)*(BETAL(1,J)**2)
      VARLM2(J) = VARL(J) + AMEANL(J)**2
      SUMXFAML = SUMXFAML + XFI(J)*AMEANL(J)

      DO 18 I =1,NN
      ALPHAL(I,J) = ALPHAL(1,J)
      BETAL(I,J) = BETAL(1,J)
      XF(I,J) = XFR(J)
      THETAL(I,J) = AMEANL(J)
      XFTHET(I,J) = XF(I,J)*THETAL(I,J)
      VARRL(I,J) = VARL(J)
      PSIL(I,J) = VARLM2(J)
      XFPSI(I,J) = XF(I,J)*PSIL(I,J)
18    CONTINUE
33    CONTINUE

      RHOLI = 0.0
      DO 35 J=1,JN
      XFMI(J) = XFI(J)*AMEANL(J)/SUMXFAML
      RHOLI = RHOLI + XFMI(J)*RHOLI1(J)
35    CONTINUE

*     INITIAL MASS OF LIQUID FUEL:
      MASS=4.D0/3.D0*3.1416D0*RDROP**3*RHOLI
```

```
      MASSEV = 0.0D0
      MASSP = MASSEV/MASS*1.D2

*************************************************************************
*    INITIAL VAPOR-LIQUID EQUILIBRIUM CALCULATION:
*************************************************************************
      SUMYFR = 0.0
      DO 44 J=1,JN
      AA(J) = SFGR*(1.D0-(A(J)/TR))
      BB(J) = B(J)/(TR-A(J))
      YFR(J) = PVAP(AA(J),BB(J),VLGAMA(J),ALPHAL(NN,J),BETAL(NN,J),PATM)
      YFR(J) = XF(NN,J)*YFR(J)/PTOT
      SUMYFR = SUMYFR + YFR(J)
44    CONTINUE

*  ALPHA, BETA, VLGAMA FOR VAPOUR PHASE IN TERMS OF MOLES
      DO 42 J=1,JN
      ALPHAV(J) = ALPHAL(NN,J)
      BETAV(J) = BETAL(NN,J)/(1.D0+(AA(J)*BB(J)*BETAL(NN,J)))
      THETA(1,J) = ALPHAV(J)*BETAV(J)+VLGAMA(J)
      VAR(1,J) = ALPHAV(J)*(BETAV(J)**2)
      VARM2(1,J) = VAR(1,J)+(THETA(1,J))**2
      SIGR(J) = DSQRT(VAR(1,J))
*
      YO(1) = YOAMB*(1.D0-SUMYFR)
      YN(1) = YNAMB/YOAMB*YO(1)
      YF(1,J) = YFR(J)
42    CONTINUE

      CALL VDENSIT

      DO 81 J=1,JN
      YMF(1,J) = YF(1,J)*THETA(1,J)/SM(1)
      YFTHET(1,J) = YF(1,J)*THETA(1,J)
      YFPSI(1,J)  = YF(1,J)*VARM2(1,J)
81    CONTINUE
*************************************************************************
*    INITIAL CONC. PROFILES OUTSIDE DROPLET:
*************************************************************************
      DO 57 J = 1,JN
      DO 20 I = 2,N
      YF(I,J) = YFINF(J)
      YMF(I,J) = YFINF(J)
      YFTHET(I,J) = YFTHIN(J)
      YFPSI(I,J) = YFPSIN(J)
      IF(YF(I,J).NE.0.0)THEN
      THETA(I,J) = YFTHET(I,J)/YF(I,J)
```

```
      VARM2(I,J) = YFPSI(I,J)/YF(I,J)
      ELSE
      THETA(I,J) = THETA(1,J)
      VARM2(I,J) = VARM2(1,J)
      VAR(I,J) = VAR(1,J)
      ENDIF
      YO(I)=YOAMB
      YN(I)=YNAMB
20    CONTINUE
57    CONTINUE

      DO 666 I=1,N
      SUMYF(I) = 0.0
      DO 555 J=1,JN
      SUMYF(I) = SUMYF(I) + YF(I,J)
555   CONTINUE
666   CONTINUE
*****************************************************************************
*    CALCULATE PROPERTIES:
*****************************************************************************
      CALL LIQDENSIT
      THETLM = RHOLI/RHOLM
      THETLMB = THETLM
      PSILMB = PSILM
      VARLM = (PSILM-THETLM**2)
      SIGLM = DSQRT(VARLM)
      THETLMBO = THETLM
      PSILMBO = PSILM
      CALL VDENSIT
      CALL VDIF
      DO 24 J=1,JN
      DO 224 I=1,NN
      GML(I,J) = GAMMA(ALPHAL(I,J))
224   CONTINUE
24    CONTINUE
      CALL LQMIXVIS
      CALL LDIF
      CALL SPECHT
      CALL THCONDK
      CALL BOILIN
      WRITE(90,512)TBOIL
512   FORMAT(/,'TBOIL=',F9.2)
```

```
*************************************************************************
*    DEFINE "OLD" VALUES OF XF, YF, ETC.
*************************************************************************
      DO 64 J=1,JN
      DO 21 I=1,N
      TOLD(I) = T(I)
      YFOLD(I,J) = YF(I,J)
      YFTHOLD(I,J) = YFTHET(I,J)
      YFPSOLD(I,J) = YFPSI(I,J)
      RHOOLD(I) = RHO(I)
21    CONTINUE
*
      DO 22 I=1,NN
      XFOLD(I,J) = XF(I,J)
      XFTHOLD(I,J) = XFTHET(I,J)
      XFPSOLD(I,J) = XFPSI(I,J)
      RHOLOLD(I) = RHOL(I)
22    CONTINUE
64    CONTINUE
*************************************************************************
*    INITIAL ESTIMATE OF SURFACE CONDITIONS FOR FIRST TIME STEP:
*************************************************************************
      CALL NEWTONIAN

      CALL THTJACB(NITR)

      DO 59 J=1,JN
      IF(ALPHAL(NN,J).LT.0.0D0.OR.BETAL(NN,J).LT.0.0D0)THEN
      WRITE(1,*) 'ALPHAL(',NN,',',J,') IS NEGATIVE'
      GOTO 6000
      ENDIF
59    CONTINUE
      GSTAR = G0

      DO 47 I=1,NN
      SUMTHETAL(I) = 0.0
      DO 48 J=1,JN
      SUMTHETAL(I) = SUMTHETAL(I) + XF(I,J)*THETAL(I,J)
48    CONTINUE
47    CONTINUE

      DO 61 I=1,N
      SUMYF(I) = 0.0
      DO 45 J=1,JN
      SUMYF(I) = SUMYF(I) + YF(I,J)
45    CONTINUE
61    CONTINUE
```

```
*************************************************************************
*    RE-CALCULATE PROPERTIES:
*************************************************************************
      CALL LIQDENSIT
      THETLM = RHOLI/RHOLM
      VARLM = (PSILM-THETLM**2)
      SIGLM = DSQRT(VARLM)
      RHOLMOLD = RHOLM
      CALL VDENSIT
      CALL VDIF
      DO 67 J=1,JN
      DO 267 I=1,NN
      GML(I,J) = GAMMA(ALPHAL(I,J))
267   CONTINUE
67    CONTINUE
      CALL LQMIXVIS
      CALL LDIF
      CALL SPECHT
      CALL THCONDK
      CALL BOILIN
      WRITE(90,512)TBOIL
*************************************************************************
*    CALCULATE VAPOR VELOCITY:
*************************************************************************
      RDOT = G0/RHOLM
      VEL(1)= G0 + (ZE3(1)-1.D0)*RDOT*(7.5D-1*RHO(1)+2.5D-1*RHO(2))
      DO 23 I=2,N-1
      VEL(I)=VEL(I-1)+ZE3D(I)*RDOT*RHO(I)
23    CONTINUE
      VELL(1) = ZLE3(1)*RHOL(1)*RDOT
      DO 37 I=2,NN-1
      VELL(I) = VELL(I-1)+ZLE3D(I)*RHOL(I)*RDOT
37    CONTINUE
*************************************************************************
*    CALCULATE QUASI-STEADY HEAT FLUX FOR THE FIRST TIME STEP:
*************************************************************************
*    HFGR AND HFG IN J/KMOL
      SUMHFG = 0.0
      DO 78 J=1,JN
      IF(G0.EQ.0.D0)THEN
      HFGR(J)=AH(J)+BH(J)*THETA(1,J)
      ELSE
      HFGR(J) = (AH(J)*YF(1,J)) - ((AH(J)*RDBAR(0,J)*DYFDR(J))/G0)
     1+(BH(J)*YFTHET(1,J))-((BH(J)*RDTWIDL(0,J)*DYFTHDR(J))/G0)
      ENDIF
      IF(HFGR(J).LT.0.D0)THEN
      HFGR(J)  = AH(J) + BH(J)*YFTHET(1,J)
```

```
      ENDIF
      TC(J) = AT + BT*THETA(1,J)
      HFG1 = HFGR(J)*((TC(J)-TR)**3.8D -1)/6.959D0
      SUMHFG = SUMHFG + HFG1
78    CONTINUE
      HFG = SUMHFG

      IF(G0.EQ.0.0D0)THEN
      QTOT = 0.0D0
      ELSE
      QTOT=G0*CPF(1)*(TFURN-TR)/(DEXP(G0*CPF(1)*R/CONDK(0))-1.D0)
      ENDIF

      IF(QTOT.LT.G0*HFG)G0=QTOT/HFG
*
      DISQ = (R*2)**2

      WRITE(*,102)TIME,TR,DISQ,MASSP,TBOIL
      WRITE(10,103)TIME,TR,MASSP,TBOIL,THETLM,DISQ
102   FORMAT(1X,F8.5,1X,F7.2,2X,E10.4,2X,F7.2,3X,F9.4)
103   FORMAT(1X,F8.5,1X,F7.2,2X,F7.2,2X,F9.3,3X,F9.3,2X,E10.4)

      DO 877 J=1,JN
      WRITE(10+J,993)TIME,XF(NN,J),THETAL(NN,J),SIGL(J)
993   FORMAT(1X,F8.5,1X,F8.5,1X,F7.3,1X,F5.1)
      WRITE(20+J,974)TIME,YFR(J),THETA(1,J),SIGR(J)
974   FORMAT(1X,F8.5,1X,F8.5,1X,F7.3,1X,F5.1)
877   CONTINUE
*************************************************************************
*    BEGIN TIME STEP
*    TIME STEP REDUCED FOR FIRST TIME STEP, ALSO AS DROPLET NEARS
*    END OF LIFETIME
*************************************************************************
1000 EMISS = 8.9D-1*(1.-DEXP(-5.4D0*R*1.D3))
      IF(IRAD.EQ.0)EMISS=0.D0
      IF(TIME.LT.DTIME0)THEN
      DTIME=DTIME0/5.D0
      ELSE
      IF(IFLAGT.EQ.0)THEN
      DTIME=DTIME0
      ENDIF
      ENDIF
      IF(MASSP.GT.8.0D1.AND.IFLAGT.LT.1)THEN
      DTIME=DTIME0/2.D0
      IFLAGT=1
      WRITE(*,654)TIME
654   FORMAT('*******TIME STEP DIVIDED BY 2 AT ',F8.5,' SEC *****')
```

```
      ENDIF
      IF(MASSP.GT.9.0D1.AND.IFLAGT.LT.2)THEN
      DTIME=DTIME0/5.D0
      IFLAGT=2
      WRITE(*,655)TIME
655   FORMAT('*******TIME STEP DIVIDED BY 5 AT ',F8.5,' SEC *****')
      ENDIF
      IF(MASSP.GT.9.5D1.AND.IFLAGT.LT.3)THEN
      DTIME=DTIME0/1.D1
      IFLAGT=3
      WRITE(*,656)TIME
656   FORMAT('*******TIME STEP DIVIDED BY 10 AT ',F8.5,' SEC *****')
      ENDIF
      IF(MASSP.GT.9.9D1.AND.IFLAGT.LT.4)THEN
      DTIME=DTIME0/2.D1
      IFLAGT=4
      WRITE(*,657)TIME
657   FORMAT('*******TIME STEP DIVIDED BY 20 AT ',F8.5,' SEC *****')
      ENDIF
      IF(MASSP.GT.9.94D1.AND.IFLAGT.LT.5)THEN
      DTIME=DTIME0/5.D1
      IFLAGT=5
      WRITE(*,658)TIME
658   FORMAT('*******TIME STEP DIVIDED BY 50 AT ',F8.5,' SEC *****')
      ENDIF

      RATIO = DTIME0/DTIME
      G0 = G0*ROLD/R
      GSTAR = G0
      DTR = DTIME/R
      GTRR = RDOT*DTR

      DO 642 I=1,N-1
      DIF(I)=ZE2DZ(I)*DTIME/R**2
642   CONTINUE

      DO 25 I=1,NN-1
      DIFLL(I)=ZLE2DZ(I)*DTIME/R**2
25    CONTINUE

      CALL COEF
*************************************************************************
*   CALCULATE TRIAL VALUE OF TR AT END OF TIME STEP:
*************************************************************************
      DTLDT = 3.D0*(QTOT - G0*HFG)/(RHOLM*CPL*ROLD)
      TRP = TROLD + DTLDT*DTIME
      IF(TRP.GE.TBOIL)TRP=TBOIL-2.5D-1
```

```
      CNTTEM=0
*************************************************************************
*    LOOP FOR TEMPERATURE, CONCENTRATION AND VELOCITY FIELDS
*************************************************************************
7000 TR = RELAX*TRP+(1.-RELAX)*TR
      T(1)=TR
      RDT=R/(3.D0*DTIME)
      DRHLMDT = (RHOLM-RHOLMOLD)/DTIME
C
C    CALCULATE VELOCITY FIELDS IN BOTH PHASES
C
      RDOT = (G0 + (R/3.D0)*DRHLMDT)/RHOLM
      GTRR = RDOT*DTR
      VEL(1) = G0+(ZE3(1)-1.D0)*(RDOT/4.D0*(3.D0*RHO(1)+
     1RHO(2))-RDT/4.D0*(3.D0*RHO(1)+RHO(2)-3.D0*RHOOLD(1)-RHOOLD(2)))

      DO 26 I=2,N-1
      VEL(I)=VEL(I-1)+ZE3D(I)*(RDOT*RHO(I)-RDT*(RHO(I)-RHOOLD(I)))
26    CONTINUE
      VELL(1) = - ZLE3(1)*(RDT*(RHOL(1)-RHOLOLD(1))-RHOL(1)*RDOT)
      DO 36 I=2,NN-1
      VELL(I) = VELL(I-1)-ZLE3D(I)*(RDT*(RHOL(I)-RHOLOLD(I))-RHOL(I)*
     1RDOT)
36    CONTINUE

      CALL YCONC
      CALL YCONCI
      CALL TEMP
      CALL XCONC

      CALL NEWTONIAN

      CALL THTJACB(NITR)

      IF(G0.LT.0.0)THEN
      WRITE(1,*) '-VE G0'
      GOTO 6000
      ENDIF

      DO 69 J=1,JN
      IF(ALPHAL(NN,J).LT.0.0D0.OR.BETAL(NN,J).LT.0.0D0)THEN
      WRITE(1,*) 'ALPHAL(',NN,',',J,') IS NEGATIVE'
      GOTO 6000
      ENDIF
69    CONTINUE
      NITER=NITER+1
```

```
      DO 77 I=1,NN
      SUMTHETAL(I) = 0.0
      DO 88 J=1,JN
      SUMTHETAL(I) = SUMTHETAL(I) + XF(I,J)*THETAL(I,J)
88    CONTINUE
77    CONTINUE

      DO 62 I=1,N
      SUMYF(I) = 0.0
      DO 135 J=1,JN
      SUMYF(I) = SUMYF(I) + YF(I,J)
135   CONTINUE
62    CONTINUE
*****************************************************************************
*   CALCULATE DROPLET HEATING
*****************************************************************************
      THETA2=(T(2)-T(1))/(TFURN-T(1))
      DTDR=DLOG(1.D0-THETA2)/(R*(1.D0-ZETA(2)))*(TFURN-T(1))

*  THERMAL RADIATION TRANSFER TO THE DROPLET:
      QRAD=SIGMA*EMISS*(T(1)**4-TRAD**4)
*
*  TOTAL HEAT FLUX DURING TIME STEP:
      QTOTP = CONDK(0)*DTDR - QRAD
      QTOT = RELAX*QTOTP + (1.D0-RELAX)*QTOT

      SUMHFG = 0.0
      DO 333 J=1,JN
      IF(G0.EQ.0.D0)THEN
      HFGR(J)=AH(J)+BH(J)*THETA(1,J)
      ELSE
      HFGR(J) = (AH(J)*YF(1,J)) - ((AH(J)*RDBAR(0,J)*DYFDR(J))/G0)
     1+(BH(J)*YFTHET(1,J))-((BH(J)*RDTWIDL(0,J)*DYFTHDR(J))/G0)
      ENDIF
      TC(J) = AT + BT*THETA(1,J)
      IF(XFI(J).EQ.0.D0)THEN
      HFG1 = 0.0
      ELSE
      HFG1 = HFGR(J)*((TC(J)-TR)**3.8D-1)/6.959D0
      ENDIF
      SUMHFG = SUMHFG + HFG1
333   CONTINUE
      HFG = SUMHFG
*
      DTLDT = 3.D0*(QTOT-G0*HFG)/(RHOLM*CPL*R)
      TRP = TROLD + DTLDT*DTIME
```

```
*************************************************************************
*    CONVERGENCE TEST - END OF TIME STEP:
*************************************************************************
*    CHECK IF CONVERGENCE HAS BEEN ACHIEVED:

      CNTTEM=CNTTEM+1
      IF(CNTTEM.GT.1000)THEN
      WRITE(1,*) 'ITERATIONS FOR TEMP. AND MOL FLUX EXCEED 100 '
     GOTO 6000
      ENDIF
      TESTT = DABS(TRP-TR)/TR
      IF(G0.NE.0.0D0)THEN
      TESTG = DABS(G0-GSTAR)/G0
      ENDIF
      GSTAR = G0
      IF(G0.EQ.0.0D0)THEN
      WRITE(*,*)' G0 IS 0 - GOING TO NEXT TIME STEP'
      WRITE(1,*)' G0 IS 0 - GOING TO NEXT TIME STEP'
     GOTO 1500
      ENDIF
      IF(TESTT.GT.CRITT.OR.TESTG.GT.CRITG)GOTO 7000
*************************************************************************
* END OF TIME STEP: UPDATE DROPLET RADIUS AND OTHER VALUES
*************************************************************************
1500 TIME=TIME+DTIME
      TR=TRP
      RHOLMOLD=RHOLM
      ROLD = R
      R = ROLD-RDOT*DTIME
      TROLD = TR
*
      DO 87 J=1,JN
      DO 28 I=1,N
      TOLD(I)=T(I)
      RHOOLD(I)=RHO(I)
      YFOLD(I,J)=YF(I,J)
      YFTHOLD(I,J) = YFTHET(I,J)
      YFPSOLD(I,J) = YFPSI(I,J)
28    CONTINUE

      DO 29 I=1,NN
      XFOLD(I,J) = XF(I,J)
      XFTHOLD(I,J) = XFTHET(I,J)
      XFPSOLD(I,J) = XFPSI(I,J)
      RHOLOLD(I) = RHOL(I)
29    CONTINUE
87    CONTINUE
```

```
*  MASS OF FUEL THAT EVAPORATED:
      MASSEV=MASSEV+4.D0/3.D0*3.1416D0*(ROLD**3-R**3)*RHOLI
      MASSP=MASSEV/MASS*1.D2
*************************************************************************
* CHECK BALANCE FOR LIQUID PHASE PROPERTIES VAPOUR SOURCE TERMS
*************************************************************************
      CALL LIQDENSIT
      THETLM = RHOLI/RHOLM
      VARLM = PSILM - THETLM**2
      SIGLM = DSQRT(VARLM)

      SUMRDTWIDL(0) = 0.0
      SUMRDHAT(0) = 0.0
      DO 339 J=1,JN
      SUMRDTWIDL(0) = SUMRDTWIDL(0) + YF(N,J)*RDTWIDL(0,J)
      SUMRDHAT(0) = SUMRDHAT(0) + YF(N,J)*RDHAT(0,J)
339   CONTINUE
      IF(SUMYF(N).GT.0.0)THEN
      SUMRDTWIDL(0) = SUMRDTWIDL(0)/SUMYF(N)
      SUMRDHAT(0) = SUMRDHAT(0)/SUMYF(N)
      ENDIF

      DO 334 I=1,NN
      SUMXFTHET(I) = 0.0
      SUMXFPSI(I) = 0.0
      DO 335 J=1,JN
      SUMXFTHET(I) = SUMXFTHET(I) + XFTHET(I,J)
      SUMXFPSI(I) = SUMXFPSI(I) + XFPSI(I,J)
335   CONTINUE
334   CONTINUE

      SUMRDTWIDLL(NN) = 0.0
      SUMRDHATL(NN) = 0.0
      DO 338 J=1,JN
      SUMRDTWIDLL(NN) = SUMRDTWIDLL(NN) + XF(NN,J)*RDTWIDLL(NN,J)
      SUMRDHATL(NN) = SUMRDHATL(NN) + XF(NN,J)*RDHATL(NN,J)
338   CONTINUE
*************************************************************************
*    UPDATE PROPERTIES:
*************************************************************************
      CALL VDENSIT
      CALL VDIF
      DO 281 J=1,JN
      DO 282 I=1,NN
      GML(I,J) = GAMMA(ALPHAL(I,J))
282   CONTINUE
281   CONTINUE
```

```
      CALL LQMIXVIS
      CALL LDIF
      CALL BOILIN
      CALL SPECHT
      CALL THCONDK
*************************************************************************
*    PRINT OUT RESULTS AT TIME INTERVALS NPRINT*DTIME0
*************************************************************************
      IF(TIME.GT.TIMELIM)GOTO 6000
      TIMETEST=TIMEPRT-DTIME0/2.D1
      IF(TIME.GE.TIMETEST)THEN
      TIMEPRT = TIMEPRT + NPRINT*DTIME0
      IF(NLP.LT.1)THEN
      IF(TIMEPRT.GE.2.3D-1)THEN
      TIMEPRT = TIMEPRT - NPRINT*DTIME0 + DTIME0
      NPRINT = 1
      NLP = NLP + 1
      ENDIF
      ENDIF
*
*  PRINT TEMPERATURE PROFILE AT END OF TIME STEP:
*
      BMF = SUMYFR/(1.D0-SUMYFR)


      DO 357 J=1,JN
      SIGL(J) = DSQRT(VARRL(NN,J))
      SIGR(J) = DSQRT(VAR(1,J))
357   CONTINUE

      DISQ = (R*2)**2

      WRITE(*,102)TIME,TR,DISQ,MASSP,TBOIL
      WRITE(10,103)TIME,TR,MASSP,TBOIL,THETLM,DISQ

      DO 673 J=1,JN
      WRITE(10+J,993)TIME,XF(NN,J),THETAL(NN,J),SIGL(J)
      WRITE(20+J,974)TIME,YFR(J),THETA(1,J),SIGR(J)
673   CONTINUE

      WRITE(11,993)XFBAR(1),XF(NN,1),THETAL(NN,1),YFR(1),XFBAR(2),
     1XF(NN,2),THETAL(NN,2),YFR(2)
*
*  PRINT LIQUID PHASE PROFILE AT END OF TIME STEP:
*
      DO 879 J=1,JN
      WRITE(30+J,*) 'LIQUID PHASE VARIABLES AS A FUNCTION OF ZETA'
```

```
      WRITE(30+J,705)
705   FORMAT(4X,'ZETAL(I)',3X,'XF(I,J)',3X,'RHOL(I)',3X,'THETAL(I,J)')
      WRITE(30+J,613)
      DO 554 I=1,NN
      WRITE(30+J,708)ZETAL(I),XF(I,J),RHOL(I),THETAL(I,J)
708   FORMAT(F8.3,3X,F7.3,3X,E10.4,3X,F7.3)
554   CONTINUE
      WRITE(30+J,613)

      WRITE(40+J,*) 'VAPOR PHASE VARIABLES AS A FUNCTION OF ZETA'
      WRITE(40+J,706)
706   FORMAT(2X,'ZETA(I)',6X,'YF(I,J)',4X,'RHO(I)',5X,'THETA(I,J)',3X,
     1'T(I)')
      WRITE(40+J,613)
      DO 556 I=1,N
      WRITE(40+J,709)ZETA(I),YF(I,J),RHO(I),THETA(I,J),T(I)
 709  FORMAT(2X,F8.3,3X,F7.5,3X,E10.4,3X,F7.3,3X,F9.3)
      WRITE(40+J,613)
556   CONTINUE
879   CONTINUE
      ENDIF
*
      NITER=0
      IF(R.GT.0.)GOTO 1000
2000  TFURN=TFURN-50.0
      TRAD=TFURN-20.0
      IF(TFURN.GE.TEND)GOTO 3000
6000  STOP
      END
*************************************************************************
      DOUBLE PRECISION FUNCTION PARAB2 (F1,F2,F3,Z1,Z2,Z3)

      IMPLICIT DOUBLE PRECISION (P,Z,F)

      PAR0 = (F2-F1)
      PAR1 = (Z2-Z1)
      PAR2 = PAR0/PAR1
      PAR3 = (F3-F1)
      PAR4 = (Z3-Z1)
      PAR5 = PAR3/PAR4
      PAR6 = PAR2-PAR5
      PAR7 = (Z2-Z3)
      PARAB1 = PAR6/PAR7
      PARAB2 = PAR2-PARAB1*PAR1
      END
*************************************************************************
```

```
      DOUBLE PRECISION FUNCTION GAMMA(ZX)
      IMPLICIT DOUBLE PRECISION (F,G,Z)

      F1 = (ZX-5.D-1)*DLOG(ZX)
      F2 = 5.D-1*DLOG(2*3.14D0)
      F3 = 1.D0/(1.2D1*ZX)
      F4 = 1.D0/(3.6D2*(ZX**3))
      F5 = 1.D0/(1.26D3*(ZX**5))
      F6 = 1.D0/(1.68D3*(ZX**7))
      GAMMA = DEXP(F1-ZX+F2+F3-F4+F5-F6)
      END
*******************************************************************************
*    YFR FROM VAPOR-LIQUID EQUILIBRIUM:

      DOUBLE PRECISION FUNCTION PVAP(F1,F2,F3,F4,F5,F6)
      IMPLICIT DOUBLE PRECISION (P,F)

      PV1 = (F1*(1.D0-F3*F2))
      PV2 = DEXP(PV1)
      PV3 = (1.D0+F1*F2*F5)
      PV4 = PV3**F4
      PVAP = PV2*F6/PV4
      END
*******************************************************************************
      SUBROUTINE  SPECHT
*******************************************************************************
      IMPLICIT DOUBLE PRECISION (A-H,O-Z)

      DIMENSION SUMTHETA(60)

      COMMON/AREA1/N,NN,JN,R
      COMMON/AREA3/CP(60),CPF(60),CPL,CPAIR(60),AO,A1,A2,A3,BO,B1,B2,B3
      COMMON/AREA5/MA,PRES,RUGC,SM(60),PATM,AVGM
      COMMON/AREA6/YOAMB,YNAMB,YF(60,5),YO(60),YN(60),YMF(60,5),
     1YMO(60),YFR(5),YFTHET(60,5),YFPSI(60,5),YFOLD(60,5),YFTHOLD(60,5),
     1YFPSOLD(60,5),SUMYF(60)
      COMMON/AREA12/TR,T(60),TOLD(60)
      COMMON/AREA13/ALPHAV(5),BETAV(5),THETA(60,5),VAR(60,5),VARM2(60,5)
      COMMON/AREA14/THETLM,AMEANL(5),VARL(5),VARLM2(5),ALPHAL(60,5),
     1BETAL(60,5),VLGAMA(5),THETAL(60,5),VARRL(60,5),PSIL(60,5),PSILM
      COMMON/AREA19/XF(60,5),XFTHET(60,5),XFPSI(60,5),XFOLD(60,5),
     1XFTHOLD(60,5),XFPSOLD(60,5),XFI(5),SUMXFTHET(60),SUMXFPSI(60)
*
*    SPECIFIC HEATS FOR FUEL AND AIR (J/KMOL.K):
*
      DO 13 I=1,N
      SUMTHETA(I) = 0.0
```

```
      DO 14 J=1,JN
      SUMTHETA(I) = SUMTHETA(I) + YF(I,J)*THETA(I,J)
14    CONTINUE
      IF(SUMYF(I).GT.0.0)THEN
      SUMTHETA(I) = SUMTHETA(I)/SUMYF(I)
      ENDIF
13    CONTINUE

      DO 15 I = 1,N
      ACP = AO + A1*T(I) + A2*T(I)**2 + A3*T(I)**3
      BCP = BO + B1*T(I) + B2*T(I)**2 + B3*T(I)**3
      CPF(I) = RUGC*1000*(ACP + BCP*SUMTHETA(I))
      CPO=(6.713D0-0.879D-6*T(I)+4.170D-6*T(I)**2-2.544D-9*T(I)**3)**4.186D3
      CPN=(7.44D0-0.324D-2*T(I)+6.400D-6*T(I)**2-2.790D-9*T(I)**3)**4.186D3
      CPAIR(I)=YOAMB*CPO+YNAMB*CPN
*  CALCULATE SPECIFIC HEAT OF MIXTURE:
      CP(I)=SUMYF(I)*CPF(I)+(1.D0 - SUMYF(I))*CPAIR(I)
15    CONTINUE
*
*  VARIABLE LIQUID SPECIFIC HEAT (J/KMOL.K)
      CPL = (0.541D0 -0.703D-3*TR+0.226D-5*TR**2)*THETLM*4.186D3
      RETURN
      END
*************************************************************************
      SUBROUTINE VDIF
*************************************************************************
      IMPLICIT DOUBLE PRECISION (A-H,O-Z)

      DIMENSION DBAR(60,5),DTWIDL(60,5),DHAT(60,5)

      COMMON/AREA1/N,NN,JN,R
      COMMON/AREA5/MA,PRES,RUGC,SM(60),PATM,AVGM
      COMMON/AREA8/RDBAR(0:60,5),RDTWIDL(0:60,5),RDHAT(0:60,5),D0(60),DIF(60)
      COMMON/AREA10/RHO(60),RHOOLD(60)
      COMMON/AREA12/TR,T(60),TOLD(60)
      COMMON/AREA13/ALPHAV(5),BETAV(5),THETA(60,5),VAR(60,5),VARM2(60,5)
      COMMON/AREA14/THETLM,AMEANL(5),VARL(5),VARLM2(5),ALPHAL(60,5),
     1BETAL(60,5),VLGAMA(5),THETAL(60,5),VARRL(60,5),PSIL(60,5),PSILM
      COMMON/AREA21/AD,BD,BPHI
*
*  DIFFUSION COEFFICIENTS (M^2/S):
*
      DO 53 J=1,JN
      DO 11 I = 1,N
      PHIDIFF = (T(I)**(5.D0/2.D0))/(PATM*(BPHI+T(I)))
      DBAR(I,J) = (AD + BD*THETA(I,J))*PHIDIFF
      DTWIDL(I,J) = (AD+BD*VARM2(I,J)/THETA(I,J))*PHIDIFF
```

```
      BETALOC = VAR(I,J)/(THETA(I,J)-VLGAMA(J))
      DHAT(I,J) = (AD+BD*(2.D0*VAR(I,J)*(BETALOC+THETA(I,J))+VARM2(I,J)
     1*THETA(I,J))/VARM2(I,J))*PHIDIFF
11    CONTINUE
*
*     PRODUCTS cD (RHO*D) ARE ASSIGNED TO EAST BOUNDARY OF CELL:
*
      RDBAR(0,J) = RHO(1)*DBAR(1,J)
      RDTWIDL(0,J) = RHO(1)*DTWIDL(1,J)
      RDHAT(0,J) = RHO(1)*DHAT(1,J)
      DO 10 I = 1,N-1
      RDBAR(I,J) = (RHO(I)*DBAR(I,J)+RHO(I+1)*DBAR(I+1,J))/2.D0
      RDTWIDL(I,J) =(RHO(I)*DTWIDL(I,J)+RHO(I+1)*DTWIDL(I+1,J))/2.D0
      RDHAT(I,J) = (RHO(I)*DHAT(I,J)+RHO(I+1)*DHAT(I+1,J))/2.D0
10    CONTINUE
53    CONTINUE
      RETURN
      END
*************************************************************************
      SUBROUTINE  THCONDK
*************************************************************************
      IMPLICIT DOUBLE PRECISION (A-H,O-Z,K)

      DIMENSION
      CONDKP(60),YAIR(60),CONDFK(60,5),CONDAK(60),SUMCONDFK(60),
     1SUMTHETA(60)

      COMMON/AREA1/N,NN,JN,R
      COMMON/AREA2/TC(5),PC,W,CPVAPA,CPVAPB,CPVAPC,CPVAPD,AL,BL,CL,DL,
     1CONDK(0:60),PCF
      COMMON/AREA3/CP(60),CPF(60),CPL,CPAIR(60),AO,A1,A2,A3,BO,B1,B2,B3
      COMMON/AREA4/TIME,DTIME,G0,VEL(60),RDOT,GTRR,DTLDT,DTR,TBOIL
      COMMON/AREA5/MA,PRES,RUGC,SM(60),PATM,AVGM
      COMMON/AREA6/YOAMB,YNAMB,YF(60,5),YO(60),YN(60),YMF(60,5),
     1YMO(60),YFR(5),YFTHET(60,5),YFPSI(60,5),YFOLD(60,5),YFTHOLD(60,5),
     1YFPSOLD(60,5),SUMYF(60)
      COMMON/AREA12/TR,T(60),TOLD(60)
      COMMON/AREA13/ALPHAV(5),BETAV(5),THETA(60,5),VAR(60,5),VARM2(60,5)
      COMMON/AREA18/VISCA,VISCF,CVA,CVF,DP,AAF,AFA,AT,BT,CT,AP,BP
      COMMON/AREA19/XF(60,5),XFTHET(60,5),XFPSI(60,5),XFOLD(60,5),
     1XFTHOLD(60,5),XFPSOLD(60,5),XFI(5),SUMXFTHET(60),SUMXFPSI(60)
*
*     THERMAL CONDUCTIVITY FOR GAS PHASE
*     FOR AIR CONDUCTIVITY, USE EUCKEN EQUATION, WITH VISCOSITY
*     FROM CHAPMAN-ENSKOG EQUATION USING THE LENNARD-JONES 12-6
*     POTENTIAL:
*
```

```
      DO 13 I=1,N
      SUMTHETA(I) = 0.0
      DO 14 J=1,JN
      IF(YF(I,J).GT.0.0)THEN
      SUMTHETA(I) = SUMTHETA(I) + YF(I,J)*THETA(I,J)
      ELSE
      SUMTHETA(I) = SUMTHETA(I) + YF(1,J)*THETA(I,J)
      ENDIF
14    CONTINUE
      IF(SUMYF(I).GT.0.0)THEN
      SUMTHETA(I) = SUMTHETA(I)/SUMYF(I)
      ENDIF
13    CONTINUE
*
      AV=1.16145D0
      BV=0.14874D0
      CV=0.52487D0
      DV=0.77320D0
      EV=2.16178D0
      FV=2.43787D0
      SA=3.711D0
      EKA=7.86D1
      TCA = 1.262D2
      PCA = 3.35D1
      KTRAA =1.0D0
      KTRFF =1.0D0
      AAA =1.0D0
      AFF =1.0D0
C
      DO 54 J = 1,JN
      DO 12 I = 1,N
*
* LENNARD-JONES PARAMETERS SIGMA AND E/K FOR FUEL
      TCF = AT + BT*THETA(I,J)
      IF(THETA(I,J).LT.2.7D2) THEN
      PCF = AP + BP*THETA(I,J)
      ELSE
      PCF = 1.1D1
      ENDIF
      SF=(TCF/PCF)**(1.D0/3.D0)*(2.3551D0-8.7D-2*W)
      EKF=TCF*(0.7915D0+0.1693D0*W)
*  SIGMA AND E/K FOR AIR-FUEL MIXTURE:
      SAF=(SA+SF)/2.D0
      EKAF=(EKA*EKF)**(1.D0/2.D0)
      TASTA=T(I)/EKA
      TASTF=T(I)/EKF
      OMGVA=AV/TASTA**BV+CV/DEXP(DV*TASTA)+EV/DEXP(FV*TASTA)
```

```
*  VISCOSITY OF AIR (MICROPOISE):
       VISCA=2.669D1*(MA*T(I))**(1.D0/2.D0)/(SA**2.D0*OMGVA)
*  EUCKEN EQUATION FOR AIR CONDUCTIVITY
       CVA=CPAIR(I)*2.39D-1/1.D3-1.99D0
       CVF=CPF(I)/4.186D3-1.99D0
       CONDAK(I)=(CVA+4.47)*VISCA*1.D-6/MA
*  CORRELATION FOR FUEL VAPOUR CONDUCTIVITY:
       AK = 2.6008D-5*T(I) - 5.6496D-3
       BK = -4.5511D-8*T(I) + 8.2873D-6
       CONDFK(I,J) = (AK + BK*THETA(I,J))*1.D-2
12     CONTINUE
54     CONTINUE

       DO 193 I=1,N
       SUMCONDFK(I) = 0.0
       DO 194 J=1,JN
       IF(YF(I,J).GT.0.0)THEN
       SUMCONDFK(I) = SUMCONDFK(I) + YF(I,J)*CONDFK(I,J)
       ELSE
       SUMCONDFK(I) = SUMCONDFK(I) + YF(1,J)*CONDFK(I,J)
       ENDIF
194    CONTINUE
       IF(SUMYF(I).GT.0.0)THEN
       SUMCONDFK(I) = SUMCONDFK(I)/SUMYF(I)
       ENDIF
193    CONTINUE
*
*  MONATOMIC VALUES OF THERMAL CONDUCTIVITY (KTR(I)/KTR(J))
*    USED FOR MIXING RULE USED TO COMBINE FUEL AND AIR K'S
*
       DO 112 I = 1,N
       TCF = AT + BT*SUMTHETA(I)
       IF(SUMTHETA(I).LT.2.7D2) THEN
       PCF = AP + BP*SUMTHETA(I)
       ELSE
       PCF = 1.1D1
       ENDIF
       TRF = T(I)/TCF
       TRA = T(I)/TCA
       GAMA = TCA**(1.D0/6.D0)*MA**5.D-1/PCA**(2.D0/3.D0)
       GAMF = TCF**(1.D0/6.D0)*SUMTHETA(I)**5.D-1/PCF**(2.D0/3.D0)
       KTRAF = (GAMF/GAMA)*((DEXP(4.64D-2*TRA) - DEXP(-2.412D-1*TRA))/
      1(DEXP(4.64D-2*TRF) - DEXP(-2.412D-1*TRF)))
       KTRFA = GAMA*(DEXP(4.64D-2*TRF) - DEXP(-2.412D-1*TRF))/
      1(GAMF*(DEXP(4.64D-2*TRA) - DEXP(-2.412D-1*TRA)))
       AAF=(1.D0+KTRAF **(1.D0/2.D0)*(MA/SUMTHETA(I))**(1.D0/4.D0))**2.D0
      1/(8.D0*(1.D0+MA/SUMTHETA(I)))**(1.D0/2.D0)
```

```
      AFA=(1.D0+KTRFA **(1.D0/2.D0)*(SUMTHETA(I)/MA)**(1.D0/4.D0))**2.D0
     1/(8.D0*(1.D0+SUMTHETA(I)/MA))**(1.D0/2.D0)
      YAIR(I) = 1.D0 - SUMYF(I)
*
*  THERMAL CONDUCTIVITY OF AIR-FUEL MIXTURE:
      CONDKP(I)=(YAIR(I)*CONDAK(I)/(YAIR(I)*AAA+SUMYF(I)*AAF)
     1+SUMYF(I)*SUMCONDFK(I)/(YAIR(I)*AFA+SUMYF(I)*AFF))*4.186D2
112   CONTINUE

      CONDK(0)=CONDKP(1)
      DO 113 I = 1,N
      CONDK(I) = (CONDKP(I)+CONDKP(I+1))/2.D0
113   CONTINUE
      RETURN
      END
**********************************************************************
      SUBROUTINE VDENSIT
**********************************************************************
      IMPLICIT DOUBLE PRECISION (A-H,O-Z)

      DIMENSION SUMYFTH(60)

      COMMON/AREA1/N,NN,JN,R
      COMMON/AREA5/MA,PRES,RUGC,SM(60),PATM,AVGM
      COMMON/AREA6/YOAMB,YNAMB,YF(60,5),YO(60),YN(60),YMF(60,5),
     1YMO(60),YFR(5),YFTHET(60,5),YFPSI(60,5),YFOLD(60,5),YFTHOLD(60,5),
     1YFPSOLD(60,5),SUMYF(60)
      COMMON/AREA9/ZETA(60),ZETAE(60),ZE2DZ(60),ZE3(60),ZE3D(60),ZETAD(60)
      COMMON/AREA10/RHO(60),RHOOLD(60)
      COMMON/AREA12/TR,T(60),TOLD(60)
      COMMON/AREA13/ALPHAV(5),BETAV(5),THETA(60,5),VAR(60,5),VARM2(60,5)
*
*  CALCULATE THE MIXTURE MOLECULAR WEIGHT AND DENSITY:
*
      MO=3.2D1
      MN=2.8D1

      DO 800 I=1,N
      SUMYFTH(I) = 0.0
      DO 900 J=1,JN
      SUMYFTH(I) = SUMYFTH(I) + YF(I,J)*THETA(I,J)
900   CONTINUE
800   CONTINUE

      DO 200 I=1,N
      SM(I)=SUMYFTH(I)+YO(I)*MO+YN(I)*MN
      RHO(I)=PRES/(RUGC*T(I))
```

```
200   CONTINUE
      AVGM = SM(1)*SM(N)/(2.D0*SM(N)/3.D0 + SM(1)/3.D0)
      RETURN
      END
*****************************************************************************
      SUBROUTINE LIQDENSIT
*****************************************************************************
*    THIS SUBROUTINE IS DONE TO CALCULATE  LIQUID DENSITY:
*
      IMPLICIT DOUBLE PRECISION (A-H,O-Z)

      DIMENSION SUMTHETAL(60),SUMPSIL(60)

      COMMON/AREA1/N,NN,JN,R
      COMMON/AREA11/RHOL(60),RHOLOLD(60),RHOLM,RHOLI,DIFLL(60),XFBAR(5)
      COMMON/AREA14/THETLM,AMEANL(5),VARL(5),VARLM2(5),ALPHAL(60,5),
     1BETAL(60,5),VLGAMA(5),THETAL(60,5),VARRL(60,5),PSIL(60,5),PSILM
      COMMON/AREA19/XF(60,5),XFTHET(60,5),XFPSI(60,5),XFOLD(60,5),
     1XFTHOLD(60,5),XFPSOLD(60,5),XFI(5),SUMXFTHET(60),SUMXFPSI(60)
      COMMON/AREA20/ZETAL(60),ZETALE(60),ZLE2DZ(60),ZLE3(60),ZLE3D(60),
     1ZETALD(60),ZLE2(60),VELL(60)
*
      DO 50 I = 1,NN
      SUMTHETAL(I) = 0.0
      SUMPSIL(I) = 0.0
      DO 51 J=1,JN
      SUMTHETAL(I) = SUMTHETAL(I) + XF(I,J)*THETAL(I,J)
      SUMPSIL(I) = SUMPSIL(I) + XF(I,J)*PSIL(I,J)
51    CONTINUE
50    CONTINUE

      DO 16 I=1,NN
      RHOL(I) = RHOLI/SUMTHETAL(I)
16    CONTINUE

      RHOLM = (RHOL(1)*ZLE3(1))+(RHOL(NN)*(1.D0-ZLE3(NN-1)))
      DO 74 I=2,NN-1
      RHOLM = RHOLM + (ZLE3D(I)*RHOL(I))
74    CONTINUE

      PSILM = SUMPSIL(1)*RHOL(1)*ZLE3(1) + SUMPSIL(NN)*RHOL(NN)
     1*(1.D0-ZLE3(NN-1))
      DO 75 I=2,NN-1
      PSILM = PSILM + (ZLE3D(I)*RHOL(I)*SUMPSIL(I))
75    CONTINUE
      PSILM = PSILM/RHOLM
```

```
      DO 99 J=1,JN
      XFBAR(J) = (RHOL(1)*XF(1,J)*ZLE3(1))+(RHOL(NN)*XF(NN,J)*
     1 (1.D0-ZLE3(NN-1)))
      DO 88 I=2,NN-1
      XFBAR(J) = XFBAR(J) + (ZLE3D(I)*RHOL(I)*XF(I,J))
88    CONTINUE
      XFBAR(J) = XFBAR(J)/RHOLM
99    CONTINUE
      RETURN
      END

*************************************************************************
      SUBROUTINE COEF
*************************************************************************
      IMPLICIT DOUBLE PRECISION (A-H,O-Z)

      COMMON/AREA1/N,NN,JN,R
      COMMON/AREA4/TIME,DTIME,G0,VEL(60),RDOT,GTRR,DTLDT,DTR,TBOIL
      COMMON/AREA8/RDBAR(0:60,5),RDTWIDL(0:60,5),RDHAT(0:60,5),D0(60),DIF(60)
      COMMON/AREA9/ZETA(60),ZETAE(60),ZE2DZ(60),ZE3(60),ZE3D(60),ZETAD(60)
      COMMON/AREA10/RHO(60),RHOOLD(60)
      COMMON/AREA12/TR,T(60),TOLD(60)
      COMMON/AREA13/ALPHAV(5),BETAV(5),THETA(60,5),VAR(60,5),VARM2(60,5)
*
*  TEMPERATURE EQUATION COEFFICIENTS THAT ARE CONSTANT:
      DO 301 I=2,N-1
      D0(I)=ZE3D(I)/3.D0*RHOOLD(I)
301   CONTINUE
      RETURN
      END
*************************************************************************
      SUBROUTINE TEMP
*************************************************************************
      IMPLICIT DOUBLE PRECISION (A-H,O-Z)

      DIMENSION SUMM(60),FCNV(60),CONDIF(60),PEPOW(60),A(60),B(60),C(60)
     1,D(60),P(60),Q(60),PSUMM(60,5)

      COMMON/AREA1/N,NN,JN,R
      COMMON/AREA2/TC(5),PC,W,CPVAPA,CPVAPB,CPVAPC,CPVAPD,AL,BL,CL,DL,
     1CONDK(0:60),PCF
      COMMON/AREA3/CP(60),CPF(60),CPL,CPAIR(60),AO,A1,A2,A3,BO,B1,B2,B3
      COMMON/AREA4/TIME,DTIME,G0,VEL(60),RDOT,GTRR,DTLDT,DTR,TBOIL
      COMMON/AREA5/MA,PRES,RUGC,SM(60),PATM,AVGM
      COMMON/AREA6/YOAMB,YNAMB,YF(60,5),YO(60),YN(60),YMF(60,5),
     1YMO(60),YFR(5),YFTHET(60,5),YFPSI(60,5),YFOLD(60,5),YFTHOLD(60,5),
     1YFPSOLD(60,5),SUMYF(60)
```

```
      COMMON/AREA8/RDBAR(0:60,5),RDTWIDL(0:60,5),RDHAT(0:60,5),D0(60),DIF(60)
      COMMON/AREA9/ZETA(60),ZETAE(60),ZE2DZ(60),ZE3(60),ZE3D(60),ZETAD(60)
      COMMON/AREA10/RHO(60),RHOOLD(60)
      COMMON/AREA12/TR,T(60),TOLD(60)
      COMMON/AREA13/ALPHAV(5),BETAV(5),THETA(60,5),VAR(60,5),VARM2(60,5)
      COMMON/AREA19/XF(60,5),XFTHET(60,5),XFPSI(60,5),XFOLD(60,5),
     1XFTHOLD(60,5),XFPSOLD(60,5),XFI(5),SUMXFTHET(60),SUMXFPSI(60)
*
*  CALCULATE THE COEFFICIENTS FOR THE ENERGY EQUATION:
*  FCNV,CONDIF AND PE CORRESPOND TO FE,DE AND PECLET IN PATANKAR
      DO 400 I=1,N-1
      ACP = RUGC*1000.*(AO + A1*T(I) + A2*T(I)**2 + A3*T(I)**3)
      BCP = RUGC*1000.*(BO + B1*T(I) + B2*T(I)**2 + B3*T(I)**3)
      SUMM(I) = 0.0
      DO 1000 J=1,JN
      PSUMM(I,J)=RDBAR(I,J)*(ACP-CPAIR(I))+RDTWIDL(I,J)*BCP*THETA(I,J)
      PSUMM(I,J)=PSUMM(I,J)*(YF(I+1,J)-YF(I,J))
      SUMM(I) = SUMM(I) + PSUMM(I,J)
1000 CONTINUE
      SUMM(I)=SUMM(I)+CONDK(I)*2.D0/(CP(I)+CP(I+1))*(CP(I+1)-CP(I))
      SUMM(I)=ZE2DZ(I)*DTIME/R**2*SUMM(I)*2.D0/(CP(I)+CP(I+1))

      FCNV(I)=VEL(I)*DTR-SUMM(I)
      CONDIF(I)=CONDK(I)*DIF(I)*2.D0/(CP(I)+CP(I+1))
      PE=FCNV(I)/CONDIF(I)
      PEPOW(I)=(1.D0-1.D-1*DABS(PE))**5

400   CONTINUE
      DO 401 I=2,N-1
      B(I)=CONDIF(I)*DMAX1(0.D0,PEPOW(I))+DMAX1(-1.D0*FCNV(I),0.D0)
      C(I)=CONDIF(I-1)*DMAX1(0.D0,PEPOW(I-1))+DMAX1(FCNV(I-1),0.D0)
      A(I)=RHO(I)/3.D0*ZE3D(I)*(1.D0-3.D0*GTRR)+SUMM(I)-SUMM(I-1)
      A(I)=A(I)+B(I)+C(I)+(FCNV(I)-FCNV(I-1))
      D(I)=D0(I)*TOLD(I)
401   CONTINUE
*
*  TRIDIAGONAL-MATRIX ALGORITHM:
      A(1)=1.0D0
      B(1)=0.0D0
      C(1)=0.0D0
      D(1)=T(1)
      P(1)=B(1)/A(1)
      Q(1)=D(1)/A(1)
      DO 403 I=2,N-1
      P(I)=B(I)/(A(I)-C(I)*P(I-1))
      Q(I)=(D(I)+C(I)*Q(I-1))/(A(I)-C(I)*P(I-1))
403   CONTINUE
```

```
      DO 404 I=N-1,2,-1
      T(I)=P(I)*T(I+1)+Q(I)
404   CONTINUE
      RETURN
      END
*****************************************************************************
      SUBROUTINE YCONC
*****************************************************************************
      IMPLICIT DOUBLE PRECISION (A-H,O-Z)

      DIMENSION FCNV(60),GAMDIF(60),PEPOW(60),A(60),B(60),C(60),D(60),P(60),
     1Q(60)

      COMMON/AREA1/N,NN,JN,R
      COMMON/AREA4/TIME,DTIME,G0,VEL(60),RDOT,GTRR,DTLDT,DTR,TBOIL
      COMMON/AREA6/YOAMB,YNAMB,YF(60,5),YO(60),YN(60),YMF(60,5),
     1YMO(60),YFR(5),YFTHET(60,5),YFPSI(60,5),YFOLD(60,5),YFTHOLD(60,5),
     1YFPSOLD(60,5),SUMYF(60)
      COMMON/AREA8/RDBAR(0:60,5),RDTWIDL(0:60,5),RDHAT(0:60,5),D0(60),DIF(60)
      COMMON/AREA9/ZETA(60),ZETAE(60),ZE2DZ(60),ZE3(60),ZE3D(60),ZETAD(60)
      COMMON/AREA10/RHO(60),RHOOLD(60)
*
*  CALCULATE THE COEFFICIENTS FOR THE DIFFUSION EQUATION:
*  FCNV,GAMDIF AND PE CORRESPOND TO FE,DE AND PECLET IN
*  PATANKAR
      DO 200 J=1,JN
      DO 100 I=1,N-1
      FCNV(I)=VEL(I)*DTR
      GAMDIF(I)=RDBAR(I,J)*DIF(I)
      PE=FCNV(I)/GAMDIF(I)
      PEPOW(I)=(1.D0-1.D-1*DABS(PE))**5
100   CONTINUE
      DO 101 I=2,N-1
      B(I)=GAMDIF(I)*DMAX1(0.D0,PEPOW(I))+DMAX1(-1.D0*FCNV(I),0.D0)
      C(I)=GAMDIF(I-1)*DMAX1(0.D0,PEPOW(I-1))+DMAX1(FCNV(I-1),0.D0)
      A(I)=B(I)+C(I)+RHO(I)/3.D0*ZE3D(I)*(1.D0-3.D0*GTRR)
      A(I)=A(I)+(FCNV(I)-FCNV(I-1))
      D(I)=D0(I)*YFOLD(I,J)
101   CONTINUE
*
*
*  TRIDIAGONAL-MATRIX ALGORITHM:
      A(1)=1.0D0
      B(1)=0.0D0
      C(1)=0.0D0
      D(1)=YF(1,J)
      P(1)=B(1)/A(1)
```

```
      Q(1)=D(1)/A(1)
      DO 103 I=2,N-1
      P(I)=B(I)/(A(I)-C(I)*P(I-1))
      Q(I)=(D(I)+C(I)*Q(I-1))/(A(I)-C(I)*P(I-1))
103   CONTINUE
      DO 104 I=N-1,2,-1
      YF(I,J)=P(I)*YF(I+1,J)+Q(I)
104   CONTINUE
200   CONTINUE
      DO 186 I=1,N
      SUMYF(I) = 0.0
      DO 187 J=1,JN
      SUMYF(I) = SUMYF(I) + YF(I,J)
187   CONTINUE
186   CONTINUE

      DO 105 I=1,N-1
      YO(I)=YOAMB*(1.D0-SUMYF(I))
      YN(I)=YO(I)*YNAMB/YOAMB
105   CONTINUE
      RETURN
      END
*******************************************************************************
      SUBROUTINE YCONCI
*******************************************************************************
      IMPLICIT DOUBLE PRECISION (A-H,O-Z)

      DIMENSION GAMDIT(60),GAMDIP(60),PET(60),PEP(60),PEPOT(60),ATH(60),
     1BTH(60),CTH(60),APS(60),BPS(60),CPS(60),DI(60),FCNV(60),PI(60),QI(60),DV(60),
     1PV(60),QV(60),PEPOW(60)

      COMMON/AREA1/N,NN,JN,R
      COMMON/AREA4/TIME,DTIME,G0,VEL(60),RDOT,GTRR,DTLDT,DTR,TBOIL
      COMMON/AREA5/MA,PRES,RUGC,SM(60),PATM,AVGM
      COMMON/AREA6/YOAMB,YNAMB,YF(60,5),YO(60),YN(60),YMF(60,5),
     1YMO(60),YFR(5),YFTHET(60,5),YFPSI(60,5),YFOLD(60,5),YFTHOLD(60,5),
     1YFPSOLD(60,5),SUMYF(60)
      COMMON/AREA8/RDBAR(0:60,5),RDTWIDL(0:60,5),RDHAT(0:60,5),D0(60),DIF(60)
      COMMON/AREA9/ZETA(60),ZETAE(60),ZE2DZ(60),ZE3(60),ZE3D(60),ZETAD(60)
      COMMON/AREA10/RHO(60),RHOOLD(60)
      COMMON/AREA12/TR,T(60),TOLD(60)
      COMMON/AREA13/ALPHAV(5),BETAV(5),THETA(60,5),VAR(60,5),VARM2(60,5)
*
*  CALCULATE THE COEFFICIENTS FOR THE DISTRIBUTION EQUATION:
*  FCNV,GAMDIF AND PE CORRESPOND TO FE,DE AND PECLET IN
* PATANKAR
C     NOTE THAT DIFFUSION COEFS. RDTWIDL, RDHAT ARE DEFINED AT
```

```
C    WEST BOUNDARY OF CELL
      DO 600 J = 1,JN
      DO 501 I = 1,N-1
      FCNV(I) = VEL(I)*DTR
      GAMDIT(I) = RDTWIDL(I,J)*DIF(I)
      GAMDIP(I) = RDHAT(I,J)*DIF(I)
      PET(I) = FCNV(I)/GAMDIT(I)
      PEP(I) = FCNV(I)/GAMDIP(I)
      PEPOT(I) = (1.D0 - 1.D-1*DABS(PET(I)))**5
      PEPOW(I) = (1.D0 - 1.D-1*DABS(PEP(I)))**5
501   CONTINUE
      DO 502 I = 2,N-1
      BTH(I) = GAMDIT(I)*DMAX1(0.D0,PEPOT(I))+DMAX1(-1.D0*FCNV(I),0.D0)
      CTH(I) = GAMDIT(I-1)*DMAX1(0.D0,PEPOT(I-1))+DMAX1(FCNV(I-1),0.D0)
      ATH(I) = BTH(I)+CTH(I)+RHO(I)/3.D0*ZE3D(I)*(1.D0-3.D0*GTRR)
      ATH(I) = ATH(I) + FCNV(I) - FCNV(I-1)
      BPS(I) = GAMDIP(I)*DMAX1(0.D0,PEPOW(I))+DMAX1(-FCNV(I),0.D0)
      CPS(I) = GAMDIP(I-1)*DMAX1(0.D0,PEPOW(I-1))+DMAX1(FCNV(I-1),0.D0)
      APS(I) = BPS(I)+CPS(I)+ RHO(I)/3.D0*ZE3D(I)*(1.D0-3.D0*GTRR)
      APS(I) = APS(I) + FCNV(I) - FCNV(I-1)
      DI(I) = D0(I)*YFTHOLD(I,J)
      DV(I) = D0(I)*YFPSOLD(I,J)
502   CONTINUE
*
*
*  TRIDIAGONAL-MATRIX ALGORITHM:
      ATH(1) = 1.0D0
      BTH(1) = 0.0D0
      CTH(1) = 0.0D0
      APS(1) = 1.0D0
      BPS(1) = 0.0D0
      CPS(1) = 0.0D0
* MEAN I TIMES YF
      DI(1) = YFTHET(1,J)
      PI(1) = BTH(1)/ATH(1)
      QI(1) = DI(1)/ATH(1)
* PSI TIMES YF
      DV(1) = YFPSI(1,J)
      PV(1) = BPS(1)/APS(1)
      QV(1) = DV(1)/APS(1)
      DO 503 I = 2,N-1
      PI(I)=BTH(I)/(ATH(I)-CTH(I)*PI(I-1))
      QI(I)=(DI(I)+CTH(I)*QI(I-1))/(ATH(I)-CTH(I)*PI(I-1))
      PV(I)=BPS(I)/(APS(I)-CPS(I)*PV(I-1))
      QV(I)=(DV(I)+CPS(I)*QV(I-1))/(APS(I)-CPS(I)*PV(I-1))
503   CONTINUE
      DO 504 I=N-1,2,-1
```

```
      YFTHET(I,J)=PI(I)*YFTHET(I+1,J)+QI(I)
      YFPSI(I,J)=PV(I)*YFPSI(I+1,J)+QV(I)
504   CONTINUE
      IFLAG = 0
      DO 106 I = 2,N
      IF (IFLAG.EQ.1)GOTO 107
      IF (YF(I,J).LT.1.D-38)THEN
      IFLAG = 1
      NFLAG = I
      GOTO 107
      ENDIF
      THETA(I,J) = YFTHET(I,J)/YF(I,J)
      VARM2(I,J) = YFPSI(I,J)/YF(I,J)
      VAR(I,J) = VARM2(I,J) - THETA(I,J)**2
      YMF(I,J) = YF(I,J)*THETA(I,J)/SM(I)
      GOTO 106
107   THETA(I,J) = THETA(NFLAG-1,J)
      VARM2(I,J) = VARM2(NFLAG-1,J)
      VAR(I,J)   = VARM2(I,J) - THETA(I,J)**2
106   CONTINUE
      YMF(1,J) = YF(1,J)*THETA(1,J)/SM(1)
600   CONTINUE
      RETURN
      END
*************************************************************************
      SUBROUTINE BOILIN
*************************************************************************
      IMPLICIT DOUBLE PRECISION (A-H,O-Z)
      INTEGER H
      DIMENSION TN(1000), F(1000),F1(1000,5),F2(1000,5),SUMF1(1000),SUMF2(1000),
     1SUMTHETAL(60)

      COMMON/AREA1/N,NN,JN,R
      COMMON/AREA4/TIME,DTIME,G0,VEL(60),RDOT,GTRR,DTLDT,DTR,TBOIL
      COMMON/AREA5/MA,PRES,RUGC,SM(60),PATM,AVGM
      COMMON/AREA14/THETLM,AMEANL(5),VARL(5),VARLM2(5),ALPHAL(60,5),
     1BETAL(60,5),VLGAMA(5),THETAL(60,5),VARRL(60,5),PSIL(60,5),PSILM
      COMMON/AREA17/A(5),B(5),SFGR
      COMMON/AREA18/VISCA,VISCF,CVA,CVF,DP,AAF,AFA,AT,BT,CT,AP,BP
      COMMON/AREA19/XF(60,5),XFTHET(60,5),XFPSI(60,5),XFOLD(60,5),
     1XFTHOLD(60,5),XFPSOLD(60,5),XFI(5),SUMXFTHET(60),SUMXFPSI(60)
*
      DO 47 I=1,NN
      SUMTHETAL(I) = 0.0
      DO 48 J=1,JN
      SUMTHETAL(I) = SUMTHETAL(I) + XF(I,J)*THETAL(I,J)
48    CONTINUE
```

```
47    CONTINUE
      H = 1000
      YFA = 1.D0
      TC = AT + BT*SUMTHETAL(NN)
      TO = 2.D2
      TF = TC
      DT = (TC-TO)/H
      TN(1) = TO
      DO 5 I=2,H
      TN(I) = TN(I-1) + DT
5     CONTINUE
      DO 10 I=1,H
      SUMF1(I) = 0.0
      DO 20 J=1,JN
      F1(I,J) = DEXP(SFGR *(1.D0-(A(J)+VLGAMA(J)*B(J))/TN(I)))/
     1((1.D0+SFGR*B(J)*BETAL(NN,J)/TN(I))**ALPHAL(NN,J))
      SUMF1(I) = SUMF1(I) + XFI(J)*F1(I,J)
20    CONTINUE
      F(I) = YFA - SUMF1(I)
      IF(I.EQ.1) GOTO 10
      JL = 0
3     P = F(I)*F(I-1)
      JL = JL+1
      IF (JL.EQ.1000) GOTO 4
      IF(P.LT.0.0D0) THEN
      TSTART = TN(I-1)
      TSTOP  = TN(I)
      TMID = (TSTART + TSTOP)/2.D0
      TDIF   = DABS(TSTOP - TSTART)
      SUMF2(I) = 0.0
      DO 15 J=1,JN
      F2(I,J) = DEXP(SFGR *(1.D0-(A(J)+VLGAMA(J)*B(J))/TMID))/
     1((1.D0+SFGR*B(J)*BETAL(NN,J)/TMID)**ALPHAL(NN,J))
      SUMF2(I) = SUMF2(I) + XFI(J)*F2(I,J)
15    CONTINUE
      IF (TDIF.LE.1.D-2) THEN
      TBOIL = TSTART
      GOTO 4
      ELSEIF (P.LT.0.0D0) THEN
      F(I) = YFA - SUMF2(I)
      TN(I) = TMID
      GOTO 3
      ELSE
      F(I-1) = YFA - SUMF2(I)
      TN(I-1) = TMID
      GOTO 3
      ENDIF
```

```
      ENDIF
10    CONTINUE
4     RETURN
      END
*****************************************************************************
      SUBROUTINE XCONC
*****************************************************************************
      IMPLICIT DOUBLE PRECISION (A-H,O-Z)

      DIMENSION ABR(60),ATH(60),APS(60),BBR(60),BTH(60),BPS(60),CBR(60)
     1,CTH(60),CPS(60),DBR(60),DTH(60),DPS(60),FCNV(60),GAMDIB(60),
     1GAMDIT(60),GAMDIP(60),PEB(60),PET(60),PEP(60),PEPOB(60),PEPOT(60),
     1PEPOP(60),PBR(60),PTH(60),PPS(60),QBR(60),QTH(60),QPS(60),TBR(60)

      COMMON/AREA1/N,NN,JN,R
      COMMON/AREA4/TIME,DTIME,G0,VEL(60),RDOT,GTRR,DTLDT,DTR,TBOIL
      COMMON/AREA11/RHOL(60),RHOLOLD(60),RHOLM,RHOLI,DIFLL(60),XFBAR(5)
      COMMON/AREA14/THETLM,AMEANL(5),VARL(5),VARLM2(5),ALPHAL(60,5),
     1BETAL(60,5),VLGAMA(5),THETAL(60,5),VARRL(60,5),PSIL(60,5),PSILM
      COMMON/AREA16/RDBARL(60,5),RDTWIDLL(60,5),RDHATL(60,5),FAC,
     1DBARL(60,5),DTWIDLL(60,5),DHATL(60,5)
      COMMON/AREA19/XF(60,5),XFTHET(60,5),XFPSI(60,5),XFOLD(60,5),
     1XFTHOLD(60,5),XFPSOLD(60,5),XFI(5),SUMXFTHET(60),SUMXFPSI(60)
      COMMON/AREA20/ZETAL(60),ZETALE(60),ZLE2DZ(60),ZLE3(60),ZLE3D(60),
     1ZETALD(60),ZLE2(60),VELL(60)
*  ***************************************************************************
*  CALCULATE THE COEFFICIENTS FOR THE DISTRIBUTION EQUATION:
*  FCNV,GAMDIF AND PE CORRESPOND TO FE,DE AND PECLET IN
*  PATANKAR NOTE THAT DIFFUSION COEFS. RDTWIDL, RDHAT ARE
*  DEFINED AT EAST BOUNDARY OF CELL
*  ***************************************************************************
      DO 20 I = 1,NN-1
      FCNV(I) = DTR*VELL(I)
20    CONTINUE
*
      DO 73 J=1,JN
      DO 21 I=1,NN-1
      GAMDIB(I) = RDBARL(I,J)*DIFLL(I)
      GAMDIT(I) = RDTWIDLL(I,J)*DIFLL(I)
      GAMDIP(I) = RDHATL(I,J)*DIFLL(I)
21    CONTINUE
*
      DO 71 I = 1,NN-1
      PEB(I) = FCNV(I)/GAMDIB(I)
      PET(I) = FCNV(I)/GAMDIT(I)
      PEP(I) = FCNV(I)/GAMDIP(I)
71    CONTINUE
```

```
*
      DO 70 I=1,NN-1
      PEPOB(I) = (1.D0 - (1.D-1)*DABS(PEB(I)))**5
      PEPOT(I) = (1.D0 - (1.D-1)*DABS(PET(I)))**5
      PEPOP(I) = (1.D0 - (1.D-1)*DABS(PEP(I)))**5
70    CONTINUE
*
*  TRIDIAGONAL-MATRIX ALGORITHM:
      ABR(1)=1.0D0
      ATH(1)=1.0D0
      APS(1)=1.0D0
      BBR(1)=1.0D0
      BTH(1)=1.0D0
      BPS(1)=1.0D0
      CBR(1)=0.0D0
      CTH(1)=0.0D0
      CPS(1)=0.0D0
      DBR(1)=0.0D0
      DTH(1)=0.0D0
      DPS(1)=0.0D0
*
      DO 23 I = 2,NN-1
      BBR(I) = GAMDIB(I)*DMAX1(0.D0,PEPOB(I))+DMAX1(-1.D0*FCNV(I),0.D0)
      BTH(I) = GAMDIT(I)*DMAX1(0.D0,PEPOT(I))+DMAX1(-1.D0*FCNV(I),0.D0)
      BPS(I) = GAMDIP(I)*DMAX1(0.D0,PEPOP(I))+DMAX1(-1.D0*FCNV(I),0.D0)

      CBR(I) = GAMDIB(I-1)*DMAX1(0.D0,PEPOB(I-1))+DMAX1(FCNV(I-1),0.D0)
      CTH(I) = GAMDIT(I-1)*DMAX1(0.D0,PEPOT(I-1))+DMAX1(FCNV(I-1),0.D0)
      CPS(I) = GAMDIP(I-1)*DMAX1(0.D0,PEPOP(I-1))+DMAX1(FCNV(I-1),0.D0)

      DBR(I) = (1.D0/3.D0)*ZLE3D(I)*RHOLOLD(I)*XFOLD(I,J)
      DTH(I) = (1.D0/3.D0)*ZLE3D(I)*RHOLOLD(I)*XFTHOLD(I,J)
      DPS(I) = (1.D0/3.D0)*ZLE3D(I)*RHOLOLD(I)*XFPSOLD(I,J)

      TBR(I) = ZLE3D(I)*RHOL(I)*((1.D0/3.D0)-GTRR)

      ABR(I) = BBR(I)+CBR(I)+TBR(I)
      ABR(I) = ABR(I)+FCNV(I)-FCNV(I-1)
      ATH(I) = BTH(I)+CTH(I)+TBR(I)
      ATH(I) = ATH(I)+FCNV(I)-FCNV(I-1)
      APS(I) = BPS(I)+CPS(I)+TBR(I)
      APS(I) = APS(I)+FCNV(I)-FCNV(I-1)

23    CONTINUE
*
      PBR(1) = BBR(1)/ABR(1)
      QBR(1) = DBR(1)/ABR(1)
```

```
      PTH(1) = BTH(1)/ATH(1)
      QTH(1) = DTH(1)/ATH(1)
      PPS(1) = BPS(1)/APS(1)
      QPS(1) = DPS(1)/APS(1)
      QBR(60) = XF(60,J)
      QTH(60) = XFTHET(60,J)
      QPS(60) = XFPSI(60,J)
*
      DO 24 I = 2,NN-1
      PBR(I)=BBR(I)/(ABR(I)-CBR(I)*PBR(I-1))
      PTH(I)=BTH(I)/(ATH(I)-CTH(I)*PTH(I-1))
      PPS(I)=BPS(I)/(APS(I)-CPS(I)*PPS(I-1))
      QBR(I)=(DBR(I)+CBR(I)*QBR(I-1))/(ABR(I)-CBR(I)*PBR(I-1))
      QTH(I)=(DTH(I)+CTH(I)*QTH(I-1))/(ATH(I)-CTH(I)*PTH(I-1))
      QPS(I)=(DPS(I)+CPS(I)*QPS(I-1))/(APS(I)-CPS(I)*PPS(I-1))
24    CONTINUE
*
      DO 25 I=NN-1,1,-1
      XF(I,J)=PBR(I)*XF(I+1,J)+QBR(I)
      XFTHET(I,J)=PTH(I)*XFTHET(I+1,J)+QTH(I)
      XFPSI(I,J)=PPS(I)*XFPSI(I+1,J)+QPS(I)
25    CONTINUE

      DO 63 I=1,NN
      IF(XF(I,J).GT.0.0D0)THEN
      THETAL(I,J) = XFTHET(I,J)/XF(I,J)
      PSIL(I,J) = XFPSI(I,J)/XF(I,J)
      VARRL(I,J) = PSIL(I,J) - THETAL(I,J)**2
      BETAL(I,J) = VARRL(I,J)/(THETAL(I,J)-VLGAMA(J))
      ALPHAL(I,J) = (THETAL(I,J)-VLGAMA(J))/BETAL(I,J)
      ENDIF
63    CONTINUE
73    CONTINUE
      RETURN
      END
*************************************************************************
      SUBROUTINE LQMIXVIS
*************************************************************************
*   THIS SUBROUTINE WILL CALCULATE THE LIQUID MIXTURE VISCOSITY
*   IN [CP] BASED ON NUMERICAL INTEGRATION FOR VLGAMA NOT EQUAL
*   TO ZERO.
*
      IMPLICIT DOUBLE PRECISION (A-G,O-Z)

      DIMENSION VISMIX1(60,5)

      COMMON/AREA1/N,NN,JN,R
```

```
      COMMON/AREA11/RHOL(60),RHOLOLD(60),RHOLM,RHOLI,DIFLL(60),XFBAR(5)
      COMMON/AREA12/TR,T(60),TOLD(60)
      COMMON/AREA14/THETLM,AMEANL(5),VARL(5),VARLM2(5),ALPHAL(60,5),
     1BETAL(60,5),VLGAMA(5),THETAL(60,5),VARRL(60,5),PSIL(60,5),PSILM
      COMMON/AREA22/VISMIX(60),GML(60,5)
      COMMON/AREA19/XF(60,5),XFTHET(60,5),XFPSI(60,5),XFOLD(60,5),
     1XFTHOLD(60,5),XFPSOLD(60,5),XFI(5),SUMXFTHET(60),SUMXFPSI(60)
      COMMON/AREA16/RDBARL(60,5),RDTWIDLL(60,5),RDHATL(60,5),FAC,
     1DBARL(60,5),DTWIDLL(60,5),DHATL(60,5)

      AV1 = -6.92D0
      AV2 = -1.5D-2
      BV1 = 2.609D2
      BV2 = 7.07D0

*     TO EVALUATE THE INTEGRAL FOR M.WT. AT EACH GRID POINT

      IF(FAC.GT.1.D0)THEN
      NLOOP = 400
      ELSE
      NLOOP = 600
      ENDIF
      DO 32 J=1,JN
      DO 33 H=1,NN
      SUM0 = 0.0D0
      TVOLD = 0.D0
      F4OLD = 0.D0
      DO 34 I= 0,NLOOP
      L = I-VLGAMA(J)
      IF(L.GT.0)THEN
      TV = L/BETAL(H,J)
      F1 = TV**(ALPHAL(H,J)-1.D0)
      F2 = DEXP(-1.D0*TV)
      F3 = DLOG(BETAL(H,J)*TV+VLGAMA(J))
      F4 = F1*F2*F3
      F5 = (F4 + F4OLD)*(TV - TVOLD)/2.D0
      TVOLD = TV
      F4OLD = F4
      SUM0 = SUM0 + F5
      ENDIF
34    CONTINUE
      TINT0 = SUM0
      TRM4 = TINT0/GML(H,J)
      TRM1 = DLOG(1.D-3*RHOLI)
      TRM2 = BV1/TR
      TRM3 = (AV2+(BV2/TR))*THETAL(H,J)
      VISMIX1(H,J) = TRM1+AV1+TRM2+TRM3+TRM4
```

```
33    CONTINUE
32    CONTINUE

      DO 38 I=1,NN
      VISMIX(I) = 0.0D0
      DO 39 J=1,JN
      VISMIX(I) = VISMIX(I) + XF(I,J)*VISMIX1(I,J)
39    CONTINUE
      VISMIX(I) = DEXP(VISMIX(I))
38    CONTINUE
      RETURN
      END
*************************************************************************
      SUBROUTINE LDIF
*************************************************************************
*     THIS SUBROUTINE WILL CALCULATE LIQUID DIFFUSION COEFFICIENTS
*     [M2/SEC] BASED ON NUMERICAL INTEGRATION FOR VLGAMA NOT
*     EQUAL TO ZERO.
*
      IMPLICIT DOUBLE PRECISION (A-G,O-Z)

      COMMON/AREA1/N,NN,JN,R
      COMMON/AREA11/RHOL(60),RHOLOLD(60),RHOLM,RHOLI,DIFLL(60),XFBAR(5)
      COMMON/AREA12/TR,T(60),TOLD(60)
      COMMON/AREA14/THETLM,AMEANL(5),VARL(5),VARLM2(5),ALPHAL(60,5),
     1BETAL(60,5),VLGAMA(5),THETAL(60,5),VARRL(60,5),PSIL(60,5),PSILM
      COMMON/AREA16/RDBARL(60,5),RDTWIDLL(60,5),RDHATL(60,5),FAC,
     1DBARL(60,5),DTWIDLL(60,5),DHATL(60,5)
      COMMON/AREA22/VISMIX(60),GML(60,5)
      COMMON/AREA19/XF(60,5),XFTHET(60,5),XFPSI(60,5),XFOLD(60,5),
     1XFTHOLD(60,5),XFPSOLD(60,5),XFI(5),SUMXFTHET(60),SUMXFPSI(60)
*
*     TO EVALUATE THE INTEGRAL FOR M.WT. AT EACH GRID POINT

      IF(FAC.GT.1.D0)THEN
      NLOOP = 400
      ELSE
      NLOOP = 600
      ENDIF
      DO 232 J=1,JN
      DO 233 H=1,NN
      SUM1 = 0.0D0
      SUM2 = 0.0D0
      SUM3 = 0.0D0
      TVOLD = 0.D0
      FF1OLD = 0.D0
      FF2OLD = 0.D0
```

```
      FF3OLD = 0.D0
      DO 34 I= 0,NLOOP
      L = I-VLGAMA(J)
      IF(L.GT.0)THEN
      TV = L/BETAL(H,J)
      F1 = TV**(ALPHAL(H,J)-1.D0)
      F2 = DEXP(-1.D0*TV)
      F3 = (BETAL(H,J)*TV+VLGAMA(J))**6.D-1
      F4 = (BETAL(H,J)*TV+VLGAMA(J))**4.D-1
      F5 = (BETAL(H,J)*TV+VLGAMA(J))**1.4D0
      FF1 = F1*F2/F3
      FF2 = F1*F2*F4
      FF3 = F1*F2*F5
      F6 = TV - TVOLD
      SS1 = (FF1 + FF1OLD)*F6/2.D0
      SS2 = (FF2 + FF2OLD)*F6/2.D0
      SS3 = (FF3 + FF3OLD)*F6/2.D0
      TVOLD = TV
      FF1OLD = FF1
      FF2OLD = FF2
      FF3OLD = FF3
      SUM1 = SUM1 + SS1
      SUM2 = SUM2 + SS2
      SUM3 = SUM3 + SS3
      ENDIF
34    CONTINUE
      TINT1 = SUM1
      TINT2 = SUM2
      TINT3 = SUM3
      CONST = ((7.4D-12)*(THETAL(H,J)**5.D-1)*((1.E-3*RHOLI)**6.D-1)
     1*TR)/(VISMIX(H)*GML(H,J))
      DBARL(H,J) = FAC*CONST*TINT1
      DTWIDLL(H,J) = FAC*CONST*TINT2/THETAL(H,J)
      DHATL(H,J) = FAC*CONST*TINT3/PSIL(H,J)
233   CONTINUE
232   CONTINUE
*
*  PRODUCTS cD (RHO*D) ARE ASSIGNED TO EAST BOUNDARY OF CELL FOR *
LIQUID
*
      DO 20 J =1,JN
      DO 19 I = 1,NN-1
      RDBARL(I,J) = (RHOL(I)*DBARL(I,J)+RHOL(I+1)*DBARL(I+1,J))/2.D0
      RDTWIDLL(I,J)=(RHOL(I)*DTWIDLL(I,J)+RHOL(I+1)*DTWIDLL(I+1,J))/2.D0
      RDHATL(I,J) = (RHOL(I)*DHATL(I,J)+RHOL(I+1)*DHATL(I+1,J))/2.D0
19    CONTINUE
      RDBARL(NN,J) = RHOL(NN)*DBARL(NN,J)
```

```
      RDTWIDLL(NN,J) = RHOL(NN)*DTWIDLL(NN,J)
      RDHATL(NN,J) = RHOL(NN)*DHATL(NN,J)
20    CONTINUE
      RETURN
      END
*****************************************************************************
      SUBROUTINE THTJACB(NITR)
*****************************************************************************
      IMPLICIT DOUBLE PRECISION (A-G,O-Z)
      INTEGER H
      DIMENSION THTL(4),FLTH(4),FVTH(4),FLPS(4),FVPS(4),PHITHT(4),PSL(4)
     1,PHIPS(4),AA(5),BB(5),G1(5)
*
      COMMON/AREA1/N,NN,JN,R
      COMMON/AREA4/TIME,DTIME,G0,VEL(60),RDOT,GTRR,DTLDT,DTR,TBOIL
      COMMON/AREA5/MA,PRES,RUGC,SM(60),PATM,AVGM
      COMMON/AREA6/YOAMB,YNAMB,YF(60,5),YO(60),YN(60),YMF(60,5),
     1YMO(60),YFR(5),YFTHET(60,5),YFPSI(60,5),YFOLD(60,5),YFTHOLD(60,5),
     1YFPSOLD(60,5),SUMYF(60)
      COMMON/AREA8/RDBAR(0:60,5),RDTWIDL(0:60,5),RDHAT(0:60,5),D0(60),DIF(60)
      COMMON/AREA9/ZETA(60),ZETAE(60),ZE2DZ(60),ZE3(60),ZE3D(60),ZETAD(60)
      COMMON/AREA10/RHO(60),RHOOLD(60)
      COMMON/AREA11/RHOL(60),RHOLOLD(60),RHOLM,RHOLI,DIFLL(60),XFBAR(5)
      COMMON/AREA12/TR,T(60),TOLD(60)
      COMMON/AREA13/ALPHAV(5),BETAV(5),THETA(60,5),VAR(60,5),VARM2(60,5)
      COMMON/AREA14/THETLM,AMEANL(5),VARL(5),VARLM2(5),ALPHAL(60,5),
     1BETAL(60,5),VLGAMA(5),THETAL(60,5),VARRL(60,5),PSIL(60,5),PSILM
      COMMON/AREA16/RDBARL(60,5),RDTWIDLL(60,5),RDHATL(60,5),FAC,
     1DBARL(60,5),DTWIDLL(60,5),DHATL(60,5)
      COMMON/AREA17/A(5),B(5),SFGR
      COMMON/AREA19/XF(60,5),XFTHET(60,5),XFPSI(60,5),XFOLD(60,5),
     1XFTHOLD(60,5),XFPSOLD(60,5),XFI(5),SUMXFTHET(60),SUMXFPSI(60)
      COMMON/AREA20/ZETAL(60),ZETALE(60),ZLE2DZ(60),ZLE3(60),ZLE3D(60),
     1ZETALD(60),ZLE2(60),VELL(60)
      COMMON/AREA22/VISMIX(60),GML(60,5)
      COMMON/AREA23/YFINF(5),YFTHIN(5),YFPSIN(5),PTOT,XFR(5),DXFDR(5),
     1DYFDR(5),DXFTHDR(5),DXFPSDR(5),DYFTHDR(5),DYFPSDR(5),THLRPF(4),
     1PSLRPF(4)
      COMMON/AREA24/SUMYFR
*
      SUMYFR = 0.0
      DO 333 J=1,JN
      IF(XFI(J).EQ.0.0)GOTO 333
      NEXIT = 0
      NITR = 0
4000  THTL(0) = THETAL(NN,J)
      PSL(0) = PSIL(NN,J)
```

```
      DTHT = 1.D-2
      DPS = 5.0D-1

      K = 1
      H = 1

5000 THTL(H) = THTL(H-1)+(DTHT*(H-1))
      PSL(K) = PSL(K-1)+(DPS*(K-1))

      IF(K.EQ.2)THTL(2)=THTL(1)
*************************************************************************
*    INITIAL LIQUID PROPERTIES:
*************************************************************************
      VARRL(NN,J) = PSL(K)-(THTL(H))**2
      VARLM2(J) = PSL(K)
      AMEANL(J) = THTL(H)
      VARL(J) = VARRL(NN,J)
      BETAL(NN,J) = VARL(J)/(AMEANL(J)-VLGAMA(J))
      ALPHAL(NN,J) = VARL(J)/(BETAL(NN,J)**2)
      IF(ALPHAL(NN,J).LT.0.0D0)THEN
      WRITE(1,*) 'NEGATIVE ALPHAL(NN,J)'
      WRITE(*,*) 'NEGATIVE ALPHAL(NN,J)'
      GOTO 6900
      ENDIF
      IF(BETAL(NN,J).LT.0.0D0)THEN
      WRITE(1,*) 'NEGATIVE BETAL(NN,J)'
      GOTO 6900
      ENDIF
*************************************************************************
*    INITIAL ESTIMATE OF CONC. PROFILES AT DROPLET SURFACE:
*************************************************************************
      XF(NN,J) = XFR(J)
      XFTHET(NN,J) = XF(NN,J)*THTL(H)
      XFPSI(NN,J) = XF(NN,J)*PSL(K)

*    YFR FROM VAPOR-LIQUID EQUILIBRIUM:

      AA(J) = SFGR*(1.D0-(A(J)/TR))
      BB(J) = B(J)/(TR-A(J))
      YFR(J) = PVAP(AA(J),BB(J),VLGAMA(J),ALPHAL(NN,J),BETAL(NN,J),PATM)
      YFR(J) = XF(NN,J)*YFR(J)/PTOT
*************************************************************************
*    ALPHA, BETA, VLGAMA FOR VAPOUR PHASE IN TERMS OF MOLES
*************************************************************************
      ALPHAV(J) = ALPHAL(NN,J)
      BETAV(J) = BETAL(NN,J)/(1.D0+(AA(J)*BB(J)*BETAL(NN,J)))
      THETA(1,J) = ALPHAV(J)*BETAV(J)+VLGAMA(J)
```

```
      VAR(1,J) = ALPHAV(J)*(BETAV(J)**2)
      VARM2(1,J) = VAR(1,J)+(THETA(1,J))**2
*
      YF(1,J) = YFR(J)
      YMF(1,J) = YF(1,J)*THETA(1,J)/SM(1)
      YFTHET(1,J) = YF(1,J)*THETA(1,J)
      YFPSI(1,J)  = YF(1,J)*VARM2(1,J)
*************************************************************************
*    CALCULATE THE INITIAL TRIAL MASS FLUX:
*************************************************************************
      DXFDR(J) = PARAB2(XF(NN,J),XF(NN-1,J),XF(NN-2,J),ZETAL(NN),
     1ZETAL(NN-1),ZETAL(NN-2))
      DXFDR(J) = DXFDR(J)/R
      DYFDR(J) = PARAB2(YF(1,J),YF(2,J),YF(3,J),ZETA(1),ZETA(2),ZETA(3))
      DYFDR(J) = DYFDR(J)/R
      G1(J)=((RDBARL(NN,J)*DXFDR(J))-(RDBAR(0,J)*DYFDR(J)))/(XFR(J)-
     1YFR(J))
      IF(NEXIT.EQ.1)THEN
      GOTO 444
      ENDIF
*************************************************************************
*    PARABOLIC FIT FOR VAPOR CONCENTRATION PROFILE NEAR SURFACE:
*************************************************************************
      DYFTHDR(J) = PARAB2(YFTHET(1,J),YFTHET(2,J),YFTHET(3,J),ZETA(1),
     1ZETA(2),ZETA(3))
      DYFTHDR(J) = DYFTHDR(J)/R
      DYFPSDR(J) = PARAB2(YFPSI(1,J),YFPSI(2,J),YFPSI(3,J),ZETA(1),
     1ZETA(2),ZETA(3))
      DYFPSDR(J) = DYFPSDR(J)/R
*************************************************************************
*    PARABOLIC FIT FOR LIQUID CONCENTRATION PROFILE NEAR SURFACE:
*************************************************************************
      DXFTHDR(J) = PARAB2(XFTHET(NN,J),XFTHET(NN-1,J),XFTHET(NN-2,J),
     1ZETAL(NN),ZETAL(NN-1),ZETAL(NN-2))
      DXFTHDR(J) = DXFTHDR(J)/R

      DXFPSDR(J) = PARAB2(XFPSI(NN,J),XFPSI(NN-1,J),XFPSI(NN-2,J),
     1ZETAL(NN),ZETAL(NN-1),ZETAL(NN-2))
      DXFPSDR(J) = DXFPSDR(J)/R
*************************************************************************
*    CALCULATE VAPOR AND LIQ. FLUXES AT THE SURFACE:
*************************************************************************
      FLTH(H) = G1(J)*XFTHET(NN,J)-RDTWIDLL(NN,J)*DXFTHDR(J)
      FVTH(H) = G1(J)*YFTHET(1,J)-RDTWIDL(0,J)*DYFTHDR(J)
      PHITHT(H) = FLTH(H)-FVTH(H)
      FLPS(H) = G1(J)*XFPSI(NN,J)-RDHATL(NN,J)*DXFPSDR(J)
      FVPS(H) = G1(J)*YFPSI(1,J)-RDHAT(0,J)*DYFPSDR(J)
```

```
      PHIPS(H) = FLPS(H)-FVPS(H)

      H = H + 1
      IF(H.EQ.2)GOTO 5000
      ENDIF

      IF(K.EQ.1)THEN
      DPHITHTDTHT = (PHITHT(2) - PHITHT(1))/DTHT
      DPHIPSDTHT = (PHIPS(2) - PHIPS(1))/DTHT
      K = 2
      H = 2
      GOTO 5000
      ELSE
      DPHIPSDPS = (PHIPS(2) - PHIPS(1))/DPS
      DPHITHTDPS = (PHITHT(2) - PHITHT(1))/DPS
      ENDIF

      DLTPS = ((-1.D0*PHITHT(1)/DPHITHTDTHT)+(PHIPS(1)/DPHIPSDTHT))
     1 /((DPHITHTDPS/DPHITHTDTHT)-(DPHIPSDPS/DPHIPSDTHT))
      DLTTHT = (-1.D0*PHITHT(1)/DPHITHTDTHT)-((DPHITHTDPS/
     1DPHITHTDTHT)*DLTPS)

      THETAL(NN,J) = THTL(1) + DLTTHT
      PSIL(NN,J) = PSL(1) + DLTPS
      VARRL(NN,J) = PSIL(NN,J)-THETAL(NN,J)**2
      CRITNEWT = 5.D-5*G1(J)*XFTHET(NN,J)
      CRITNEWP = 5.D-5*G1(J)*XFPSI(NN,J)

      NITR = NITR+1

    IF(DABS(PHITHT(1)).LT.CRITNEWT.AND.DABS(PHIPS(1)).LT.CRITNEWP)THEN
C       UPDATE SURFACE CONDITIONS AND G0
      NEXIT = 1
      GOTO 4000
      ELSE
      IF(NITR.GT.50)GOTO 6900
      GOTO 4000
      ENDIF
444   SUMYFR = SUMYFR + YFR(J)
333   CONTINUE

      G0 = G1(1)
6900 RETURN
      END
```

```
**************************************************************************
      SUBROUTINE NEWTONIAN
**************************************************************************
      IMPLICIT DOUBLE PRECISION (A-G,O-Z)
      INTEGER H

      DIMENSION AA(5),BB(5),XFRL(100),PHI(100),FL(100),FV(100)
*
      COMMON/AREA1/N,NN,JN,R
      COMMON/AREA4/TIME,DTIME,G0,VEL(60),RDOT,GTRR,DTLDT,DTR,
     1TBOIL
      COMMON/AREA5/MA,PRES,RUGC,SM(60),PATM,AVGM
      COMMON/AREA6/YOAMB,YNAMB,YF(60,5),YO(60),YN(60),YMF(60,5),
     1YMO(60),YFR(5),YFTHET(60,5),YFPSI(60,5),YFOLD(60,5),YFTHOLD(60,5),
     1YFPSOLD(60,5),SUMYF(60)
      COMMON/AREA8/RDBAR(0:60,5),RDTWIDL(0:60,5),RDHAT(0:60,5),D0(60),
     1DIF(60)
      COMMON/AREA9/ZETA(60),ZETAE(60),ZE2DZ(60),ZE3(60),ZE3D(60),
     1ZETAD(60)
      COMMON/AREA10/RHO(60),RHOOLD(60)
      COMMON/AREA11/RHOL(60),RHOLOLD(60),RHOLM,RHOLI,DIFLL(60),
     1XFBAR(5)
      COMMON/AREA12/TR,T(60),TOLD(60)
      COMMON/AREA13/ALPHAV(5),BETAV(5),THETA(60,5),VAR(60,5),
     1VARM2(60,5)
      COMMON/AREA14/THETLM,AMEANL(5),VARL(5),VARLM2(5),
     1ALPHAL(60,5),BETAL(60,5),VLGAMA(5),THETAL(60,5),VARRL(60,5),
     1PSIL(60,5),PSILM
      COMMON/AREA16/RDBARL(60,5),RDTWIDLL(60,5),RDHATL(60,5),FAC,
     1DBARL(60,5),DTWIDLL(60,5),DHATL(60,5)
      COMMON/AREA17/A(5),B(5),SFGR
      COMMON/AREA19/XF(60,5),XFTHET(60,5),XFPSI(60,5),XFOLD(60,5),
     1XFTHOLD(60,5),XFPSOLD(60,5),XFI(5),SUMXFTHET(60),SUMXFPSI(60)
      COMMON/AREA20/ZETAL(60),ZETALE(60),ZLE2DZ(60),ZLE3(60),ZLE3D(60
     1),ZETALD(60),ZLE2(60),VELL(60)
      COMMON/AREA22/VISMIX(60),GML(60,5)
      COMMON/AREA23/YFINF(5),YFTHIN(5),YFPSIN(5),PTOT,XFR(5),DXFDR(5),
     1DYFDR(5),DXFTHDR(5),DXFPSDR(5),DYFTHDR(5),DYFPSDR(5),
     1THLRPF(4),PSLRPF(4)
      COMMON/AREA24/SUMYFR
*
      J = 1
      NEXIT = 0
      NITR = 0

4000 XFRL(0) = XFR(J)
      DXF = 1.D-4
```

```
      H = 1
5000 XFRL(H) = XFRL(H-1)+(DXF*(H-1))
      IF(XFRL(H).EQ.1.D0)GOTO 6900
      IF(XFRL(H).GT.1.D0)THEN
      XFRL(H) = XFRL(H-1) - (DXF*(H-1))
      ENDIF

      SUMYFR = 0.0
      SUM1 = 0.0
      SUM2 = 0.0
      DO 333 J = 1,JN
*************************************************************************
*   INITIAL ESTIMATE OF CONC. PROFILES AT DROPLET SURFACE:
*************************************************************************
      IF(J.EQ.1)THEN
      XF(NN,J) = XFRL(H)
      ELSE
      XF(NN,J) = 1.D0 - XFRL(H)
      ENDIF
*    YFR FROM VAPOR-LIQUID EQUILIBRIUM:

      AA(J) = SFGR*(1.D0-(A(J)/TR))
      BB(J) = B(J)/(TR-A(J))
      YFR(J) = PVAP(AA(J),BB(J),VLGAMA(J),ALPHAL(NN,J),BETAL(NN,J),PATM)
      YFR(J) = XF(NN,J)*YFR(J)/PTOT
      SUMYFR = SUMYFR + YFR(J)
*************************************************************************
*    ALPHA, BETA, VLGAMA FOR VAPOUR PHASE IN TERMS OF MOLES
*************************************************************************
      ALPHAV(J) = ALPHAL(NN,J)
      BETAV(J) = BETAL(NN,J)/(1.D0+(AA(J)*BB(J)*BETAL(NN,J)))

      THETA(1,J) = ALPHAV(J)*BETAV(J)+VLGAMA(J)
      VAR(1,J) = ALPHAV(J)*(BETAV(J)**2)
      VARM2(1,J) = VAR(1,J)+(THETA(1,J))**2
*
      YF(1,J) = YFR(J)
      YMF(1,J) = YF(1,J)*THETA(1,J)/SM(1)
      YFTHET(1,J) = YF(1,J)*THETA(1,J)
      YFPSI(1,J)  = YF(1,J)*VARM2(1,J)
*************************************************************************
*    CALCULATE THE INITIAL TRIAL MASS FLUX:
*************************************************************************
      DXFDR(J) = PARAB2(XF(NN,J),XF(NN-1,J),XF(NN-2,J),ZETAL(NN),
     1ZETAL(NN-1),ZETAL(NN-2))
      DXFDR(J) = DXFDR(J)/R
```

```
      SUM1 = SUM1 + RDBARL(NN,J)*DXFDR(J)

      DYFDR(J) = PARAB2(YF(1,J),YF(2,J),YF(3,J),ZETA(1),ZETA(2),ZETA(3))
      DYFDR(J) = DYFDR(J)/R

      SUM2 = SUM2 + RDBAR(0,J)*DYFDR(J)

333   CONTINUE

*************************************************************************
*    CALCULATE VAPOR AND LIQ. FLUXES AT THE SURFACE:
*************************************************************************
      G0 = (SUM1 - SUM2)/(1.D0 - SUMYFR)
      FL(H) = G0*XF(NN,1)-RDBARL(NN,1)*DXFDR(1)
      FV(H) = G0*YFR(1)-RDBAR(0,1)*DYFDR(1)
      PHI(H) = FL(H) - FV(H)

      H = H + 1
      IF(H.EQ.2)GOTO 5000
      DPHIDXF = (PHI(2) - PHI(1))/DXF
      XFRLN = XFRL(2) - (PHI(2)/DPHIDXF)

      CRITNEW = 5.D-5*G0
      NITR = NITR+1

      IF(DABS(PHI(1)).LT.CRITNEW)THEN
      XFR(1) = XFRL(1)
      XFR(2) = 1.D0 - XFRL(1)
      ELSE
      IF(NITR.GT.50)GOTO 6900
      J = 1
      XFR(J) = XFRLN
      GOTO 4000
      ENDIF

6900  RETURN
      END
```